

Developing an experimental murine autoimmune model of nephrotic syndrome driven by a podocytopathic humoral response

Marie Ashley Ste-Croix, MSc

Department of Microbiology and Immunology

Faculty of Medicine and Health Sciences

McGill University

Montréal, Québec, Canada

April 2023

A Thesis submitted to McGill University Graduate and Post-Doctoral Studies

In partial fulfillment of the requirements of the degree of

Master of Science

Copyright © 2023 by Marie Ashley Ste-Croix

Table of Contents

LIST OF FIGURES AND TABLES	5
ABSTRACT	6
RÉSUMÉ	7
ACKNOWLEDGEMENTS	9
CONTRIBUTION OF AUTHORS	11
ABBREVIATIONS	12
Chapter 1: INTRODUCTION	16
1.1 AUTOIMMUNITY	16
1.1.1 MECHANISMS OF TOLERANCE	17
1.1.1.1 Central tolerance and T cell education in the thymus	17
1.1.1.2 Central tolerance and B cell education in the bone marrow	18
1.1.1.3 Mechanisms of peripheral tolerance	18
1.1.1.3.1 Control of self-tolerance and immune homeostasis by FoxP3⁺ T_{REG} cells	18
1.1.1.3.2 Anergy and activation-induced cell death in T and B cells	19
1.1.2 BREAKDOWN OF IMMUNE TOLERANCE	20
1.1.2.1 Defects in central tolerance	20
1.1.2.2 Defects in peripheral tolerance	20
1.1.2.2.1 Developmental, homeostatic, or functional deficits in FoxP3⁺ T_{REG} cells	21
1.1.2.2.2 Auto-antigen presentation on MHC-II risk alleles	21
1.1.2.2.3 Peripheral survival of auto-reactive lymphocytes	22
1.1.3 ROLES OF CELLULAR RESPONSES MEDIATING AUTOIMMUNE DISORDERS	22
1.1.3.1 Lineage-committed differentiation of auto-reactive CD4⁺ Th cells	23
1.1.3.2 CD4⁺ Th1 and Th17 cells: key mediators of autoimmunity	23
1.1.4 ANTIBODY-MEDIATED AUTOIMMUNITY	24
1.1.4.1 Auto-antigen presentation to CD4⁺ T cells by B cells	24
1.1.4.2 CD4⁺ Tfh cells: key drivers of humoral responses	25
1.1.4.3 Auto-antigen ligation, pathogenic B cell activation, and auto-antibody production	25
1.1.4.4 GC reactions: CD4⁺ T cell-dependent B cell activation & plasma cell differentiation	26
1.1.4.4.1 B cell activation – Memory B cells	27
1.1.4.4.2 B cell activation – high-affinity auto-antibody secreting plasma cells	28
1.2 RENAL AUTOIMMUNE DISORDERS	30
1.2.1 KIDNEY ANATOMY	30

1.2.1.1	Nephron anatomy and function	30
1.2.1.2	Glomeruli – The filtration unit of the kidneys.....	31
1.2.1.3	Podocyte anatomy and function.....	31
1.2.2	GLOMERULAR AUTOIMMUNE DISEASE.....	32
1.2.2.1	Inflammatory nephritic verses non-inflammatory nephrotic syndromes.....	32
1.2.2.2	Idiopathic nephrotic syndrome (INS).....	33
1.2.2.2.1	Membranous nephropathy (MN)	33
1.2.2.2.2	Focal segmental glomerulosclerosis (FSGS).....	34
1.2.2.2.3	Minimal change disease (MCD)	34
1.2.3	EVIDENCE OF IMMUNE CELL INVOLVEMENT IN MCD PATHOLOGY	35
1.2.3.1	Historical evidence of T cell activity in MCD	35
1.2.3.2	Emerging evidence of B cell involvement in MCD.....	36
1.2.4	MURINE MODELS OF NEPHROTIC SYNDROME TO STUDY THE CD4 ⁺ T-B CELL CROSSTALK 37	
1.2.4.1	Limitations of current murine models.....	37
1.2.4.2	Experimental autoimmune nephrotic syndrome (EANS) model	38
1.3	KNOWLEDGE GAPS, HYPOTHESIS & EXPERIMENTAL OBJECTIVES.....	40
Chapter 2: MATERIALS & METHODS.....		42
2.1	Materials.....	42
2.2	Mice	43
2.3	Mouse recombinant Crb2 (rCrb2) protein production.....	43
2.4	Protein purification	44
2.4.1	Column purification.....	44
2.4.2	Protein dialysis	44
2.5	rCrb2 emulsification	44
2.6	rCrb2 immunization.....	45
2.7	Necropsy and sample collection	45
2.8	Secondary lymphoid organ and kidney tissue processing (immune cell isolation)	45
2.8.1	Kidney processing.....	45
2.8.2	Secondary lymphoid organs.....	46
2.9	Lymphocyte cytokine stimulation	46
2.10	Immunophenotyping (flow cytometry).....	46
2.11	Enzyme-linked immunosorbent assay (ELISA)	47

2.11.1	Albuminuria (uACR).....	47
2.11.2	Serum anti-Crb2 poly-IgG titre.....	47
2.12	Histology – H&E staining.....	48
2.13	Immunofluorescent glomerular staining.....	48
2.14	rCrb2-specific CD4 ⁺ T cell restimulation	49
2.15	Passive transfer	49
2.16	FTY720 treatment.....	49
2.17	Statistics.....	49
Chapter 3: RESULTS	51
3.1	Generation of experimental autoimmune nephrotic syndrome (EANS) model	51
3.1.1	Immunization with rCrb2 induced nephrotic-range proteinuria in C3H/HeN mice.....	51
3.1.2	Key clinical features of human MCD are recapitulated in EANS.	52
3.2	Podocyte-binding auto-antibodies are associated with EANS severity.	53
3.3	Activation of isotype-switched memory B cells preceded proteinuria.	54
3.4	The characterization of CD4 ⁺ T _{EFF} cells & FoxP3 ⁺ T _{REG} cells during EANS.....	55
3.4.1	Effector CD4 ⁺ T cells arise prior to proteinuria.....	56
3.4.2	FoxP3 ⁺ T _{REG} cells were not perturbed during active EANS.	57
3.5	Effector CD4 ⁺ T cell harbour rCrb2-reactive clones.	57
3.6	FTY720-treatment suppressed germinal centres abrogating humoral auto-reactivity.	58
3.7	BALB/c mice are susceptible to EANS.....	60
Chapter 4: DISCUSSION	63
4.1	SUMMARY AND DISCUSSION	63
4.1.1	How does this model recapitulates key humoral responses and clinical aspects of human MCD?	63
4.1.2	How are germinal centre reactions key in determining auto-antibody generations?.....	66
4.1.3	How are humoral responses and effector functions linked in the pathogenesis of MCD?	
	70	
4.2	EXPLORING THE ROLE OF THE CD4⁺ T-B CELL CROSSTALK IN THE DEVELOPMENT OF MCD AND THE INTERPLAY BETWEEN HUMORAL & CELLULAR FUNCTIONS	73
4.2.1	How are humoral responses mediating podocyte cytoskeletal rearrangement and continued podocyte injury?	73
4.2.2	How is the T-B cell crosstalk mechanistically involved in podocyte injury and MCD pathogenesis in the murine EANS model?	77
Chapter 5: CONCLUSION	80

FIGURES & TABLES	81
REFERENCES	118

LIST OF FIGURES AND TABLES

Figure 1. Activation and differentiation of CD4 ⁺ T cells and B cells.	82
Figure 2. The T-B cell crosstalk is critical for protective immunity and represents a key junction in the development of autoimmunity.	84
Figure 3. Glomerular filtration is the renal process where ultrafiltrate from the blood is filtered through the podocytes.....	85
Figure 4. Podocyte foot process effacement causes proteinuria – a common symptom in nephrotic syndrome.	86
Figure 5. Evidence of immune cell involvement in MCD pathology.	87
Figure 6. Immunization protocol of C3H/HeN mice with podocyte-specific Crb2.....	88
Figure 7. rCrb2-immunized mice developed nephrotic injury with histological features resembling MCD.90	
Figure 8. Anti-rCrb2 antibody responses were increased in rCrb2-immunized mice with glomerular deposition and podocyte binding.....	92
Figure 9. Switch-memory B cells with IgG BCR and increase MHC-II expression preceded proteinuria development in EANS.....	94
Figure 10. Memory CD4 ⁺ T _{EFF} cells expressing the co-stimulatory activator molecule accumulated in iLN of EANS mice prior to proteinuria detection.	96
Figure 11. FoxP3 ⁺ T _{REG} cell frequencies showed no changes in iLN and kidneys in EANS.	98
Figure 12. Increased proliferation in vitro following restimulation with rCrb2 denotes expansion of rCrb2-specific CD4 ⁺ T cells.	100
Figure 13. FTY720-treatment attenuated auto-antibody production and inhibited proteinuria development in rCrb2-immunized mice.....	102
Figure 14. Prolonged FTY720-treatment significantly reduced proliferation responses in CD4 ⁺ T _{EFF} cells within iLN of EANS mice.	104
Figure 15. Migrating the EANS immunization model into the BALB/c mouse strain.	106
Figure 16. Renal LN acquisition from rCrb2-immunized BALB/c mice revealed accumulation of activated CD4 ⁺ T _{EFF} cells.	108
Figure 17. Induction of EANS in BALB/c with rCrb2-immunization showed no changes in renal CD4 ⁺ T _{EFF} and FoxP3 ⁺ T _{REG} cell proportions.	110
Table 1. Historically used animal models of podocyte injury.	111
Table 2. List of antibodies.....	112

ABSTRACT

Idiopathic nephrotic syndrome (INS) is a rare pediatric disease characterized by severe proteinuria of unknown etiology, with most cases presenting as Minimal Change Disease (MCD), displaying severe podocyte effacement. MCD shows no clear evidence of inflammation, immune cell infiltration or antibody (Ab) deposition within the kidney yet responds readily to immunosuppressive drugs. Recent evidence suggests the involvement of autoimmune responses in the pathogenesis of INS, significantly the detection of podocyte-targeting auto-Abs. The lack of an immune-mediated murine model hinders our understanding of the pathology, so we aim to develop an immune-driven *in-vivo* model to investigate the mechanisms of immune dysregulation mediating podocytopathy in INS with MCD-like lesions. We hypothesize podocyte antigens activate T and B cell responses, initiating anti-podocyte auto-Abs responses leading to MCD pathology. C3H/HeN mice were immunized with recombinant Crb2 (rCrb2), a podocyte transmembrane protein. Pathological measurements and podocyte injury was evaluated by urine albumin-to-creatinine ratios, histology assessing glomerular integrity, and serum Ab titres. Flow cytometry characterized immunophenotypes of CD4⁺ T and B cells within the kidneys and periphery by fluorescently targeting key identifying markers, co-stimulatory, and antigen-presenting molecules. rCrb2-immunized C3H/HeN mice recapitulated key features of human MCD injury, including nephrotic-range proteinuria, anti-Crb2 auto-Ab production, intact glomerular structural integrity, and lack of renal immune cell infiltration. High serum titres of auto-Abs were detected with glomerular deposition and podocyte binding. Activation of IgG⁺ B cell and memory CD4⁺ T_{EFF} cells were observed. There were no detectable changes in FoxP3⁺ T_{REG} cell populations in mice with experimental autoimmune nephrotic syndrome (EANS), possibly suggesting a dysregulation in suppressor functions. Germinal centre (GC) reactions were found to be critical for anti-Crb2 auto-Ab maturation in EANS. Lastly, successful induction of EANS in BALB/c mice may be used as an alternative strain for the EANS model. Overall, evidence showed activated T and B cells are communicating during GC reactions to produce high-affinity auto-Abs leading to EANS. CD4⁺ T cells may be involved in the deposition of auto-Abs to the glomeruli by generating factors to allow access to the podocytes. The use of this model will begin to fill the knowledge gaps regarding the cellular and molecular mechanisms underlying the break in immune tolerance mediating podocytopathy in MCD, however future experimentation is required.

RÉSUMÉ

Le syndrome idiopathique néphrotique (SIN) est une maladie pédiatrique rare caractérisée par une protéinurie sévère d'étiologie inconnue et un effacement des pieds podocytaires. La majorité des cas se présente comme un Syndrome Néphrotique à Lésions Glomérulaires Minimales (SNLGM) avec une absence d'inflammation, d'infiltration immunitaire ou de dépôts d'anticorps significatifs sur le rein, mais répond pourtant aux traitements immunosuppresseurs. La découverte récente d'auto-anticorps anti-podocytes suggère une origine auto-immune à la pathogenèse du SIN. Toutefois, l'absence de modèle murin de la maladie limite notre compréhension de sa physiopathologie. Ainsi, nous cherchons à développer un modèle de syndrome néphrotique expérimental auto-immun (SNEA) afin d'étudier les mécanismes de dérégulation immunitaire qui induisent la podocytopathie. Nous émettons l'hypothèse que des antigènes podocytaires induisent une activation des réponses lymphocytaires B et T, déclenchant la production d'auto-anticorps anti-podocytes et conduisant au SNLGM. Nous avons immunisé des souris C3H/HeN avec une protéine Crb2 recombinante (rCrb2), habituellement exprimée à la membrane des podocytes. La pathologie et les lésions glomérulaires furent mesurées par le ratio albumine: créatinine urinaire, une évaluation histologique de l'intégrité des glomérules et les titres sériques d'anticorps. Nous avons caractérisé par cytométrie en flux le phénotype des lymphocytes B et T résidant dans le rein et les ganglions lymphatiques périphériques en quantifiant leur expression de marqueurs de co-stimulation et de présentation d'antigène. Les souris C3H/HeN immunisées contre rCrb2 ont présenté plusieurs caractéristiques pathognomoniques de SNLGM, avec une protéinurie d'ordre néphrotique, la production d'auto-anticorps anti-Crb2, une structure glomérulaire intacte et une absence d'infiltration immunitaire substantielle au niveau rénal. Nous avons détecté des titres sériques élevés d'auto-anticorps avec dépôts glomérulaires et liaison aux podocytes. Nous avons noté une activation des lymphocytes B IgG⁺ et des lymphocytes T_{eff} CD4⁺. Nous n'avons pas détecté de réduction du nombre de lymphocytes T régulateurs Foxp3⁺, ce qui suggère une possible altération de leur fonction suppressive. La réaction du centre germinatif était essentielle à la maturation des auto-anticorps anti-Crb2 dans notre modèle. Enfin, l'induction dans des souris BALB/c pourrait représenter un modèle alternatif de SNEA. Dans l'ensemble, nous avons observé que l'activation des réponses lymphocytaires B et T coopèrent durant la réaction du centre germinatif pour produire des auto-anticorps de haute affinité qui induisent un SNEA. Les

lymphocytes T CD4⁺ pourraient être impliqués dans le dépôt des auto-anticorps en produisant des facteurs qui induisent un accès aux podocytes. L'utilisation de ce modèle permet de combler des manques dans notre compréhension des mécanismes moléculaires et cellulaires à l'origine de la perte de tolérance immunitaire qui sous-tendent la podocytopathie dans le SNLGM.

ACKNOWLEDGEMENTS

There are numerous people I would like to express my thanks and gratitude here for their unwavering support through my Master's progress.

First, I would like to give my biggest thanks to my supervisors, Dr. Ciriaco Piccirillo and Dr. Tomoko Takano, for taking me on and providing guidance, support, and patience throughout this Master's study. Not only has they provided me the opportunity and research resources to conduct the Thesis work presented here, but they have always inspired and pushed me to be a more of a critical thinker and a leader. I know that what I have learned here during my time as their student will benefit me greatly both professionally and personally as I advance further into my scientific career.

Next, I'd like to thank my committee members, Dr. Javier Di Noia and Dr. Woong-Kyung Suh for observing the progression of this Thesis work and giving valuable insight and critics on the work itself. They pushed the boundaries of my knowledge and motivated me to think of the bigger picture. They were always understanding, willing to help, patient, as well as gave value critiques to better my research and myself.

To Tho-Alfakar Al-Aubodah, Fernando Alvarez, Mikhaël Attias, Roman Istomine, Geneviève Genest, ZhiYang Liu, Helen Mason, Céleste Pilon, Harshita Patel, Lamine Aoudjit, and Simon Leclerc, my fellow lab members and friends, I extend my deepest gratitude. Every day they were always there ready to help when asked, for the invaluable training, and just all the wonderful conversations whether about our work or lives. Most importantly, I especially want to thank Tho, Simon, and Lamine for their major contributions of this Thesis work including all they have done with the proteinuria ELISAs, immunofluorescent microscopy, and human studies for which this work is extended from. I would also like to thank Dr. Kunimasa Yan at Kyorin University (Tokyo, Japan) for generously gifting the rCrb2-expression plasmids and purified rCrb2 mAb that made this project possible.

To McGill University and the Department of Microbiology Immunology, thank you for accepting me into this program and providing opportunities to grow academically, professionally, and personally. All the professors, faculty, and other students were always willing to help, friendly, and encouraged me to succeed.

Thank you to the CIHR (Canadian Institute of Health Research) for funding this research.

Last, but certainly not least, with all my heart I thank my friends and family. They have been my rock throughout this entire journey and got me through all the highlights and the challenges that came with it, especially my parents (Jennifer and Brian Ste-Croix), my brother (Kevin Ste-Croix), and my loving husband (Tim Keding). They are always supportive in whatever I chose, and they continue to be supportive to this day as I advance further into my scientific career, wherever that leads me.

To everyone who I have not mentioned, I wanted to thank them as well in their support and encouragement for which I hold dear. You know who you are, my friends.

Thank you!

I, Marie Ashley Ste-Croix, have read, understood, and abided by all norms and regulations of academic integrity of McGill University.

CONTRIBUTION OF AUTHORS

In collaboration with Dr. Ciriaco Piccirillo and Dr. Tomoko Takano, I was responsible for the experimental designs, execution, data analysis, and writing of the Thesis presented. Results from human pediatric INS studies where data cannot be cited was provided from the work conducted by Tho-Alfakar Al-Aubodah, a Ph.D. student in Dr. Piccirillo's laboratory, which have yet to be published at the time of Thesis writing/submission. As the work progressed, Simon Leclerc, a PhD candidate in Dr. Takano's laboratory contributed to the Thesis with his immunofluorescent staining and quantification of renal tissue sections obtained from immunization experiments I have designed.

ABBREVIATIONS

°C	Degrees Celsius	CD44	Homing-associated cell adhesion molecule (H-CAM)
Ab	Antibody	CD62L	L-selectin
ACAD	T cell autonomous death	CFA	Complete Freund's Adjuvant
Ack	Ammonium-Chloride-Potassium	CO ₂	Carbon dioxide
AD	Atopic dermatitis	COVID-19	SAR-CoV2
ADCC	Antibody-dependent cellular cytotoxicity	Crb2	Crumbs Cell Polarity Complex Component 2
ADR	Adriamycin	cRPMI	Complete RPMI-1640 media
Ag	Antigen	CSR	Class switch recombination
AICD	Auto-reactive lymphocytes through activation-induced cell death	CTV	Cell tracer violet
AID	Activation-induced cytidine deaminase	DC	Dendritic cell
ANCA	Anti-neutrophil cytoplasmic antibodies	ddH ₂ O	Double distilled water
APC	Antigen presenting cell	DNase	Deoxyribonuclease
ax/brLN	Axillary-brachial lymph nodes	DP	Double positive
B6C3F1	C3H/HeN x C57BL/6 first generation hybrid mouse strain	DZ	Dark zone
Bcl-6	B-cell lymphoma 6	<i>E. coli</i>	<i>Escherichia coli</i>
BCR	B cell receptor	E. tubes	Eppendorf tubes
BL/6	C57BL/6 mouse strain	EAE	Experimental autoimmune encephalomyelitis
BM	Bone marrow	EANS	Experimental autoimmune nephrotic syndrome
BSA	Bovine serum albumin	EDTA	Ethylenediaminetetraacetic acid
C3H	C3H/HeN mouse strain	ELISA	Enzyme-linked immunosorbent assay
Ca ²⁺	Calcium	EtOH	Ethanol
CD25	IL-2 receptor	F(ab) ₂	Antibody variable region
		Fas	Cell death receptor
		FasL	Fas ligand

FBS	Fetal bovine serum	Hr	Hour
Fc	Antibody constant region	HRP	Horseradish peroxidase
FcR	Fc receptor	HSC	Haematopoietic stem cells
FcRn	Neonatal Fc receptor	IC	Immune complex
FDC	Follicular dendritic cell	ICOS	Inducible T Cell Costimulator
FERM	4.1/ezrin/radixin/moesin	ICOS-L	Inducible T cell Co-stimulator ligand
Fig.	Figure	IF	Immunofluorescent
FoxP3	Forkhead box protein 3	IFA	Incomplete Freund's Adjuvant
FSGS	Focal segmental glomerulosclerosis	IFN γ	Interferon γ
FTY720	Fingolimod	Ig	Immunoglobulin
g	Gravity	IgA	Immunoglobulin A
GATA3	GATA Binding Protein 3	IgD	Immunoglobulin D
GBM	Glomerular basement membrane	IgE	Immunoglobulin E
GC	Germinal centre	IgG	Immunoglobulin G
GC	Glucocorticoid	IgM	Immunoglobulin M
gm	Gram	IL	Interleukin
gMFI	Geometric mean fluorescent intensity	iLN	Inguinal lymph nodes
GN	Glomerulonephritis	INS	Idiopathic nephrotic syndrome
H&E	Hematoxylin and eosin	IPEX	Immune dysregulation, poly-endocrinopathy, enteropathy, X-linked disorder
H ₂ O	Water	IPTG	Isopropyl β -D-1-thiogalactopyranoside
H ₂ SO ₄	Sulfuric acid	KANK	Kidney ankyrin
HBSS	Hanks' Balanced Salt Solution	kg	Kilogram
HCl	Hydrochloric acid	KO	Knockout
hi	High	LB	Lysogeny broth
HIV	Human immunodeficiency virus	LN	Lupus nephritis
HLA	Human leukocyte antigen		

LN	Lymph nodes	NTS	Nephrotoxic serum nephritis
lo	Low	ON	Overnight
LPS	Lipopolysaccharide	PAN	Puromycin aminonucleoside nephrosis
LZ	Light zone	PBMC	Peripheral blood mononuclear cells
m ²	Meter ²	PBS	Phosphate-Buffered Saline
M	Molar	PC	Plasma cell
MCD	Minimal change disease	PCR	Polymerase chain reaction
mg	Milligram	PD-1	Programmed death-1
Mg ²⁺	Magnesium	PD-1L	Programmed death-1 ligand
MHC-I	Major histocompatibility complex class I	Pen-Strep	Penicillin and streptomycin
MHC-II	Major histocompatibility complex class II	PFA	Paraformaldehyde
Min	Minute	PI3K	Phosphoinositol 3-kinase
ml	Millilitre	pIgG	Polyclonal IgG
mM	Millimolar	PLA2R1	Phospholipase A2 receptor
MN	Membranous nephropathy	PM	Plasma membrane
MS	Multiple sclerosis	PMA	Phorbol myristate acetate
N	Normality	pT _{REG}	Peripherally induced regulatory T cell
NaCl	Sodium chloride	RA	Rheumatoid arthritis
NF- κB	Nuclear factor-κB	rCrb2	Recombinant Crb2
ng	Nanogram	RI-MUHC	Research Institute of the McGill University Health Centre
nm	Nanometre	rLN	Renal lymph nodes
NON/SCID	Nonobese diabetic/severe combined immunodeficiency	RORγt	RAR-related orphan receptor γ
<i>NPHS1</i> & <i>NPHS2</i>	Nephrin genes	rpm	Rotation per minute
NS	Nephrotic syndrome	RSV	Human respiratory syncytial virus
NSM	Non-switched memory	RT	Room temperature
		RTX	Rituximab

S1P	Sphingosine 1-phosphate	THSD7A	Thrombospondin type-1 domain containing protein 7A
S1P-R	Sphingosine 1-phosphate receptor	TLR	Toll-like receptor
Saline	0.9% NaCl in ddH ₂ O	TMB	Reaction substrate
sec	Second	TMG	TitreMax Gold
SHM	Somatic Hypermutation	TNE	Tris-HCl; NaCl; EDTA
SLE	Systemic lupus erythematosus	TNF- α	Tumor necrosis factor- α
SM	Isotype-switched memory	T _{REG}	Regulatory T cell
T-bet	T-box transcription factor TBX21	tT _{REG}	Thymic-derived regulatory T cell
TCR	T cell receptor	uACR	Urine albumin creatinine ratio
T _{EFF}	Effector T cell	μ g	Microgram
Tfh	Follicular helper T cell	μ l	Microlitre
TGF- β	Transforming growth factor β	μ m	Micron
Th	Helper T cell		

Chapter 1: INTRODUCTION

Idiopathic nephrotic syndrome (INS) is a rare pediatric disease characterized by severe proteinuria of unknown etiology. Clinical manifestation of INS can be presented in the histological forms of membranous nephropathy (MN), focal segmental glomerulosclerosis (FSGS), and minimal change disease (MCD) [1-3]. The majority of pediatric INS (90%) cases present as MCD, displaying severe podocyte effacement which responds readily to immunosuppressive drugs [4-6]. While the exact cause of MCD is not known, it was generally not considered an autoimmune disorder, as it was thought to be caused by an abnormal immune response not directed against the glomerular basement membrane (GBM) or podocytes as characterized unlike in MN and FSGS [4, 7, 8]. Recent discoveries in human MCD patients however have revealed hallmarks of auto-reactive immune responses against podocyte proteins, which have prompted a closer look into possible immune mechanisms of podocytopathy, including the activation of pathogenic T and B cells and auto-antibody (Ab) production targeting podocytes [9-12]. A comprehensive understanding of the immune system's ability to develop tolerance to self-antigens (Ag), as well as the mechanisms that lead to autoimmune responses when this tolerance is disrupted, is imperative in elucidating the processes that underlie nephrotic injury in MCD. This knowledge can aid in the development of better diagnostic and treatment strategies for the disease. The goal of the current work is to fill known knowledge gaps of MCD, particularly with regards to its autoimmune nature, by aiming to explore the immune mechanisms responsible for podocyte injury and proteinuria.

1.1 AUTOIMMUNITY

An autoimmune disorder is a condition in which a break in immune tolerance leads immune cells to attack and damage healthy cells, tissues, and organs in the body [13]. This is driven by genetic, epigenetic, and environmental triggers that precipitate a loss of peripheral tolerance [14]. The immunological mechanisms engaged during the onset and maintenance of autoimmune disorders are complex, and largely unexplored in diseases like MCD. Peripheral tolerance involves a complex balance between efficient thymic T cell education, the elimination of self-reactive B cells, the generation of suppressive regulatory T (T_{REG}) cells as well as an array of peripheral signals inhibiting the activation and survival of self-reactive T and B cells.

1.1.1 MECHANISMS OF TOLERANCE

Adaptive immunity, also referred to as acquired immunity, is one of two major branches of the immune system. Unlike innate immune responses, which are generally non-specific towards an invading pathogen, adaptive immune responses mediated by B and T cells, are activated through specific recognition of Ag or derived peptides, respectively, and develop immune memory upon re-exposure to Ag [15]. The adaptive immune response is also characterized by its ability to discriminate self- from non-self-Ags thus preventing auto-reactive responses leading to autoimmunity through central and peripheral tolerance mechanisms [16]. Central tolerance is developed in the thymus and bone marrow (BM), eliminating self-reactive lymphocytes during their initial development. Peripheral tolerance in secondary lymphoid organs prevents over-reactivity or elimination of self-reactive lymphocytes which have escaped the mechanism of central tolerance [17].

1.1.1.1 Central tolerance and T cell education in the thymus

Central tolerance begins with the generation of productive T cell receptor (TCR) and B cell receptors (BCR) during the development of early T and B cell progenitors. Both lymphocytes derive from haematopoietic stem cells (HSC) precursors in the BM [18-20]. From there, early T cell progenitors migrate to the thymus and undergo several distinct stages of development. As they progress through the early stage of TCR development, a CD3 $\alpha\beta$ complex forms on pre-T cells and gives rise to CD4⁺CD8⁺ double positive (DP) thymocytes [20]. DP thymocytes interact with self-Ags presented on major histocompatibility complex (MHC) -I (MHC-I) or MHC-II molecules. T cells recognizing peptide/MHC complexes with the appropriate level of affinity binding are given survival signals (positive selection), whereas those with weak affinity die by apoptosis. Surviving DP thymocytes undergo further TCR rearrangement prior to negative selection, a process by which T cells recognizing self-Ags with high affinity are eliminated through a process of clonal deletion, in turn, preventing autoimmunity. Thymocytes surviving negative selection differentiate into either single positive CD4⁺ or CD8⁺ naïve T cells, egress from the thymus to the periphery for ensuing immune responses [21].

1.1.1.2 Central tolerance and B cell education in the bone marrow

From common lymphocyte precursor cells differentiated from HSCs, pro-B cells develop within the BM. They express immunoglobulin (Ig) heterodimers Ig- α and Ig- β , which are necessary for downstream intracellular signaling during BCR ligation [22-25]. As pro-B cells develop into pre-B cells, the heavy and light chains Ig gene undergo genetic rearrangement through V(D)J recombination [26, 27]. From this recombination process, immature B cells with IgM BCR expression are capable of binding to a diverse array of Ags; however, prior to exiting the BM the BCR must be tested to ensure no auto-reactivity [28]. Immature B cells with strong self-reactivity are not permitted to progress into mature naïve B cells co-expressing IgM and IgD to leave the BM, otherwise they either undergo clonal deletion through apoptosis or endure an additional round of receptor editing to reprogram the existing BCR [29].

1.1.1.3 Mechanisms of peripheral tolerance

Auto-reactive T and B cells can escape central tolerance and migrate to the periphery. Peripheral tolerance refers to the process by which the immune responses is regulated within secondary lymphoid organs and tissues after naïve T and B lymphocytes have undergone V(D)J rearrangement and present a mature TCR and BCR, respectively [21]. These mechanisms include 1) active suppression by specialized T_{REG} cells, 2) the generation of anergy by neglect, and 3) active deletion by apoptosis [30, 31].

1.1.1.3.1 Control of self-tolerance and immune homeostasis by FoxP3⁺ T_{REG} cells

T_{REG} cells are a specialized subset of CD4⁺ T cells involved in immune regulation, homeostasis, and immune tolerance, positioning them as the central master-switch of peripheral tolerance [30, 32]. Development of T_{REG} cells occurs in the thymus when TCR:MCH-II interaction with self-peptides expresses intermediate-high reactivity and therefore escapes negative selection. T_{REG} cells express the master-switch transcription factor Forkhead box protein 3 (FoxP3), comprising approximately 5-10% of all CD4⁺ T cells in mice and 1-2% in humans [32-38]. The expression of FoxP3 is induced through STAT5 signaling which is linked to the constitutive surface expression of interleukin (IL)-2 receptor (CD25) and the binding of IL-2, an indispensable cytokine for T cell activation, proliferation, differentiation, and function [38, 39]. FoxP3⁺ T_{REG} cells are essential in ensuring unresponsiveness of auto-Ags and regulating the size and duration of

inflammatory responses during pathogen clearance [40]. The suppressive function of FoxP3⁺ T_{REG} cells can be achieved through several mechanisms exploited in context-dependent settings in secondary lymphoid tissues and sites of inflammation [34]. They include 1) the production of anti-inflammatory cytokines IL-10, transforming growth factor (TGF)- β , and IL-35 [41], 2) metabolic disruption [42, 43], 3) cytolysis by producing pro-apoptotic proteins granzyme A/B and perforin [44], and 4) disruption of dendritic cell (DC) maturation and Ag-presentation cell (APC) function [45-47]. The details regarding these mechanisms of FoxP3⁺ T_{REG} cell suppression is outside of the scope of this Thesis.

Peripheral naïve CD4⁺ T cells TCR-activated in the presence of TGF- β and IL-2 have been shown to induce FoxP3 expression, thus allowing them to contribute to the regulation of emerging immune responses [38]. Since both express high levels of FoxP3, although with different kinetics and dynamics, distinct markers have been proposed to differentiate between thymic-derived T_{REG} (tT_{REG}) cells from peripherally-induced T_{REG} (pT_{REG}) including the transcription factor Helios [33].

1.1.1.3.2 Anergy and activation-induced cell death in T and B cells

In addition to FoxP3⁺ T_{REG} cells, peripheral tolerance is enforced through other means by anergy, clonal deletion, and BCR revision [48, 49]. Models of T cell anergy are either categorized as clonal anergy or adaptive tolerance/*in vivo* anergy. Clonal anergy arises from incomplete T cell activation in the absence of secondary signals [50]. CD4⁺ T cell activation is highly regulated, requiring three signals: 1) MHC-II:TCR binding, 2) co-stimulatory binding (ex. CD28:CD80/86, CD40L:CD40, ICOS:ICOS-L, etc.), and 3) cytokine production. These signals are vital for CD4⁺ T cell activation (signal 1), survival (signal 2), and differentiation (signal 3) [51]. In absence of these collaborative signals, naïve T cells will become refractory to subsequent Ag-TCR engagement [50]. This strategy is designed to prevent self-reactive CD4⁺ T cells from undergoing clonal expansion or premature T cell activation in the absence of inflammation [52]. Anergic B cells arise when there is continuous BCR binding with Ag, leading to unproductive BCR signaling and desensitization. B cell anergy can additionally be mediated by lack of co-stimulatory signaling, BCR editing to avoid self-recognition, clonal deletion, and receipt of anergy-inducing signals [53]. Once anergic, B cells are unable to elicit the help of T cells, are excluded from follicles in the germinal centres (GC), and therefore cannot differentiate into memory B cells or long-lived plasma cells (PC) [48, 54].

Programmed cell death, or apoptosis, is important in maintaining peripheral tolerance once auto-reactive immune cells are activated [55]. Engagement of the cell death receptor Fas (CD95) on T and B cells with Fas ligand (FasL) on APC's and cytotoxic CD8⁺ T cells is a key process in activation-induced cell death (AICD) [56-58]. AICD serves dual functions for maintaining cell homeostasis: 1) limits the expansion of reactive T cell clone after Ag clearance, and 2) inactivates auto-reactive T and B cells [56, 59].

Lymphocyte interactions with distinct Ags can engage multiple unique mechanisms that prevent potentially detrimental activation of these cells to self-Ags. Dysregulation of individual or multiple tolerance junction however lead to auto-reactivity [31].

1.1.2 BREAKDOWN OF IMMUNE TOLERANCE

While mechanisms involved in both central and peripheral immune tolerance are to ensure the identification and elimination of auto-reactive immune cells, the breakdown of these mechanisms results in pathogenesis of autoimmune disorders.

1.1.2.1 Defects in central tolerance

During the final stages of naïve T and B cell development in the thymus and BM, negative selection deletes potentially auto-reactive cells, thus limiting reactivity to self-Ags. Defects during the negative selection process of central tolerance development though bring rise to the escape of these cells [60, 61]. One instance of this defect is mutations in autoimmune regulator (AIRE), an important transcriptional regulator controlling the expression of tissue-restrict Ags in the thymus. Thymic escape of self-reactive T cells and defective FoxP3⁺ tT_{REG} cells therefore are associated with AIRE gene dysfunction [60, 62-64]. In addition, the repertoire of self-Ags in humans is extensive, and not all self-Ags are readily available for effective negative selection. This can sometimes cause the mechanisms of central tolerance to be “leaky” [65, 66], though these cells are typically controlled by mechanisms of peripheral tolerance.

1.1.2.2 Defects in peripheral tolerance

Peripheral tolerance ensures the prevention and suppression of auto-reactive T and B cells which have managed to escape the mechanism of central tolerance as reviewed [21, 29]. Like central tolerance, defects in peripheral tolerance can lead to the development of autoimmune disease. These could be caused from failure of FoxP3⁺ T_{REG} cells, abnormal expression of co-

stimulatory molecules, dysregulation of cytokine production, defects in peripheral clonal deletion and in some instances molecular mimicry [66-72].

1.1.2.2.1 Developmental, homeostatic, or functional deficits in FoxP3⁺ T_{REG} cells

FoxP3⁺ T_{REG} cells are the central mediator of immune suppression and have a key role in peripheral tolerance, as reviewed [30, 32], where dysregulation in their function will lead to autoimmunity [73]. An extreme example of ineffective FoxP3⁺ T_{REG} cell function is the immune dysregulation, poly-endocrinopathy, enteropathy, X-linked (IPEX) recessive disorder. Impairment of FoxP3⁺ T_{REG} cell function is caused by mutation within the FoxP3 master regulator protein, leading to systemic autoimmune disorders and primary immunodeficiency [74, 75]. Dysregulation of suppressor function are known to occur disorders such as multiple sclerosis (MS) and type-1 diabetes. These impairments may be caused from mutations in *ctla-4* and *cd25* genes, decrease production of IL-10, or from effects of pro-inflammatory cytokines secreted by CD4⁺ effector T (T_{EFF}) cells [76-78]. Additionally, ineffective immune regulation could be caused through failure to activate FoxP3⁺ T_{REG} cells [79]. FoxP3⁺ T_{REG} cells comprise of approximately 10% of all circulating CD4⁺ T cells [32-38], however in some autoimmune patients (ex. systemic lupus erythematosus, SLE), reduced levels of circulating FoxP3⁺ T_{REG} cells have been reported, which has been suggested to be caused by impaired proliferation of these cell due to decrease in CD25-dependent activation [79, 80].

1.1.2.2.2 Auto-antigen presentation on MHC-II risk alleles

Tissue damage in autoimmune disorders is caused by both auto-Abs and pathogenic CD4⁺ T_{EFF} cells. While CD4⁺ T_{EFF} cell responses may not be apparent in pathology, they are crucial for the production of auto-Abs through the CD4⁺ T-B cell crosstalk [81]. Autoreactive B cells, acting as professional APC's, can directly break CD4⁺ T cell tolerance by presenting auto-Ags with their MHC-II molecule [82]. Disease-predisposed MHC-II alleles (human leukocyte Ag, HLA, in humans and H2 in mice) have been implicated in presenting immunogenic auto-Ags to auto-reactive CD4⁺ T cells who have escaped central tolerance [83-85]. The interaction between TCR and MHC-II however can trigger autoimmune reactions in the absence of auto-Ags due to molecular mimicry resulting from viral infections [86].

1.1.2.2.3 Peripheral survival of auto-reactive lymphocytes

Abnormal expression of co-stimulatory molecules regulating lymphocyte activation have been linked in the activation and expansion of auto-reactive clones in some autoimmune disorders. These include CD28:CD80/86, CTLA-4:CD80/86, CD40L:CD40, PD-1:PD-1L, and ICOS:ICOS-L [67, 81, 87]. Dysregulated CD28:CD80/86 interactions between T-B cells have negative consequences, as CD28 promotes excessive proliferation and effector functions of CD4⁺ T_{EFF} cells. As a master-switch opposing CD28, CLTA-4 is a negative regulatory signaling molecule that interacts with CD80/86 to prevent excessive CD28 activity [88]. CD80/86 ligands on B cells have also been linked to autoimmune disorders, making B cells highly susceptible to pathogenic T cell influence [69]. Next, CD40:CD40L activity and expressions have been linked to multiple clinical settings and increased auto-Ab production [70]. Patients with renal-inflammatory glomerulonephritis (GN) have been reported to have increased expression levels of CD40L on CD4⁺ T cells which contributed to disease onset and severity [70, 71]. Likewise, inducible co-stimulation (ICOS) dysregulation can lead to autoimmune disorders, particularly when overexpressed on CD4⁺ follicular helper T (T_{fh}) cells as characterized in SLE patients with increased anti-dsDNA serum Ab production [72].

Defects in clonal deletion have been reported as a factor in defective peripheral tolerance [89]. Apoptosis deletes auto-reactive lymphocytes through AICD and T cell autonomous death (ACAD). During GC reactions, apoptosis can be triggered through the binding of the programmed death (PD)-1 receptor and PD-1 ligand (PD-1L) on T and B cells, respectively. The engagement inhibits over-activation and proliferation, with defects in this junctio linked to autoimmunity and is currently an active area of investigation [37, 90, 91]. Regardless of how immune tolerance is broken, auto-Abs are a common product from pathogenic CD4⁺ T-B cell interactions. As a major focus point for this Thesis work, it is important to understand how the T-B crosstalk influence CD4⁺ helper T (Th) cell differentiation and auto-Ab production mediating MCD pathogenesis.

1.1.3 ROLES OF CELLULAR RESPONSES MEDIATING AUTOIMMUNE DISORDERS

Once initial TCR activation and co-stimulatory binding occur, CD4⁺ T cells differentiate into effector Th cell subsets Th1, Th2, Th17, and T_{fh} cells (**Fig. 1, top**). The diversity in CD4⁺ Th cell subsets allow the immune system to mediate a response tailored to a particular infection. For

example, CD4⁺ Th1 cells defend against intracellular pathogens such as viruses by secreting interferon- γ (IFN γ), activating macrophages to enhance microbial destruction, and induce Ab secretion for complement activation [92]. Parasitic infections, allergy responses, and humoral immunity are mediated by Th2-mediated responses via IL-4, IL-5, and IL-13 [93, 94]. Lastly, Th17 mediated responses defend against extracellular bacteria and fungi with secreted IL-17A [92]. The cytokine milieu at the time of B cell activation is vital in influencing the type of humoral responses and will be discussed in greater detail [95].

1.1.3.1 Lineage-committed differentiation of auto-reactive CD4⁺ Th cells

CD4⁺ Th cell subsets are characterized by their master regulator expression and response type; this lineage differentiation is highly influenced by the cytokine signals they received during initial TCR activation [96]. IFN γ and IL-12 control Th1 lineage differentiation, Th2 differentiation is mediated by IL-4, Th17 from exposure to TGF- β plus IL-6, IL-21, and IL-23 in the absence of IL-12 and IL-4 cytokines influencing Th1 and Th2 lineage differentiation, and lastly IL-6 and IL-21 mediating Tfh cell lineage fate (**Fig. 1, top**) [97]. These cytokines mediate lineage differentiation is through the binding of their respective Janus kinase-signal transducer and activator of transcription (JAK-STAT) pathway. Signals are transferred from cell-membrane receptors to the nucleus to collaborate with master transcription factors T-bet (STAT1/4), GATA3 (STAT5/6), ROR γ t (STAT3), or Bcl-6 (STAT3) involved in lineage differentiation of Th1, Th2, Th17 and Tfh cells, respectively [98-102].

1.1.3.2 CD4⁺ Th1 and Th17 cells: key mediators of autoimmunity

CD4⁺ Th1 and Th17 cells have been well documented in the development of organ-specific and systemic autoimmunity such as rheumatoid arthritis (RA), SLE, and MS, through production of pro-inflammatory cytokines and interactions with B cells [103, 104]. Th1 cell-derived IFN γ is a potent factor in cell-mediated immunity recruiting CD8⁺ cytotoxic T cells, causing direct cell destruction and delayed-type hypersensitivity reaction [105]. Binding of Th1-secreted IFN γ to auto-Ag presenting B cells promotes GC reactions, which in turn leads to class-switching and production of IgG auto-Abs involved in complement fixation, Ab-opsonization, and Ab-dependent cell cytotoxicity (ADCC) [106]. In autoimmune disorders where B cells play a role in pathology, such as SLE, IL-4, IL-13, and IL-17A co-produced from CD4⁺ Th2 and Th17 cells have been shown to

induce pro-inflammatory responses [107]. While Th2-secreted IL-4 and IL-13 have strong associations with high-affinity B cells responses and class-switching fate [108], the role of IL-17A as a B cell helper for strong proliferation, Ab maturation, and GC formation is a well-studied mediator in autoimmune disorders [109]. The Th17/T_{REG} cell balance is crucial, as they mediate opposing immune function, and both subsets share a common signaling pathway mediated by TGF- β [110]. Th17 cells produce pro-inflammatory cytokines to recruit innate cells and promote tissue inflammation, while FoxP3⁺ T_{REG} cells secrete anti-inflammatory cytokines to suppress effector responses [111]. This balance however can be disruption through many factors, as mentioned in previous sections describing mechanisms involved in the break of peripheral tolerance. This disruption can lead to an increase in Th17 cell function and reduction in T_{REG} cell activity [111, 112].

The initial activation and differentiation signals for auto-reactive B cell are provided by CD4⁺ Tfh cells and subsequent re-activation of humoral response can be mediated via other CD4⁺ Th cell subsets [95, 113]. This interaction will be described in greater detail to better understand how the resulting humoral responses mediate autoimmune renal disorders.

1.1.4 ANTIBODY-MEDIATED AUTOIMMUNITY

The T-B cell crosstalk refers to the bidirectional communication between CD4⁺ T cells and B cells, essential for the generation of a robust immune responses against pathogens (**Fig. 2**). This interaction is a complex process involving multiple signaling pathways with physical and soluble interactions received by both lymphocytes. In response against pathogens and or in accidental reactivity to self-Ags, this interaction dictates GC formation and B cell differentiation to high-affinity Ab-secreting long-lived PC and memory B cells [11, 12].

1.1.4.1 Auto-antigen presentation to CD4⁺ T cells by B cells

Due to the nature of effector responses by T cells after activation, TCR ligation requires the corresponding Ag to be presented on MHC molecules. For the purpose of this Thesis, the focus is on CD4⁺ T cell TCR binding to Ags presented on MHC-II [114]. For CD4⁺ T cell TCR ligation, Ag from typically extracellular pathogens are captured, internalized, and processed on MHC-II molecules [115]. The mechanisms underlying the generation and MHC-II presentation of auto-Ags are of considerable interest in autoimmune research. It could be as simple as self-Ags stochastically

obtained by DC's during an incident of cell destruction (ex. allergies, viral infections, physical tissue trauma, transplantation, etc.) and presented to auto-reactive CD4⁺ T cells [116]. In other incidences, viral Ags triggered auto-reactive immune cells through molecular mimicry or bystander activation when engrossed in a pro-inflammatory environment [67, 86, 117]. There are also examples of Ag discordance when T cells and B cells may be activated by the same Ag but immunogenic recognition may differ based on TCR/BCR specificity and how the Ag was processed for MHC-II presentation [118]. Once TCR:MHC-II ligation is confirmed, activated pathogenic CD4⁺ T cell are then able to proliferation and differentiation into their distinctive helper subsets [115].

1.1.4.2 CD4⁺ Tfh cells: key drivers of humoral responses

CD4⁺ Tfh cells are a specialized subset of CD4⁺ Th cells with a critical role in humoral responses by providing essential activation signals to B cells for their activation, differentiation, and maturation into memory B cells and Ab-secreting PCs during GC reactions [119]. Characterized by their expression of the B cell lymphoma 6 (Bcl-6) transcription factor triggered through the Jak-STAT3 pathway (**Fig. 1, top**), Tfh cells are primarily found in the GC within lymphoid tissues. Tfh cells express high levels of the chemokine receptor CXCR5, allowing them to migrate into the follicular zones of lymphoid organs, where they interact with follicular DCs (FDCs) and B cells [119]. They also express high levels of PD-1, ICOS, and CD40L, in addition to secreting IL-21, which are critical for their interaction with B cells and for the regulation of the GC reaction [120].

Dysregulation of Tfh cell function has been implicated in various autoimmune and inflammatory diseases, as well as in the pathogenesis of some infections [121]. For example, overexpression of ICOS binding to B cells could lead to increased auto-Ab production as characterized in SLE patients with increased anti-dsDNA serum Ab production [122]. Overproduction of IL-21 has been linked to renal diseases and early mortality. In order to combat this, interventions to disrupt the ICOS:ICOS-L interactions have been studied and while they are successful, they also negatively affect general humoral responses [72].

1.1.4.3 Auto-antigen ligation, pathogenic B cell activation, and auto-antibody production

Conventional B cells are vital as they provide immune protection via humoral and memory responses [123]. The humoral response relies on Abs directed against specific Ags and are secreted by long-lived PC. The memory response is mediated by Ag-primed memory B cells held in reserve

within the GC's of the lymphatic system, and are reactivated with Ag re-exposure [123]. Both responses are mediated through membrane-bound (BCR) or secreted (Ab) Ig molecules [124, 125]. Regardless of the form, Ig are heterodimeric proteins comprised of two heavy chains and two light chains [25, 126]. The heavy chains (constant regions, Fc) distinguish the Ig class-type, providing diversity in responses against pathogens and disease progression [125, 127, 128]. The light chains (variable regions, F(ab)₂) give binding-specificity and binding-affinity to target Ags [129]. Crucial in the generation of high-affinity Ab production, FDCs capture and retain foreign and self-Ags on their surfaces for presentation to B cells in the GC (**Fig. 2**) [130]. This interaction with the GC B cells modulates the clonal diversity through permissive selection. Unfortunately, this could give rise to auto-reactive B cell clones through epitope spreading [131]. Epitope spreading is a phenomenon that occurs during an immune response in which new immune responses are generated against epitopes not originally targeted by the immune system; it also provides an opportunity for auto-Ag recognition and auto-reactivity [132]. Overall, epitope spreading is a complex process that involves the activation of new immune responses against previously unrecognized epitopes by auto-reactive lymphocytes who have escaped central tolerance [132].

The differentiation of naïve B cells to memory B cells and long-lived PCs and thus the overall shaping of humoral responses against foreign or self-Ags are typically dependent on the CD4⁺ T-B cell crosstalk. Thus, we will next review where in the secondary lymphoid organs and GC these interactions take place and how these interactions influence the type of humoral response to better characterize this process during renal autoimmune onset and progression.

1.1.4.4 GC reactions: CD4⁺ T cell-dependent B cell activation & plasma cell differentiation

The lymphoid structure can be broken down into four zones: 1) the T cell-rich zone, 2) B cell-rich follicles within the T cell zone, 3) the GC which form within the B cell follicle during Ag-ligation to BCRs, and 4) the PC-rich zone [133, 134]. It is generally accepted for the successful GC formation signals need to be provided from 1) the engagement of Ag to naïve B cells and 2) Ag presentation from activated B cell to CD4⁺ Tfh cells (i.e. the T-B cell crosstalk) [135]. This can be referred as a two-phase response (**Fig. 2**).

Upon Ag recognition, activated lymphocytes travel to secondary lymphoid organs through specialized high endothelial venules, where GC structures are formed [136, 137]. GCs are critical

sites of Ab affinity maturation, and PC and memory B cell generation [138, 139]. GC reactions are associated with T cell-dependent activation of B cells when they congregate at the T cell zone-B cell follicles boundary and are engaged in T-B cell interactions [138]. B cells receiving strong BCR signaling will rapidly proliferate, forming the dark zone (DZ) of the GC. This signaling strength is dependent on downstream phosphoinositol 3-kinase (PI3K) signaling initiated with CD19 binding and enhanced by co-stimulatory signals from CD40 and ICOS-L binding with activated CD4⁺ Tfh cells [140, 141]. B cells receiving weaker BCR signals quickly differentiate into extrafollicular short-lived PCs secreting low-affinity IgM, mounting a quick primary immune response [142]. Continuing within the DZ, the BCR's undergo somatic hypermutation (SHM) of the Ig variable region genes via the enzyme activation-induced cytidine deaminase (AID) causing point mutations in the genes to increase affinity-binding [143-145]. Afterwards, with the aid of their surface CXCR5, the B cells turned centroblasts will follow a CXCL13 chemokine gradient to the light zone (LZ) of the GC. It is here where B cells must out-complete other BCR clones to interact with Ag-primed CD4⁺ Tfh cells; BCR clones with increased Ag binding affinity are selected, survive, and undergo differentiation into long-lived PCs and memory B cells [143]. Additional edits of the BCR's can be performed in the LZ through class switch recombination (CSR), resulting in isotype switching of the Fc heavy chain from IgM to IgG, IgA, or IgE [146]. Centroblasts whose BCRs were not selected can re-enter the DZ to undergo supplementary SHM recombination to improve BCR-Ag affinity, otherwise, non-improved BCR maturation or auto-reactive BCR's undergo negative selection through apoptosis [147, 148]. Finally, high-affinity long-lived PC or memory B cells expressing a non-switched (IgM) or isotype-switched (IgG, IgA, or IgE) BCR receive signals to exit the GC and reside in the BM, mobilizing humoral and cellular responses (**Fig. 1, bottom**) [149].

1.1.4.4.1 B cell activation – Memory B cells

After a primary immune response against an Ag has resolved, Ag-primed memory B cells are kept in reserve within the lymphoid organs, particularly the spleen, in a quiescent state. This reserve allows for a quicker and stronger response against Ag re-exposure [150, 151]. Upon re-activation, memory B cells will differentiate in GC B cells once again, undergoing BCR modifications to further increase Ag affinity, and differentiate into PC [123]. While high-affinity IgG⁺ memory B cells tend to be retained over IgM⁺ cells [152], IgM⁺ memory B cells are able to provide immediate

protection against reoccurring pathogens [153], whereas IgG⁺ memory B cells tended to be fated towards PC differentiation [154]. T cell-dependent differentiation of PCs can be followed by the expression of surface markers CD20 and CD138 as indicated in **Fig. 1 (bottom)** [155]. Utilization of these markers provide a valuable tool to map-out how memory B cell activity and PC differentiation mediate autoimmune disorder pathology.

1.1.4.4.2 B cell activation – high-affinity auto-antibody secreting plasma cells

Residing in the BM, PC are the main cells responsible for humoral immunity, secreting high-affinity Abs [156]. Abs impose their effector function to their target Ag, cell, or tissues in four distinct actions: 1) neutralization, 2) opsonization by macrophage ingestion, 3) ADCC, and 4) complement activation and stimulation of effector responses through exposed Fc region binding [157].

In conjunction with binding-affinity influencing Ab function, the Ig constant chain isotype mediates the type of humoral response against a target Ag [150, 158-160]. Secreted in early response by short-lived PC, low-affinity IgM Abs are highly effective in activating the complement system due to their pentameric shape [161]. Next, as the principle secreted Ab, IgG is secreted in the serum, extracellular fluid, and deposited in target tissues with efficiency in pathogen opsonization and complement activation [126, 162]. For mucosal immunity, the dimeric IgA accumulates in mucosal secretions and in breast milk for passive immune transfer [163-165]. Due to their dimeric shape, IgA cannot activate the complement system effectively, rather they function through neutralization of pathogen. Lastly, commonly associated in allergic reactions, IgE binds to mast cells to release powerful chemical mediators causing allergy responses [126, 166]. The IgD isotype is the only Ig subclass which does not have a secreted form. Remaining membrane-bound on naïve B cells, it is typically co-expressed with IgM prior to Ag stimulation [167]. Recently, it has been experimentally shown in C57BL/6 (BL/6) mice that IgD-deficiency leads to accelerated B cell responses and inability to control subsequent affinity maturation and Ab production. This highlighted the essential regulatory role of IgD in the activation of naïve mature B cells to switched/non-switched mature B cells [168]. The Ig subclass secreted in response against a pathogen is heavily influenced by signals provided through the CD4⁺ T-B cell crosstalk, especially by cytokines produced from the CD4⁺ Th cells (**Fig. 2**). Cytokines can promote or inhibit the initial

germline transcription of the selected heavy chain exon, depending on the cytokine-responsive promoters, and thus the production of a particular Ig [95]. For example, IFN γ enhances secretion of IgG2a and prevents switching to IgG1, IgG2b, IgG3 and IgE in mice, IL-4 promotes class-switching to IgG (e.g. non-complement neutralizing IgG4 in humans or IgG1 in mice) and IgE while inhibiting IgA, TGF- β induces IgG2b (in mice) and IgA, IL-10 increases IgA, and IL-2 increases secretion of IgM and IgG [95, 169, 170].

Lastly, immune complexes (IC) can be subjected to humoral-mediated responses mentioned including complement activation, opsonization, and neutralization [171]. In a way, IC bridges humoral and cellular responses upon ligation of the Ab Fc region to Fc receptors (FcR) expressed on immune cells and some non-immune cells, including podocytes [172-174]. The subclass of FcR expressed is based on the type of Ig isotype they recognize and their signaling properties: Fc γ R recognize IgG, Fc α R to IgA, Fc ϵ R binding IgE, and Fc μ R to IgM [173]. The most common signaling function of FcR's is the activation of phagocytosis/endocytosis in order to internalize Ab-coated Ag for destruction or MHC-II processing [175]. Furthermore, FcR engagement on leukocytes can trigger a signaling cascade to initiate production of various pro- and anti-inflammatory cytokines, in conjunction with other modulatory mechanisms of the adaptive immune response [173]. FcR are also involved in the last Ab function mentioned which is ADCC. This triggered with Ag-Fc:FcR binding on Natural killer cells, stimulates release of cytotoxic molecules from granules, lysing Ab-covered target cell [157, 176].

A characteristic autoimmune disorders share is the increased levels of auto-Abs, whether they target a particular cell type, organ, or cause destruction systemically. Up to this point, various mechanisms and interactions that can lead to a breakdown of tolerance have been discussed. These can occur at the T cell level and B cell levels, either centrally or peripherally, as well as at various junction points during the T-B cell crosstalk. Regardless of the cause, for which is still a major point of inquiry for various autoimmune disorders, they result in the production of auto-Abs. In this Thesis research, we aim to understand if and how auto-Abs may influence renal autoimmune disorders and an insight into MCD pathology.

1.2 RENAL AUTOIMMUNE DISORDERS

Autoimmune responses can play a significant role in the development of glomerular disorders, which are a group of diseases that affect the tiny blood vessels in the kidneys called glomeruli. In these disorders, the immune system attacks the glomeruli, causing inflammation and damage [13]. There are several ways in which autoimmune responses can lead to glomerular injury. For example, they can develop as a consequence to pre-existing autoimmune disorders such as lupus nephritis (LN) and RA, formation and glomerular deposition of auto-Ag IC's causing inflammation (e.g. LN and IgA nephropathy), direct damage of the GBM by anti-GBM auto-Abs, and Ab-mediated kidney transplant rejection [177-182]. Understanding how auto-reactive immune responses are mediating glomerular disease is vital to further develop specialized treatments.

1.2.1 KIDNEY ANATOMY

Located in the abdomen, the kidneys play a unique and central role in preserving our physiological well-being. The kidneys' primary function is to remove toxic metabolic waste and excess water from the blood, maintain salt balance all the while preventing excretion of essential proteins, sugars, and amino acids [183], in addition to secondary functions including regulation of body pH, production of hormones through the endocrine gland, and gluconeogenesis [183, 184]. Kidney structure can be defined by two sections: the cortex (outer region) and the medulla (inner region). Both regions are comprised of nephrons, blood vessels, lymphatics, and nerves. Blood to be filtered is supplied into the kidneys by the renal artery, branching into the medulla and medulla pyramids. They progressively branch into the glomerular capillaries, forming a secondary network to supply unfiltered blood to the nephron (**Fig. 3**).

1.2.1.1 Nephron anatomy and function

The functional unit of the kidneys are the nephrons, with each kidney containing 1-1.5 million units [183]. Pre-filtered blood from the renal artery enters the nephron at the renal corpuscle, the proximal component of the nephron consisting of the glomerular capillaries (tuft) encompassed in the Bowman's capsule (**Fig. 3**) [185]. Here, the blood is subjected to ultrafiltration before leaving the renal corpuscle through the efferent arteriole. Waste filtered from the blood enters the urinary space of the Bowman's capsule and from there it descends into the medulla via

the proximal tubule, to the loop of Henle in the inner medulla, and ascends out of the medulla towards the collecting ducts via the distal tubule [183]. This juxtamedullary structure of the nephron creates an environment for the concentration of urinary components within the medulla and then expelled. While the filtration functions are fundamental in the reabsorption of most of the water, nutrients, and salts from the ultrafiltrate and regulating the final acid-base balance [183, 186], the details are outside the scope of this Thesis work.

1.2.1.2 Glomeruli – The filtration unit of the kidneys

At the proximal end of the nephron, located in the cortex, are the glomeruli. They are the filtration unit of the kidneys containing the glomerular tuft enclosed with the Bowman's capsule [187]. The glomeruli typically filters a collective 90-120ml/min/1.73m² of blood, removing toxins, urea, and other small molecule into the Bowman's space to be later modified in the tubules into urine [187]. The filtration barrier of the glomeruli is comprised of fenestrated endothelial cells, the proteinaceous charged GBM, and interlocking podocytes (**Fig. 4**). Together, these three major components collaborate to form a size- and charge-selective filtration barrier, permitting urea and other small molecules into the Bowman's space to then be excreted [183, 188, 189].

1.2.1.3 Podocyte anatomy and function

Podocytes are terminally differentiated specialized epithelial cells with three distinct structural elements: 1) a large cellular body, 2) major extending process, and 3) foot processes [190]. To adhere to the GBM, podocytes utilize transmembrane adhesion receptors, cell-cell, and cell-matrix adhesion which have recently been reviewed elsewhere [191, 192]. While the cytoskeletal morphology of podocytes is what maintains the kidney filtration barrier, it is the foot processes that allow for glomerular ultrafiltration [193]. To build the filtration barrier, podocytes wrap their foot processes around the glomerular capillaries (**Fig. 3 & 4**). Adjacent foot processes interlock with neighboring podocyte's foot processes, forming an intercellular junction known as the slit diaphragm [188, 194-196]. A major constituent of the slit diaphragm is nephrin (*NPHS1*), a podocyte specific transmembrane protein which, which generate nephrin-nephrin homotypic interactions between adjacent foot processes as seen in **Fig. 4** [194, 197]. Belonging to the Ig superfamily, nephrin regulates a diverse group of signalling processes controlling podocyte cell adhesion, cytoskeletal arrangement, survival, lamellipodia formation for cellular migration, and

endocytosis after tyrosine-phosphorylation by the Src-family kinase Fyn. Phosphorylation of nephrin's intracellular domain provides a scaffold for signaling protein recruitment and downstream signalling [198, 199]. Due to the incredibly vital role in the filtration function of podocytes, mutations in *NPHS1* causes congenital nephrotic syndrome of the Finnish type, an autosomal recessive disease characterized by podocyte foot process effacement and massive proteinuria shortly after birth [200, 201]. Other impairments of nephrin signaling and filtration function can lead to kidney disease and defective kidney function and has been prominently studied in glomerular disease.

1.2.2 GLOMERULAR AUTOIMMUNE DISEASE

Glomerular disorders comprise a family of kidney diseases where damage to the glomerular filtration barrier impedes the kidney's ability to properly filter blood. This damage leads to hematuria (blood in urine), proteinuria (protein in urine), edema (water retention), poor blood pressure control, and dyslipidemia. If left untreated, glomerular diseases can progress into end-stage renal disease requiring life-long dialysis or eventual kidney transplantation. There are two distinct forms of pediatric glomerular diseases, inflammatory nephritic disease and non-inflammatory nephrotic disease [202].

1.2.2.1 Inflammatory nephritic versus non-inflammatory nephrotic syndromes

Nephritic syndrome, or GN, is characterized by robust glomerular inflammation, hematuria, and mild non-nephrotic-range proteinuria (e.g. <3.5 gm/day) [203]. The cause of GN can occur following infections such as strep throat (proliferative GN) and upper respiratory tract infections (Henoch-Schönlein purpura), or arising as a consequence of autoimmunity such as lupus GN, IgA nephropathy, membranoproliferative GN, anti-neutrophil cytoplasmic Abs (ANCA)-associated GN, anti-GBM disease [203, 204]. Largely Ab-mediated, deposition of auto-Abs along the GBM activates the complement system which in turn recruits inflammatory CD4⁺ T_{EFF} cells and cell-destructing innate immune cells, leading to GBM disruption and damage to podocyte cellular layer [204].

While some characteristics are shared between the two glomerular disease types including edema and podocyte injury, the main differences between nephritic and nephrotic syndromes (NS) are the lack of inflammation, hematuria, low blood albumin levels (hypoalbuminemia), and

increase in protein leakage (>3.5 gm/day) in the latter [205]. NS can be caused in children through different means, such as genetics, other diseases or infections, and medications [206]. Congenital NS, also known as Finnish-type NS, is an autosomal recessive disorder with a high infant mortality rate. Mutations are commonly observed in the *NPHS1* or *NPHS2* genes (chromosome 19) which transcribe for nephrin and podocin, respectively. As key components of the podocyte slit diaphragm, mutations lead to the development of tubular dilation, variable mesangial sclerosis, no Ig deposition, and podocyte foot process effacement [201, 207]. Case studies have indicated NS can be associated with other disorders such as Henoch-Schönlein purpura, SLE, and blood cancers (leukemia and lymphoma), infections from hepatitis B, human immunodeficiency virus (HIV), malaria, and from the use of certain medications, linking the immune response to secondary NS [206]. The most common form of NS in children is primary or INS, with over 90% of young pediatric glomerular disease cases and between 15-30% of adult cases [208].

1.2.2.2 Idiopathic nephrotic syndrome (INS)

INS is a spectrum of rare relapsing-remitting primary glomerular disease with unknown etiology, characterized by the triad of edema, proteinuria, and hypoalbuminemia [208, 209]. Currently, first-line of treatment for INS includes immunosuppressive therapy with glucocorticoids (GC) and GC-sparing cyclophosphamide which is successful in establishing remission in 80-90% of pediatric patients for a short period of time [5, 6, 210-213]. Unfortunately, majority of patients who have gone into remission will relapse (75-80%), with 40-50% of those individuals having multiple relapses (steroid-dependence), running the risk for severe consequences including steroid toxicity, susceptibility to systemic infections, and other serious side effects [210, 211, 214, 215]. While the pathophysiology of INS remains unclear, evidence collected from case studies, responsiveness to immunosuppressive treatments, and experimental research strongly suggests an immunological link [216]. Clinical manifestation of INS can be presented in the histological forms of MN, FSGS, and MCD, with approximately 2-17/100,000 incidences of pediatric INS per year [1-3].

1.2.2.2.1 Membranous nephropathy (MN)

MN is an Ab-mediated autoimmune renal disorder affecting less than 5% of pediatric patients [217]. Targeting phospholipase A2 receptor 1 (PLA2R1) and thrombospondin type-1

domain containing protein 7A (THSD7A), granular pseudo-linear IgG auto-Abs deposition occurs along the outer GBM wall, causing the thickening of the glomerular capillary walls [217-220]. This deposition triggers the second hallmark of MN pathology which is the activation of the classical (dominant), alternative, and lectin complement pathways, disrupting podocyte structure morphology and inducing proteinuria [221].

1.2.2.2.2 Focal segmental glomerulosclerosis (FSGS)

Another cause of pediatric INS is FSGS, making up to 20% of pediatric cases [222, 223]. FSGS is characterized histologically by partial scarring (segmental) in majority of glomeruli (focal), altering glomerular permeability, leading to massive proteinuria, and declining renal function over time [224]. As a result of this, FSGS is the most common cause of end-stage renal failure of INS, leading to kidney transplantation [222, 224]. Like other INS histological forms, while the cause of FSGS remains unknown, there is evidence of an immune link to FSGS pathology. For example, it has been observed in renal transplant recipients with a history of FSGS the re-occurrence of FSGS as early as a few hours post-transplantation, strongly suggesting permeating soluble factors (cytokines) causing podocyte foot effacement and proteinuria [225]. The theory of soluble factors influencing glomerular injury was supported through exposure *in vitro* and *in vivo* animal studies using serum from FSGS positive patients and their capacity to increase glomerular permeability [225]. Recent immunofluorescent (IF) staining of adult patient renal biopsies revealed IgM deposition of C3 activation in the sclerotic areas of secondary FSGS patients [226], giving rise of possible anti-glomerular auto-Ab responses aiding in disease progression and severity.

1.2.2.2.3 Minimal change disease (MCD)

The most common form of INS in children is MCD, representing up to 85% of cases in pediatric patients [4]. Pediatric MCD diagnosis is confirmed of every 2-7 per 100,000 cases, affecting a higher ratio of males to females (2:1), and having a higher prevalence in children under the age of 5 [227]. While pathophysiology of INS remains unclear, MCD was and still is regarded as an immunological enigma showing no clear evidence inflammation, immune cell infiltration or Ab deposition within the kidneys [4, 7]. Additionally, unlike FSGS and MN, morphological changes are not observable under bright light microscopy, only by electron microscopy severe podocyte injury is visible, hence the name Minimal Change [228].

1.2.3 EVIDENCE OF IMMUNE CELL INVOLVEMENT IN MCD PATHOLOGY

In the last decade, there has been increased frequency of cases studies and research studies being released giving compelling evidence of T and B immune cell involvement in the pathology of MCD.

1.2.3.1 Historical evidence of T cell activity in MCD

It was postulated that MCD is T cell-mediated based on four main clinical observations: 1) a natural remission of MCD following a natural measles infection-induced cell-mediated immunosuppression, 2) MCD may occur in cases of T cell lymphomas, 3) responsiveness to immunosuppressive drugs such as GC's, and 4) co-occurrence of MCD with atopic diseases have been reported (**Fig. 5, left**) [7, 208, 229]. It was proposed that inflammatory cytokines like tumor necrosis factor (TNF)- α , soluble IL-2R, IL-4, IL-5, IL-9, and IL-13, produced by abnormal CD4⁺ T cell populations can trigger glomerular podocyte injury as serum from nephrotic patients and can induce proteinuria in healthy rodents [229, 230]. Specifically, evidence of the CD4⁺ Th2 cell-associated cytokine, IL-13, may directly lead to morphological changes in podocytes, coinciding with case studies of patients in sustained remission showing significant decrease in IL-13 [229, 231].

Furthermore, a group developed a humanized NOD/SCID BALB/c mouse model of FSGS and MCD describing the induction of disease after adoptive transfer of peripheral blood mononuclear cells (PBMCs) or CD34⁺ stem cells from MCD patients. Additionally, those transferred CD34⁺ stem cells from MCD patients differentiated into T cells [228]. In other autoimmune disorders such as GN and LN, though they are inflammatory disorders, it has been reported IL-17 produced from CD4⁺ T_{EFF} cells (i.e. Th17) promoted renal impairment by supporting self-reactive B cell survival, differentiation and Ab secretion, promoting inflammation in infiltrated tissues [232, 233]. When studying CD4⁺ T cell subset populations in adult MCD patients, an imbalance in the Th17/T_{REG} cell subset ratio was reported. In ongoing adult MCD patients, there was a skew towards a higher Th17/T_{REG} cell ratio with a reset back to normal ratios post-GC treatments, leading researchers hypothesizing Th17 may be a strong driver of steroid resistance NS and have influence on resistance to GC treatment [234, 235]. With accumulating evidence of dysregulated CD4⁺ T_{EFF} cell subsets and functions, FoxP3⁺ T_{REG} cell function was analyzed. In case studies with GC-resistance

adult MCD patients experiencing early relapse, it was revealed FoxP3⁺ T_{REG} cell populations were lower than compared to MCD patients in sustained remission and healthy controls (**Fig. 5, left**), therefore FoxP3⁺ T_{REG} cell levels could possibly predict early relapse [231, 236]. After additional treatment with other immunosuppressant drugs such as rituximab (RTX), FoxP3⁺ T_{REG} cells frequencies increased, and majority of patients (70%) sustained long-term remission [237, 238].

1.2.3.2 Emerging evidence of B cell involvement in MCD

RTX, a B cell-specific chimeric monoclonal anti-CD20 Ab, has recently been utilized and successful in promoting prolonged remission in MCD patients, suggesting an important role for B cells in pathogenesis (**Fig. 5, right**) [7, 239-241]. This is significant as pathogenic B cells have the dual capability of 1) orchestrating CD4⁺ T cell activation and differentiation through Ag presentation and pro-inflammatory cytokine production, and 2) differentiating into PC to produce and secrete auto-reactive Abs [241, 242]. Our lab demonstrated while RTX therapy of pediatric INS patients mediates a strong shift in the B cell profile towards immature phenotypes following complete ablation, the resurgence of isotype-switched memory (SM) B cells was often correlated with proteinuric relapses. Additionally, evidence obtained by flow cytometry revealed hyperactive B cell responses in patients during disease relapse characterized by atypical B cells (**unpublished data**). In various other autoimmune disorders, pathogenic memory B cells have been linked to the dysfunction of FoxP3⁺ T_{REG} cell suppressor mechanisms [243]. This has led to inquiries if recurrence of pathogenic memory B cells in relapsing MCD patients may also be linked to FoxP3⁺ T_{REG} cell dysfunction. In studies with GC-resistant patients post-RTX treatment, low FoxP3⁺ T_{REG} cell populations and IL-2 and IFN γ levels have been reported [231, 236]. Thus, it is essential to gain a better understanding of INS by investigating the CD4⁺ T-B cell crosstalk during disease progression. This is particularly important given that evidence suggests a T cell origin and the effectiveness of RTX treatments points towards a B cell involvement.

In the last couple of years, new evidence has surfaced strengthening the theory of a B cell role in MCD pathogenesis [8]. In MCD, auto-Abs were generally not thought of as a factor in disease progression as Ab deposition was not observed in renal biopsies [8]. Recent case studies in adult and pediatric MCD patients however indicated incidences of Ig levels predicting MCD onset or relapse (**Fig. 5, right**). Indeed, auto-reactive IgG and IgE are predictive risk factors in some cases of

adult MCD prior to renal biopsy [244]. Moreover, auto-reactive IgM positive adult patients with MCD have been reported to have higher frequency of relapse compared to MCD patients not displaying these auto-Abs [245]. In some cases, patients present uncommon symptoms of NS (i.e. superimposed MCD) with IgA-mediated nephropathy characterized by nephrotic-range proteinuria and extensive foot process effacement [246]. More impressively, a report was released documenting approximately 20% of relapsing adult MCD patients had detectable levels of anti-nephrin auto-Abs in their serum, with weak IgG deposits along the glomerular capillary wall [10]. After the release of that study, more reports of serum anti-podocyte auto-Abs targeting annexin A₂, vinculin, myosin-9, Crb2, and others in INS were published [247-249]. As such, these observations suggest the role of auto-Abs, while not a hallmark of pediatric MCD, may be underestimated. Further characterization of the role of B cells – in both their Ag-presenting capacity and their recognition of auto-Ag – is warranted in this disease.

1.2.4 MURINE MODELS OF NEPHROTIC SYNDROME TO STUDY THE CD4⁺ T-B CELL CROSSTALK

Recently, a review was released recapping INS case studies post-RTX treatment which have observed a decrease in the Th1/Th2 and Th17/Treg ratios, production of IL-4-, IL-13 (Th2-associated cytokines), and IL-5, and an increase in soluble CD40L shed by activated T cells [250], which are consequences linked to dysfunction of the CD4⁺ T-B cell crosstalk [251]. As convincing as all these findings are in strongly suggesting the CD4⁺ T-B cell crosstalk could be involved in MCD pathology, they do not show where and how these interactions are taking place. Since CD4⁺ T-B cell interactions cannot be observed in PBMCs obtained from human patients, as these interactions take place in the secondary lymph nodes (LN), it is imperative that immune-mediated *in vivo* models be developed to study these interactions.

1.2.4.1 Limitations of current murine models

Currently, there are rodent models capable of mimicking some aspects of MCD-like injury either through animal strains possessing a genetic susceptibility or using podocytopathic agents ultimately yielding nephrotic-range proteinuria (summarized in **Table 1**). The most commonly used model of induced proteinuria to study MCD was the puromycin aminonucleoside nephrosis (PAN) model in rats [252]. While severe proteinuria and classical histology features of MCD can be obtained with a single injection of puromycin aminonucleoside, there is a limitation to the model.

This included a dose-dependent effect on GC-sensitivity and this model often resulting in FSGS due to direct podocyte injury [252, 253]. The other commonly used model of podocytopathy is injections with lipopolysaccharide (LPS), activating immune responses through toll-like receptor (TLR) activation [253, 254]. However, proteinuria levels tends to be mild and developed systemic or septic effects with the use of LPS [252]. Another common chemical-induced proteinuria model is the Adriamycin (ADR)-induced nephropathy model with a single high dose of ADR being sufficient to induce proteinuria in rats and mice [255]. The major limitation of this model for MCD analysis is there is a dose-dependent toxicity as proteinuria and injury tends to progress to FSGS-like injury, has pleiotropic effects on podocytes, and murine strain susceptibility is severely limited to those like BALB/c [256-260]. While no longer used as a model of MCD, protamine sulfate nephropathy was used to study molecular changes associated with reversible transient foot process effacement in rats and mice [252, 259]. To summarize, there are histologically MCD- and FSGS-like injury models induced chemically or using sheep anti-rat whole glomerular nephrotoxic serum in mice which can promote proteinuria and classical injury morphology. These methods differ from human pathology overall as induction may be dose-dependent, have an effect on GC-sensitivity, or be independent of the complement system, leukocytes, or fibrin during heterologous phase [252].

In 2018, Takeuchi *et al.* utilized anti-nephrin Abs, which led to the induction of proteinuria 24-hrs post-injection in transgenic BL/6 mice. These mice exhibited injury resembling FSGS with a brief initial phase of MCD-like injury prior to progressing into FSGS [261]. However, these are models for FSGS, which have a different model of mechanism for podocytopathy than MCD (i.e. C3 complement with IgG deposition with glomeruli scarring), and they still bypass the initial immunological responses for which Abs are produced after B cell activation. To comprehend how the activation of immune responses leads to proteinuria with MCD-like injury, a model where podocyte injury is immune mediated is vital.

1.2.4.2 Experimental autoimmune nephrotic syndrome (EANS) model

Recently, our collaborators in Japan released a study describing a novel murine model of podocyte injury, immunizing C3H/HeN (C3H) mice with recombinant form of the Crumbs and Par (apical complexes) and Scribble (basal complex) extracellular domain (rCrb2) emulsified in

TitreMax Gold (TMG) adjuvant [249]. Crb2 is a podocyte-specific transmembrane I protein expressed in the apical membrane involved in cell polarity and in the slit diaphragm [262]. In patients with steroid-resistant NS, mutations in Crb2 have been reported to be a causing factor [263]. Using podocyte-specific Crb2 knockout (Crb2^{KO}) mice, heavy proteinuria and podocyte foot process effacement with FSGS-like injury were the resulting consequences as Crb2 along with nephrin has a role in maintaining the actin cytoskeleton [264]. Moreover, further analysis in the slit diaphragm in podocyte-specific Crb2^{KO} mice revealed not only a decrease in nephrin expression, but demonstrated Crb2 can interact with nephrin via their extracellular domains due to their adjacent clustering in the slit diaphragm [262, 264]. Thus, the use of Crb2 extracellular domain as the immunogen of choice for induction of anti-podocytes autoimmunity via immunization was a suitable choice.

Hada *et al.* showed induction of heavy proteinuria and podocytes foot process effacement approximately 4-5 weeks post-initial immunization with rCrb2; histologically, the induced NS resembles that of human MCD [249]. Interestingly, the presence of anti-Crb2 auto-Ab responses in the serum of immunized C3H mice with IgG deposition in the glomeruli, resembled humoral responses that are increasingly being reported in relapsing MCD patients. Biochemically, it was reported the phosphorylation of ezrin, a plasma membrane (PM) cytoskeleton-link protein connecting Crb2 to the cytoskeleton and involved in signaling transduction [265], was increased with altered Crb2 localization and actin distribution [249]. While this study was extensive and provided a novel mouse model of INS with MCD-like injury, there are limitations for which we aim to fill the knowledge gap on. For starters, the time it takes to induce significant nephrotic-range proteinuria levels in immunized mice is lengthy and therefore adaptations of this EANS model are of interest. Secondly, and most importantly, it is unclear if the EANS model recapitulated human immune responses (e.g. pathogenic B cell phenotypes, CD4⁺ T_{EFF} responses, FoxP3⁺ T_{REG} cell function, etc.) in the onset and progression of NS as there was a lack of immune analysis conducted. Finally, the use of the C3H mouse strain background severely limits future in-depth analysis regarding the CD4⁺ T-B cell crosstalk and immune mechanisms of podocytopathy as the C3H background lacks additional genetic models (e.g. Cre-lox KO, or congenic markers).

1.3 KNOWLEDGE GAPS, HYPOTHESIS & EXPERIMENTAL OBJECTIVES

In summary, several pieces of historical evidence indicate a T cell origin, and the success of RTX and evidence of B cell abnormalities, indicate a B cell role in MCD onset and progression. Importantly, evidence of auto-Abs targeting podocytes in patients with MCD suggest a role of humoral immunity in podocyte injury. The exact mechanisms of how these pathogenic immune cells are activated, when they are activated and inducing their effector responses, and the type of responses occurring are still unclear. The recent detection of auto-Abs targeting podocytes in patients with MCD further highlights the role of humoral immunity in podocyte injury. Nonetheless, it is still unknown what role these newly discovered podocyte-targeting auto-Abs has in the initiation, progression, and maintenance of podocyte injury and proteinuria induction in MCD patients. Addressing these knowledge gaps can help us understand the mechanisms behind the disease and identify new therapeutic targets.

Prior murine models failed to fully recapitulate key features of MCD, leading to an incomplete understanding of the immune mechanisms involved. To better understand the immune processes involved in B cell-mediated pathology, a model encompassing the full immune cascade of self-Ag recognition is required. Despite some limitations, auto-Ag immunization murine models have provided key insights into the role of autoreactive T cells in each disease; examples include the experimental autoimmune encephalomyelitis (EAE) model for MS research and RA [266, 267]. With the successful development of MCD-like injury in mice through the immunization against podocyte-specific Crb2 [249], it is imperative to answer the overarching question of why does this model result in autoimmune NS with an emphasis to MCD-like injury? It is hypothesized that immunization with podocyte Ags activates T and B cell responses, initiating anti-podocyte auto-Abs responses leading to MCD-like pathology in the novel EANS model.

In order to better understand how the CD4⁺ T-B cell crosstalk influences MCD pathology in this model, the primary aim of this Thesis work is to 1) utilize the novel immune-mediated murine model of NS to characterize the immune environment throughout disease pathogenesis, 2) detect anti-podocyte auto-Ab production in the EANS model and characterizing their function in podocytopathy, and 3) characterize the immune effectors driving disease onset and progression in the EANS murine model. Using this EANS model, we aim to answer two overarching questions:

1) what is the function of anti-podocyte auto-Abs in the immunopathology of EANS, and 2) how do T and B cells interact to induce disease onset or aggression after showing to be involved? To characterize the immune environment throughout disease progression, the immunization protocol described by Hada *et al.* [249] was modified to emulsify the rCrb2 Ag with Complete/Incomplete Freund's Adjuvants (CFA/IFA). The aim of this modification was to enhance cellular responses using CFA/IFA while maintaining high serum Ab titres [268, 269], in addition to potentially accelerate development of nephrotic-range proteinuria.

Chapter 2: MATERIALS & METHODS

2.1 Materials

Ampicillin (Cat. AMP201) from BioShop (Burlington, ON, Canada), isopropyl β -D-1-thiogalactopyranoside (IPTG, Cat. I5502) from Sigma-Aldrich (St. Louis, MI, USA), Bio-Safe Coomassie Stain (Cat. 1610786) from Bio-Rad (Hercules, CA, USA), and urea (Cat. 57-13-6) from Millipore Burlington, MA, USA) were utilized during protein induction and purification. For protein purification, the 3ml resin bed HisPur™ Ni-NTA Spin Column (Cat. 88226) and 3-12ml 10,000 membrane molecular-weight cut-off Slide-A-Lyzer Dialysis Cassettes kit (8-pack, Cat. 66807) were purchased from ThermoFisher Scientific (Waltham, MA, USA). Cell culture components such as 2-mercaptoethanol (2-ME, Cat. 60-24-2) from Sigma-Aldrich (St. Louis, MI, USA), IL-2 (Cat. 202-IL) from R&D systems (Minneapolis, MN, USA), and Golgi stop (Cat. 554724) from BD Biosciences (San Jose, CA, USA), were required with various other solutions purchased from Multicell Wisent Bioproducts (Montréal, QC, Canada) including sterile phosphate-buffered saline (PBS, Cat. 311-425-CL), RPMI-1640 media with L-glutamine and sodium bicarbonate (Cat. 350-000-CL), fetal bovine serum (FBS, Cat. 080-910), penicillin-streptomycin (Pen-Strep, Cat. 450-201-EL), 1M HEPES Solution (Cat. 330-050-EL), MEM Non-essential amino acids (Cat. 321-011-EL), sodium pyruvate (Cat. 600-110-EL), gentamicin (Cat. 450-135-XL), and HBSS cell culture media (containing Ca^{2+} and Mg^{2+} , Cat. 311-510-CL). Sigma-Aldrich (St. Louis, MI, USA) provided 3-way luer-lock valve system (Cat. S7521), and Complete and Incomplete Freund's Adjuvant (Cat. F5881 & F5506, respectively) for immunization preparation, in addition to Formalin (Cat. 50-00-0), Collagenase D (Cat. 11088866001), DNase (Cat. DN25-100MG), phorbol 12-myristate 13-acetate (PMA, Cat. P1585-1MG), ionomycin (Cat. 10634-1MG), Tween-20. (Cat. P7949), and lastly Fingolimod (FTY720, Cat. SML0700-25MG) for drug treatment. Experiments involving flow cytometry utilized eBioscience™ Fixation/Permeabilization Concentrate (Cat. 00-5123-43), Permeabilization Buffer (10X, Cat. 00-8333-56), and Fixation/Permeabilization Diluent (Cat. 00-5223-56) purchased from Invitrogen (Carlsbad, CA, USA), in addition to flat-bottom and V-bottom 96-well plates (Cat. 83.1835 and Cat. 83.3926, respectively) from Sarstedt (Nümbrecht, Germany). Sarstedt also provided Microtest 96-well flat-bottom ELISA plates (Cat. 82.1581) which were utilized along with products for ELISA's such as the mouse albumin ELISA quantitation set (Cat. E99-134) and mouse reference serum (Cat. RS10-101-5) from Bethyl (Waltham, MA, United States), the creatinine (urinary) colorimetric assay

kit (Cat. 500701) distributed by the Cayman Chemical Company (Ann Arbor, MI, USA), albumin bovine serum (BSA, Cat. ALB001.250), and TMB One Component HRP reaction substrate (Cat. AMP201) both by BioShop (Burlington, ON, Canada). Lastly, IF staining preparation required O.C.T compound cryostat embedding medium (Cat. 23-730-625), 4',6-diamidino-2-phenylindole (Dapi, Cat. D21490), and Aqua Mount (Cat. 14-390-5) from ThermoFisher Scientific (Waltham, MA, USA). All Abs used throughout this Thesis for flow cytometry, IF staining, and ELISA's are listed in **Table 2**.

2.2 Mice

C3H/HeN mice were purchased from Charles River Laboratories and then subsequently bred for more than seven generations. Inbred WT BALB/c were purchased from Charles River laboratories. Inbred male C57BL/6 mice (Jackson Laboratories) were bred with inbred female C3H/HeN mice to generate a first generation (F1) B6C3F1 strain; the male hybrids were utilized for *ex vivo* analysis. All mice were used at 8–12 weeks of age, housed and bred under specific pathogen-free conditions, and used according to institutional guidelines at McGill University.

2.3 Mouse recombinant Crb2 (rCrb2) protein production

Transformed competent pET-22b(+) *Escherichia coli* (*E.coli*) with the rCrb2-expression plasmid was generously gifted from Dr. Kunimasa Yan at Kyorin University (Tokyo, Japan). The plasmid was constructed as described [249], containing the sequence for the extracellular domain of Crb2 with additional tag inserts, including a terminal His₆-tag for later protein purification processes. The construct of rCrb2 can be observed in **Fig. 6A**. To produce mouse recombinant Crb2 (rCrb2), frozen *E.coli* stocks were thawed and cultured in LB medium (10g/L Bio Tryptone, 10g/L NaCl, 5g/L yeast extract in ddH₂O) with 100µg/ml ampicillin, at 37°C, shaking, until A₆₆₀ optimal density of -0.5. Production of rCrb2 was induced with 0.1mM IPTG, for 3hrs, at 37°C, shaking. After induction, the culture was spun down at 4,000g, 4°C, for 20min to form a bacterial pellet, and the supernatant was decanted. *E. coli* pellet was lysed using TNE buffer (50mM Tris-HCl, 100mM NaCl, 0.1mM EDTA, pH 7.4). rCrb2 production was confirmed with Coomassie blue staining prior to purification.

2.4 Protein purification

2.4.1 Column purification

Mouse rCrb2 protein was purified using the manufacture protocol provided with the 3ml resin bed HisPur™ Ni-NTA Spin Column (ThermoFisher Scientific) with slight modifications to the buffers. Protein samples were purified twice, first in denaturing conditions and again to increased reducing conditions. Conducting these purification protocols one immediately after the other removed un-specifically bound proteins in the final product. Firstly, 6M guanidine-HCl was added to the Equilibrium buffer (PBS + 6M guanidine-HCl + 10 mM imidazole, pH 7.4), wash buffer (PBS + 6M guanidine-HCl + 25 mM imidazole, pH 7.4), and Elution buffer (PBS + 6M guanidine-HCl + 250 mM imidazole, pH 7.4). The protein isolation was conducted as described by the provided protocol (ThermoFisher Scientific). To increase reducing conditions to remove non-specific proteins, 150mM NaCl was added to wash buffer (PBS + 6M guanidine-HCl + 25 mM imidazole + 150 mM NaCl, pH 6.3) only. The Equilibrium buffer and Elution buffer were unchanged from the previous column purification process. The protein isolation was conducted as described by the provided protocol (ThermoFisher Scientific). Coomassie blue staining confirmed rCrb2 isolation.

2.4.2 Protein dialysis

Column purified mouse rCrb2 samples were dialyzed to diffuse protein samples from the elution buffer to PBS. Dialysis was performed according to manufacture protocol provided [270] with the 3-12ml 10,000 membrane molecular-weight cut-off Slide-A-Lyzer Dialysis Cassettes kit (ThermoFisher Scientific). Dialysis was performed at 4°C, with protein samples within the cassettes dialyzed over-night (ON) in an initial dialysis solution of 8M urea in PBS, slowing rotating. The next day, dialysis solution was changed every 3hrs, decreasing concentration of urea every change (4M urea, 2M urea, 1M urea, to 0.5M urea in PBS) until the final dialysis solution of PBS (no urea). Protein samples with dialyzed ON in PBS and then removed from the cassettes. Mouse rCrb2 purity and concentration was determined using the NanoDrop 2000 Spectrophotometer (Thermo Scientific). Mouse rCrb2 in PBS was aliquoted and stored in -80°C.

2.5 rCrb2 emulsification

Emulsification of purified rCrb2 Ag was prepared in accordance with the manufacture protocol provided with use of CFA and IFA (Sigma-Aldrich). 50µg rCrb2/mouse was obtained and suspended in sterile PBS for a final volume of 100µl/mouse. The solution was then uptaken into a

3cc luer-lock syringe. In a separate 3cc syringe, an equal volume of CFA or IFA was acquired. The syringes were connected through the luer lock fitting to the 3-way valve (Sigma-Aldrich) and the solution was emulsified as instructed.

2.6 rCrb2 immunization

The immunization protocol utilized was adapted from Hada *et al.*, 2022 [249], displayed in **Fig. 6B**. At timepoint 0-weeks, male C3H mice 8-12 weeks of age were bilaterally injected at the base of tail with 100µl emulsification of rCrb2 in 1:1 CFA, for a total of 50µg rCrb2 in 200µl. For subsequent booster immunizations at 2- and 4-weeks, mice were injected with rCrb2 emulsified in 1:1 IFA bilaterally on the flanks. Control mice were immunized with a 1:1 emulsification of PBS and CFA/IFA. Mice were sedated with isoflurane as according to institutional guidelines at McGill University.

Blood and urine samples were collected approximately weekly as indicated in **Fig. 6B**. Blood samples collected through saphenous vein bleeds or cardiac punctures during necropsies, were left to rest for 30-45min at room temperature (RT) to coagulate. Samples were spun down for 15min at 1500rpm, RT. Separated serum was transferred into 200µl PCR microtubes. Samples were stored in -20°C until analyzed.

2.7 Necropsy and sample collection

At experimental endpoints (weeks 3, 6, and 10), mice were euthanized by CO₂ inhalation after anesthetized via isoflurane. Cardiac puncture was performed on the deceased mice to collect final blood serum samples for subsequent experimentation. Spleens, draining inguinal LN (iLN), renal LN (rLN), and kidneys were extracted and placed in 15ml falcon tubes (spleens and kidney) or FACs tubes (LN) with cRPMI (RPMI-1640 media, 10% FBS, 1% PenStrep, 1% 1M HEPES Solution, 1% MEM non-essential amino acids, 1% sodium pyruvate, gentamicin, 2-ME) for functional analysis and immunophenotyping. Kidney sections for histology were collected in E.tubes with 10% formalin (H&E staining) or PBS (frozen sections).

2.8 Secondary lymphoid organ and kidney tissue processing (immune cell isolation)

2.8.1 Kidney processing

Kidney tissue was homogenized to a single cell suspension and resuspended in cold HBSS media with Ca²⁺ and Mg²⁺. Digestion media (5mg/ml collagenase D and 5mg/ml DNase) was mixed

to the resuspended kidneys (final concentration of 1mg/ml each). Tubes were placed in the 37°C incubator (no CO₂) for 45min. After incubation, collagenase activity was quenched with FBS and washed with HBSS media. Samples were resuspended in HBSS media and gently mixed to ensure lymphocyte suspension. Over a 50ml falcon tube, the supernatant was filtered through 70µm basket filter. Cells were spun down, supernatant decanted, and resuspended in 1ml cRPMI media. Cells were transferred to sterile FACs tubes through a sterile 70µm neon mesh filter prior to counting and staining.

2.8.2 Secondary lymphoid organs

Spleens and LNs were homogenized, washed with cRPMI media, spun down for 5min at 1450rpm, 4°C, and the supernatant decanted. Red blood cells in the spleens were lysed with 1ml Ack lysis buffer (NH₄Cl, KHCO₃, 0.5M EDTA in PBS, 7.2-7.4 pH) for 30-60sec and then washed with cRPMI media. Cells were resuspended in cRPMI media and transferred to sterile FACs tubes through a sterile 70µm neon mesh filter prior to counting.

2.9 Lymphocyte cytokine stimulation

In a flat-bottom 96-well plate (Sarstedt), approximately 1x10⁶ cells from secondary lymphoid organs were pipetted for cytokine stimulation of T cells. A 2X solution of simulant consisting of PMA (0.1µg/ml final concentration), ionomycin (0.5µg/ml final concentration), and Golgi stop (diluted 1:1000) was added to the cells and left to incubate in a 37°C, 5% CO₂ incubator for 3hrs [271, 272]. No PMA stimulant controls were prepared using approximately 1x10⁶ cells isolated from iLNs and cRPMI media. After stimulation, cells were transferred to a V-bottom 96-well plate (Sarstedt), spun down for 5min at 1450rpm, 4°C and washed with 200µl PBS. Cells were stained for viability (v780), and extracellularly stains for CD3 (BUV737), CD4 (AF700), and CD8β (BV510). Once stained, cells were fixed overnight at 4°C, covered, permeabilized, and internally stained with CD4 (AF700), CD8β (BV510), IFNγ (PE-Cy7), IL-4 (PE), IL-13 (v450), IL-17A (APC), Ki67 (BUV395), and FoxP3 (FITC) (see **Table 2**). Fluorescence data was collected using BD LSRFortessa™ X-20 flow cytometer (BD Bioscience) and analyzed with FlowJo version 10.3.0.

2.10 Immunophenotyping (flow cytometry)

Immune cells isolated from secondary lymphoid organs and kidneys ([section 2.8](#)), were extracellularly and intracellularly stained for markers associated with T and B cell activation and

memory responses. The staining protocol utilized was as described in [section 2.9](#). All fluorescently-conjugated Abs used in panels are listed in **Table 2**, with specific Ab combinations for the different panels can be reviewed in their respective Figure titles. Cells were acquired with BD LSRFortessa™ X-20 flow cytometry and raw data was analyzed with FlowJo version 10.3.0.

2.11 Enzyme-linked immunosorbent assay (ELISA)

2.11.1 Albuminuria (uACR)

Albuminuria, or proteinuria for the purpose of this Thesis, was reported as a ratio of albumin to creatinine concentrations (uACR) in urine samples collected. Quantification of urine albumin and creatinine concentrations were obtained in separate ELISA protocols. Urine albumin ELISA was conducted with the manufacturer protocol provided in the kit purchased from Bethyl laboratories Inc., which provided the mouse reference serum for standards, and both anti-Mouse Albumin Coating and anti-Mouse albumin HRP conjugated Abs (**Table 2**). Prior to incubation in plate(s) coated with 1µg anti-mouse albumin Ab , urine samples were diluted 1:5000 in diluent. For the creatinine ELISA, it was conducted using the Creatinine (urinary) Colorimetric Assay kit (Cayman Chemical Company). Urine samples were diluted 1:30 and the remaining assay was conducted following the manufacturer protocol provided.

For both ELISAs, absorbance was read at 450nm using the Tecan infinite (M200 Pro) plate reader. Albumin titres (mg/ml) were calculated from the absorbance values and interpolation of standard absorbance values; creatinine titres (mg/dl) were derived from the difference between final and initial absorbance values and linear best line of fit determined via the standard curve. Quantification of uACR (mg/mg) were calculated by dividing albumin concentrations by creatinine concentrations.

2.11.2 Serum anti-Crb2 poly-IgG titre

Quantification of anti-Crb2 polyclonal IgG (pIgG) titres from serum collected from immunized mice was conducted via indirect ELISA using the protocol described by ThermoFisher Scientific with modifications [273]. Wells of Microtest 96-well flat-bottom ELISA plates (Sarstedt) were coated with 1µg rCrb2 Ag in 100µl 0.2M sodium carbonate bicarbonate, and incubated ON at 4°C, covered. After washes, plates were blocked with 200µl blocking buffer (2% BSA and 0.05% Tween-20 in PBS) for 1-2hrs, covered, at RT. 100µl diluted samples and standards were pipetted

in duplicates and incubated covered at RT for 2-3hrs. Serum samples were diluted 1:1000 and 1:5000 in blocking buffer. Standards (500ng/ml, 250ng/ml, 125ng/ml, 62.5ng/ml, 31.3ng/ml, 15.6ng/ml, 7.8ng/ml, plus blank) were created by diluting 1mg/ml purified anti-Crb2 pIgG gifted from Dr. Kunimasa Yan's lab (Kyorin University, Tokyo, Japan, [249]) in blocking buffer. After washing, 100µl goat pAb to mouse IgG-HRP diluted 1:1000 in blocking buffer was added to each well and incubated cover at RT for 1hr. Lastly, 100µl TMB One Component HRP reaction substrate was added to each well and developed at RT covered for 1-2min and then 50µl 2N H₂SO₄ halted the reaction. Absorbance was read at 450nm with reference correlation (λ) at 570nm using the Tecan infinite (M200 Pro) plate reader. Anti-Crb2 pIgG titres (μ g/ml) were calculated from the absorbance values and interpolation of standard absorbance values.

2.12 Histology – H&E staining

Renal sections of the cortex were collected at the respective experimental endpoints mentioned and fixed with 10% formalin. After three 30min PBS washes, tissue samples were preserved in 70% EtOH in PBS and stored in 4°C until ready for histology processing. The histology core at the Glen of the RI-MUHC provided services which prepared 3-4µm kidney sections on microscope slides, stained with hematoxylin & eosin (H&E), and scanned for analysis.

2.13 Immunofluorescent glomerular staining

Renal tissue samples were prepared by freezing in O.C.T compound cryostat embedding medium and stored in -80°C until ready for use. Tissues sections were cut (4µm) and mounted on glass slides, airdried, and washed in cold acetone. Slide were fixed in 4% PFA for 15min after PBS washes and blocked for 30min in blocking buffer (3% BSA in PBS) at RT. Renal samples underwent a secondary blocking treatment with donkey anti-mouse IgG (diluted in 3% BSA solution) to remove non-specific binding. Primary staining with anti-nephrin Ab in 3% BSA solution (**Table 2**) took place overnight at 4°C, covered. The next day, sections were washed with PBS and then co-stained with secondary fluorochrome-conjugated IgG-448 (nephrin) and anti-mouse IgG-555 (mouse IgG) at RT for 1hr, separately (**Table 2**). Finally, slides were stained with Dapi, and mounted using Aqua Mount. Confocal images were captured with the Zeiss LSM780 confocal microscopy and Zen software (version 8.1.0.484); mean fluorescent intensity was quantified for nephrin and mouse IgG from 40-80 pooled glomeruli.

2.14 rCrb2-specific CD4⁺ T cell restimulation

Male C3H Mice were bilaterally immunized at 0- and 2-weeks with 50µg rCrb2 emulsified in 1:1 CFA and IFA, respectively. On day 17, mice were euthanized and their draining iLN and control axillary/brachial LNs (ax/brLN) were collected. Immune cells were isolated, filtered, and plated in 48-well tissue culture plates at 5×10^5 cells/well with 10µg rCrb2 and 100 units IL-2. Cells were left to incubated at 37°C, 5% CO₂ for 5-days. At the end of the 5-days, media was removed and replaced with fresh cRPMI media containing 10µg rCrb2 and Golgi Stop (1:2000), and incubated at 37°C, 5% CO₂ for 3hrs. At the end of 3hrs, cells were washed and stained for flow cytometry analysis.

2.15 Passive transfer

Naïve male C3H mice were passively injected intraperitoneal (i.p.) or intravenously (i.v.) with 200µl of raw serum from disease positive rCrb2-immunized C3H mice 6-weeks post-initial immunization. Urine samples were collected on days 0, 1, 3, 5, and 7 post-serum transfer and analyzed by ELISA.

2.16 FTY720 treatment

Male C3H mice were immunized following the protocol mentioned in [section 2.6](#). From 2-weeks post-initial immunization to 5-weeks, mice were given daily i.p. injections of FTY720 (Sigma-Aldrich) in saline (0.9% NaCl in ddH₂O) at a dosage of 1mg/kg [274, 275]. To serve as controls, rCrb2-immunized mice were i.p. injected daily with 200µl saline. Urine and serum were collected weekly. Secondary lymphoid organs, kidneys, and renal tissue sections were collected 5-weeks post-initial rCrb2-immunization, to be processed and analyzed.

2.17 Statistics

Throughout experimental analysis, different statistical analyzes were utilized and p-values < 0.05 were considered significant. Two-way ANOVA Šídák multiple comparisons test determined statistical relevance for results on body weight change, uACR and serum ELISA titres. For IF staining, live lymphocyte counts within secondary lymphoid organs and kidneys, and data gathered and displayed from flow cytometry, unpaired parametric two-tailed t tests were conducted. Lastly, Pearson correlation coefficients analysis with 95% confidence interval with

simple linear regression were performed for all correlation analysis. $p \geq 0.05$ (ns), $p < 0.05$ (*), $p < 0.01$ (**), $p < 0.001$ (***), $p < 0.0001$ (****).

Chapter 3: RESULTS

Research into a novel mouse model that mediates podocyte injury and NS is crucial for several reasons. First, it is well established that the CD4⁺ T-B cell crosstalk plays a critical role in the onset and progression of autoimmune diseases. T cells can stimulate the production of auto-Abs by triggering PC differentiation, which can bind to and induce effector functions on their target tissue. Conversely, B cells can activate T cells by presenting auto-Ags, leading to the activation of autoreactive T cells that can secrete pro-inflammatory cytokines [81, 82]. Second, immunosuppressant treatments have shown some success in treating NS, and recent studies have detected auto-Abs in MCD before and during the disease, suggesting T and B cells play a role in the pathogenesis of MCD [7, 9, 10, 216, 247, 248, 276]. However, the cellular functions of pathogenic T cells and the exact mechanisms of immune-mediated podocytopathy are largely unknown due to limitations in past murine models. Therefore, developing a novel mouse model that initiates auto-responses against podocytes leading to podocyte injury and proteinuria can provide insight into the underlying mechanisms of immune-mediated podocytopathy. Once confirmed, this model can be used to further dissect the mechanisms of immune-mediated podocytopathy and may lead to the development of new treatments for NS.

3.1 Generation of experimental autoimmune nephrotic syndrome (EANS) model

The use of an immunization mouse model with auto-Ags to prime immune responses is a powerful tool to study the T-B cell crosstalk and humoral responses in autoimmune diseases. This approach has been used successfully in other models, such as the EAE model for MS for which the T-B cell crosstalk has been extensively studied and has provided insight into the mechanisms of MS pathogenesis [267]. Therefore, the development of this model approach could help elucidate the cellular and molecular mechanisms underlying the dysregulation of immune responses mediating podocytopathy in INS with MCD-like injury.

3.1.1 Immunization with rCrb2 induced nephrotic-range proteinuria in C3H/HeN mice.

Activation of pathogenic CD4⁺ T and B cells by podocyte auto-Ags following an initial tissue injury has been theorized to cause MCD, leading to the production of anti-podocyte auto-Abs and effector responses [7, 67, 208, 229]. Therefore, if these conditions were mimicked through auto-Ag immunization, which are successfully utilized in multiple autoimmune murine models [221,

277-280], EANS could be induced and give a platform to study the immunological mechanisms of podocytopathy. Recently, it was discovered biweekly immunizations of C3H mice with recombinant Crb2 (rCrb2) with TMG adjuvant was able to induce proteinuria at 4-weeks post-initial immunization [249]. This model was also able to induce podocyte foot effacement, while maintaining glomerular structure integrity, thus recapitulating key clinical attributes observed in human MCD patients [249]. There were some limitations to the study for which we aimed to address, particularly the lack of immune phenotyping and mechanism analysis leading up to disease onset.

Seeking to recapitulate the observations, the EANS model was established in C3H mice using a modified rCrb2 immunization protocol, initially described by Hada *et al.* [249]. Specifically, rather than bilaterally injecting mice subcutaneously biweekly (weeks 0, 2, and 4) with rCrb2 in TMG, the rCrb2 Ag was emulsified in CFA and IFA, as shown in **Fig 6B**. We had a goal to investigate whether different adjuvants could stimulate effective pathogenic cellular responses, while maintaining reported serum anti-Crb2 IgG titres and histological features of the glomeruli. Adjuvants that can produce high effector and T cell-dependent humoral responses are known to be effective, such as CFA/IFA [281, 282]. The aim was to perform in-depth immunophenotyping and mechanistic studies to determine if these adjuvants could induce efficient pathogenic cellular responses. Onset and severity of NS in our EANS model was tracked by uACR, a measurement of proteinuria. Weekly urine samples were collected and analyzed via ELISA. Proteinuria was observed approximately 4-weeks post-initial rCrb2 immunization, similar to what was described [249]. By 5-weeks post-immunization, proteinuria levels were significantly higher than PBS controls, and surpassed the nephrotic-range uACR threshold (e.g. uACR >3mg/mg) (**Fig. 7A**). Therefore, we confirmed immunization of C3H mice against the podocyte auto-Ag Crb2 with CFA (primary immunization) and IFA (booster immunizations) was able to induce EANS and nephrotic-range proteinuria.

3.1.2 Key clinical features of human MCD are recapitulated in EANS.

During the immunization process, CFA/rCrb2- (primary) and IFA/rCrb2-immunized (booster) mice showed no difference in weight in comparison to the PBS controls (**Fig. 7B**). To ensure the nephrotic injury in this EANS model shared histological features comparable to human MCD patients, renal sections stained with H&E reviewed no changes in glomerular structural

integrity or evidence of increased immune cell infiltration in rCrb2-immunized mice (**Fig. 7C**). Lastly, total live lymphocyte cell counts were quantified in the spleens (not displayed), draining iLN, and kidneys of rCrb2 and PBS immunized mice with CFA/IFA. While there was the predicted increase in immune cells within iLN of rCrb2-immunized mice compared to their PBS counterparts, there were no changes in cell numbers within the kidneys of rCrb2-immunized mice (**Fig. 7D**), confirming lack of infiltrating immune cells observed through histology. Overall, these results confirmed immunizing C3H mice with rCrb2 emulsified in CFA/IFA recapitulates key features of NS and MCD-like injury as reported [249].

3.2 Podocyte-binding auto-antibodies are associated with EANS severity.

With increasing accounts of auto-Abs present in MCD patients [9, 10, 245, 276], we hypothesized auto-Abs have a role in MCD pathogenesis by interacting with targeted surface proteins on podocytes and triggering downstream cytoskeletal rearrangement. In this model, the next step was to determine if rCrb2-immunized mice produced anti-Crb2 auto-Abs and if these auto-Abs drove disease onset. ELISA targeting mouse anti-Crb2 pIgG titres in blood serum was conducted from serum collected at various timepoints post-initial immunization. Significant serum anti-Crb2 pIgG production was detected as early as day 10 post-initial immunization with titres increasing and remain high as long as 9-10 weeks (**Fig. 8A**).

Traditionally, it was reported in clinical studies no evidence of glomerular Ig deposition within biopsies taken from adult human MCD patients [245, 283, 284]. However, two recent studies have shown podocyte auto-Ab binding in renal biopsy samples of MCD patients using IF staining [10, 247]. One study demonstrated glomerular Ig deposition were caused from anti-podocyte auto-Abs by eluting Ig with the podocyte protein annexin A₂ from frozen renal biopsies of MCD patients [247]. Therefore, this new evidence supports the theory that Ig's are depositing within the kidneys, though likely not as high as intensity seen in other nephrotic injuries, such as MN and IgA nephropathy [285-287]. In the EANS model, IF staining analysis was conducted by staining for anti-mouse IgG on frozen renal sections obtained from C3H mice immunized against rCrb2 or PBS. IgG deposition was confirmed within the glomeruli of rCrb2-immunized mice with podocyte-specific binding with co-staining against nephrin (**Fig. 8B**), a protein necessary for the maintenance and function of the podocyte slit diaphragm [194, 197]. A significant increase in glomerular IgG

deposition was observed with podocyte-specific binding as anti-IgG fluorescence overlapped with fluorescence from nephrin (**Fig. 8C**). These results further support the theory of auto-Abs having a role in MCD pathogenesis.

Variability in recorded proteinuria severity and serum anti-Crb2 IgG titres of rCrb2-immunized C3H mice (**Fig. 7A & 8A**), prompted an inquiry of whether the level of auto-Abs produced was associated with disease severity. Correlation analysis displayed a significant positive correlation ($r = 0.6418$; $p\text{-value} = 0.0074$) between serum anti-Crb2 IgG titres of rCrb2-immunized mice and their proteinuria severity 3-weeks post-initial immunization (**Fig. 8D**). This positive correlation may be dependent on the progression of NS within these mice as at 6-weeks there was still a positive correlation though no longer significant ($r = 0.5036$; $p\text{-value} = 0.1378$), and at 9-weeks a negative correlation was observed ($r = -0.002049$; $p\text{-value} = 0.0210$). Interestingly, the presence of serum IgG preceded the detection of nephrotic-range proteinuria, so it was tested if auto-Abs mediated disease onset in EANS. Male naïve C3H mice (6-8 weeks of age) were passively transferred (i.p. or i.v. injections) once with 200 μ l raw serum collected from high-responsive mice; these were mice with high uACR values and high serum anti-Crb2 IgG titres. Approximately 1mg of anti-Crb2 IgG per 200 μ l of serum was injected in naïve recipient mice. Urine samples were collected on days 0 (baseline), 1, 3, 5, and 7 for uACR quantification. The raw serum was unsuccessful at inducing proteinuria in naïve C3H mice, regardless if they were i.p. or i.v. injected (**Fig. 8E**). Presence of anti-Crb2 IgG were detected in the recipient mice with nearly a 10-fold decrease from initial titres 4-days post transfer (**data not shown**). A limitation of this experiment may be the concentration of raw serum Abs may not have been sufficient to induce initial injury and a titration with purified anti-Crb2 IgG could be conducted. Although, the biological interpretation makes for a strong hypothesis that a cellular response, followed by humoral response, are needed to initiate podocyte injury.

3.3 Activation of isotype-switched memory B cells preceded proteinuria.

The activation of pathogenic B cells and their differentiation into PC's is a complex process that involves several signals and interactions with CD4⁺ T cells. B cells are activated after Ag-BCR ligation. This recognition triggers a cascade of signals inside the B cell that lead to its activation, proliferation, and differentiation into auto-Ab secreting PC's [11, 12]. The presence of podocyte

targeting auto-Abs suggested pathogenic B cells are becoming activated and differentiating into Ab-secreting PC's. Additionally, B cells function as professional APCs to CD4⁺ T cells through MHC-II:TCR ligation plus co-stimulatory signals [81, 288-290]. To characterize cellular responses and memory status of CD4⁺ T and B cells, spleens, draining iLN, rLN, and kidneys were obtained from rCrb2- and PBS-immunized C3H mice 3-, 6-, and 9-weeks post-initial immunization (**Fig. 6B**). Immune cells were isolated and stained with fluorescently-labelled monoclonal Abs directed against surface, intracellular and intranuclear proteins for multiparametric flow cytometry analysis. Based on the presence of podocyte auto-Abs being significantly elevated prior to proteinuria detection (i.e. 3-weeks) and high serum titres associated with high uACR, cellular response 3- and 6-weeks post-initial immunization were analyzed. Due to insufficient cell numbers, results obtained from rLN's were excluded as they would not accurately represent the immune environment or reactions occurring within the secondary lymphoid organ during EANS induction. Within the iLN-resident CD19⁺ B cell population in rCrb2-immunized mice (**Fig. 9A**), a high frequency of class-switched CD19⁺ B cells with IgG⁺ BCR's was observed prior to the onset proteinuria at 3-weeks (**Fig. 9B-C**). CD19⁺ B cells displayed a greater activated phenotype, as per MHC-II expression (gMFI), in rCrb2-immunized, pre-proteinuric mice compared to PBS controls. Though at nephrotic-range disease (i.e. 6-weeks) there was no significant difference (**Fig. 9D**). Taken together, these findings demonstrate that the activation and differentiation of B cells in response to rCrb2-immunization take place in the early stages of EANS, preceding nephrotic-range disease, leading to the generation of class-switched B cells with IgG⁺ BCRs and auto-Ab secreting PCs. However, the lack of significant differences at the nephrotic-range disease stage between the rCrb2-immunized and control mice may indicate potential changes in the dynamics of B cell activation as the disease progresses from the early stage. Further investigations are warranted to understand the underlying mechanisms governing these changes and their implication for autoimmune responses and disease development.

3.4 The characterization of CD4⁺ T_{EFF} cells & FoxP3⁺ T_{REG} cells during EANS

A significant increase in B cell activity was observed, particularly with increased in MHC-II expression and class-switching to IgG⁺ BCR (**Fig. 9**), which are indicative of CD4⁺ T cell-dependent activation [291]. Hence, CD4⁺ T cell effector and regulatory activity was analyzed.

3.4.1 Effector CD4⁺ T cells arise prior to proteinuria.

Effective CD4⁺ T_{EFF} cell responses require TCR:MHC-II interactions and secondary co-stimulatory binding with APCs, which include B cells [96]. Activated CD4⁺ T cells present within the T cell zone, or paracortex, of draining LNs modulate the expression two distinct adhesion molecules, L-selectin (CD62L) and H-CAM (CD44) [133]. CD62L expression which is required for naïve CD4⁺ T cells to migrate to the draining LN gives way to the expression of CD44 which allow Ag-experienced memory CD4⁺ T cells to egress to target tissue [292, 293]. To observe CD4⁺ T cell responses at prior to and immediately after nephrotic-range proteinuria (3- and 6-weeks, respectively) of EANS, we aimed to determine if 1) there was increased CD4⁺ T cell activation, and 2) if these responses are observed in the kidneys. Therefore, to evaluate the evolution of CD4⁺ T cell responses during EANS induction, we assessed the frequency of naïve CD4⁺ T_{EFF} cells (CD62L^{hi}CD44^{lo}) and memory CD4⁺ T_{EFF} cells (CD62L^{lo}CD44^{hi}) by flow cytometry in the draining iLN and kidneys of rCrb2- and PBS-immunized C3H mice at various timepoints post-immunization [294]. To track activation, CD4⁺ T_{EFF} cells were gated on the ICOS marker along with CD44. As a member of CD28/CTLA-4 co-stimulators specific to T cells, ICOS is involved in T cell proliferation and cytokine secretion [295]. Unlike CD28 where it binds to B7 on all APCs [296], ICOS's ligand B7H/B7RP-1 is expressed on B cells [297]. In addition to this B cell link, it is widely accepted that ICOS is essential, along with IL-4 production, for the development of humoral responses [297]. Therefore, it was highly attractive to use this marker for memory CD4⁺ T_{EFF} cell activation during EANS. Memory CD4⁺ T_{EFF} cells within the draining iLN were significantly increased in rCrb2-immunized mice both 3- and 6-weeks post-initial immunization compared to their PBS-immunized counterparts (**Fig. 10A**). Regarding the activation status iLN, an overall increase in the frequency and number of activated memory CD4⁺ T_{EFF} cells was observed with significantly elevated ICOS expression (gMFI) after 3-weeks (**Fig. 10C**). At 6-weeks, ICOS expression and frequency of activated memory CD4⁺ T_{EFF} cells in rCrb2-immunized C3H mice were observed to not be as prominent. Much like the cellular B cell responses reported (**Fig. 9**), this decrease in T cell activity within the iLN during EANS induction may be evidence of pathogenic immune cells migrating from the draining secondary lymphoid organs to the target tissue and its associated LN (e.g. the kidneys and rLN). Memory CD4⁺ T_{EFF} cell frequency and numbers in the kidneys were unchanged between rCrb2-immunized and PBS control C3H mice (**Fig. 10B**). Therefore, the lack of infiltrating immune

cells observed in renal histologies (**Fig. 7C**) and detectable changes in frequencies by flow cytometry within the kidneys of immunized mice with EANS suggests cellular responses initiating and/or moderating proteinuria and NS induction are occurring in the peripheral LNs.

3.4.2 FoxP3⁺ T_{REG} cells were not perturbed during active EANS.

With the decline of activated memory CD4⁺ T_{EFF} cell responses by week 6 in rCrb2-immunized mice, particularly within the draining iLN, we inquired if FoxP3⁺ T_{REG} cells were suppressing responses. In both rCrb2-immunized and PBS mice, there were no significant changes in FoxP3⁺ T_{REG} frequency or numbers in the iLN and kidneys at 3- or 6-weeks (**Fig. 11A-B**). This was particularly intriguing find as human MCD patients have been reported to have lower levels of FoxP3⁺ T_{REG} cells immediately prior and during disease relapse [231].

The expression of the transcription factor Helios differentiates FoxP3⁺ T_{REG} cells that are either thymic derived (Helios⁺ tT_{REG}) or induced from conventional CD4⁺ T_{EFF} cells in the periphery (Helios⁻ pT_{REG}) [33, 298]. Helios provides stability and enhanced suppressor functions in tT_{REG} cells through activation of the IL-2R α -STAT5 pathway downstream of CD25 binding, compared to their induced Helios⁻ T_{REG} cell counterparts where lineage stability is weaker [298-300]. Therefore, the Helios⁺ tT_{REG} cell subgroup were analyzed. Like general FoxP3⁺ T_{REG} cell results reported, there were no changes in Helios⁺ T_{REG} cells in the iLN or kidneys of rCrb2-immunized mice at either 3- or 6-weeks (**Fig. 11C-D**). Helios⁺ T_{REG} cells are critical in a secondary memory response and have also been associated with increased expression of ICOS and PD-1 [33, 298, 301]; an in-depth analysis determining if there is an association of peripheral Helios⁺ T_{REG} cells to disease progression and T_{EFF} cell activity will need to be conducted. Taken together, effector responses in this EANS model are suggested to occur in the peripheral secondary organs. Additionally, with no detectable changes in FoxP3⁺ T_{REG} cell populations in mice with EANS, it suggests there may be a dysregulation in suppressor functions towards the podocyte immunogen.

3.5 Effector CD4⁺ T cell harbour rCrb2-reactive clones.

Pathogenic CD4⁺ T_{EFF} cells secrete pro-inflammatory cytokines to generate an inflammatory environment leading to tissue injury [289]. These cytokines in-turn influence B cell isotype-switching and Ab production [108, 302-304]. Lastly, studies propose glomerular podocyte injury in INS could be triggered from cytokines, including TNF- α , soluble IL-2R, IL-4, IL-5, IL-9, and

IL-13 [229, 230]. With evidence of activated memory CD4⁺ T_{EFF} cells within the draining iLN, characterizing the functions of these cells was essential for understanding the type of responses occurring, giving a better idea on how these soluble factors influence humoral responses and possibly podocyte injury in future studies. From the *in vivo* studies, we did not observe any difference in Th1, Th2, or Th17-associated cytokine production following CD4⁺ T_{EFF} cell activation with rCrb2-immunization at 3- or 6-weeks (**data not shown**). As such, cytokine quantification was conducted from rCrb2-primed CD4⁺ T cells and APCs isolated from rCrb2-immunized mice and restimulated with rCrb2 *in vitro*. Doing so would clonally expand Crb2-specific CD4⁺ T cells to analyze by flow cytometry. After co-culturing for 7 days, cells were stimulated with Golgi stop, fixed, and fluorescently stained to analyze their cytokine production (**Fig. 12A**).

CD4⁺ T_{EFF} cells from rCrb2-immunized mice proliferated vigorously in response to *in vitro* re-stimulation with rCrb2 as indicated by the increased frequency of Ki67⁺ T cells (**Fig. 12B**), thus indicating responding T cells were rCrb2-specific. Cytokines associated with lineage-differentiated CD4⁺ T_{EFF} cells were stained, with particular interest in IFN γ (Th1-associated), IL-4 and IL-13 (Th2-associated), and IL-17A (Th17-associated). There was a slight increase in IL-4-producing CD4⁺ T_{EFF} cells frequency isolated from the iLN compared to their PBS counterparts (**Fig. 12C, bottom**). No significant changes in IFN γ , IL-13, or IL-17A levels were detected (**Fig. 12C-E**). With these current results, the re-activation of rCrb2-specific CD4⁺ T_{EFF} cells isolated from immunized mice showed evidence of Th2-associated cytokine production which coincides with what has been reported in human MCD patients [229].

3.6 FTY720-treatment suppressed germinal centres abrogating humoral auto-reactivity.

Thus far, previous analysis showed strong evidence of CD4⁺ T_{EFF} cell and B cell activation early in EANS disease through surface markers involved in the T-B cell crosstalk and class-switching to IgG⁺ BCRs. However, they still did not show how this interaction influenced podocytopathy in the EANS model. To determine the importance of adaptive immune responses influencing and/or instigating nephrotic injury in EANS, lymphocyte migration out of active LN's and downstream autoimmune responses were hindered using the sphingosine 1-phosphate (S1P) agonist FTY720 (Fingolimod). FTY720 equalizes the S1P gradient between tissues and secondary lymphoid organs. Doing so prevents the egression of activated matured lymphocytes with increased expression of

S1P receptor (S1P-R) from the draining LNs [305]. In a MP4- EAE mouse model of MS, BL/6 mice were treated daily with 1mg/kg body weight of FTY720 for either 30-days at peak disease (acute treatment), or 50-days (chronic treatment) immediately after disease onset [306]. In this study, it was reported FTY720-treatment (acute and chronic) significantly reduced circulating T cells while B cells were slightly diminished. Within the B cell compartment, there was no observable effects on memory B cell or serum Ab production, where B220⁺ B cells were significantly increased within the spleens after FTY720-treatment [306]. These results were what inspired the use of FTY720 during rCrb2-immunization. Male C3H mice were immunized with rCrb2 using the standard protocol. Starting 2-weeks post-initial immunization along with the first booster immunization, mice underwent daily i.p. injections of 1mg/kg FTY720; serving as controls, a group of rCrb2-immunized mice were treated daily with saline injections (**Fig.13A**). Since FTY720 is a treatment used for autoimmune conditions [307], mice were sacrificed 5-weeks post-initial immunization to minimize adverse effects. Like previous rCrb2-immunization cohorts, urine, blood, spleens, draining iLN, and kidneys were collected for immunophenotyping analysis by flow cytometry. Histologically, glomeruli integrity remained unchanged, nor were there signs of increased infiltrating lymphocytes (**Fig. 13B**).

We hypothesized with FTY720-treatment, activated CD4⁺ T and B cells will continue to be present in the draining iLN while serum anti-Crb2 IgG migrated into the glomeruli and trigger proteinuria. We based this hypothesis on our observations of uACRs, serum auto-Ab titres, and correlation analysis, particularly at 3- and 6-weeks post-initial immunization, as shown in **Fig. 7A and 8A,D**. Surprisingly, what was observed was the opposite as FTY720-treatment seemed to have prevented proteinuria development in rCrb2-immunized mice while those that were treated with saline still developed proteinuria (**Fig. 13C**). Moreover, serum anti-Crb2 IgG began declining after approximately one-week with FTY720-treatment (**Fig. 13D**). IF staining of mouse IgG in the glomeruli displayed a significant decrease in IgG deposition in FTY720-treated rCrb2-immunized mice compared to their saline-treated counterparts (**Fig. 13E**). With the decline in serum auto-Ab production, B cell activity within the GC (CD95 and GL-7) within the draining iLN were quantified using flow cytometry. Firstly, FTY720-treatment significantly inhibited general CD19⁺ B cell GC reactions (**Fig. 13F**). Due to decrease in GC B cell activity, there was a significant decrease in class-

switching to IgG⁺ B cells in rCrb2-immunized C3H mice treated with FTY720 compared to EANS mice treated with saline (**Fig. 13G**).

Lastly, while there were no observable changes in memory CD4⁺ T_{EFF} cell frequency, numbers nor their activation (i.e. ICOS expression) with FTY720-treatment, proliferation of CD4⁺ T_{EFF} cells were significantly decreased in the draining iLN (**Fig. 14A, C-D**). While overall lymphocyte numbers were unchanged in kidneys of saline and FTY720-treated mice (**data not shown**) as observed in **Fig. 13B**, frequency of memory CD4⁺ T_{EFF} cells were overall increased in FTY720-treated mice while cellular numbers remained consistent (**Fig. 14B**). This may be due to circulating naïve T cells not returning to the kidneys. Much like what was observed between rCrb2- and PBS-immunized mice in previous studies, FoxP3⁺ T_{REG} cell populations were unaffected within the iLN regardless if mice were treated with saline or FTY720 (**Fig. 14E**). What was striking was the effects observed in the FoxP3⁺ T_{REG} cell populations in the kidneys of FTY720-treated rCrb2-immunized mice, which were significantly decreased after drug treatment (**Fig. 14F**). However, it was unclear if this was due to decrease in overall CD4⁺ T cells or a decrease in FoxP3⁺ T_{REG} cell migration as we reported no change in iLN FoxP3⁺ T_{REG} cells population. Further analysis utilizing markers for tissue residency are needed. Overall, these results depicted potential off-target immunosuppressive effects of FTY720 beyond restriction of activated S1P-R expressing CD4⁺ T and B cells in iLNs, leading to decreased cellular responses, downstream humoral activity, and proteinuria development.

3.7 BALB/c mice are susceptible to EANS.

The C3H mouse strain is known to be limited in terms of variable genetic models. This includes not possessing genetic models such as the Cre-Lox models, TCR deficient mice, reporter genes, congenic strains such as Ly5.1/CD45.1 for adoptive transfer, etc. Considering these limitations, we sought to investigate the possibility of transposing this model to a strain that is commercially available in various genetic strains or has been developed in our lab. With the rCrb2-immunization protocol utilized throughout this Thesis work, induction of the EANS model was first attempted in wildtype BL/6 mice. No proteinuria developed during the experiment (**Fig. 15A**). Previous immunization attempts with rCrb2 emulsified with TMG adjuvant have shown detectable high serum titres of anti-Crb2 IgG in BL/6 mice; again, no proteinuria developed (**data not available**). Regarding the BL/6 mouse strain, it has been known in past attempts by other research

groups to be notoriously resistant to glomerular injury [256]. Therefore, the first generation hybrid offspring of BL/6 and C3H mice (B6C3F1) were immunized with rCrb2 in a pilot experiment to observe if the immunoreactive factors of the C3H mice could be transferred to the BL/6 background and induce proteinuria and NS. However, while uACR increased slightly in the hybrid B6C3F1 mice, it did not reach the level was considered significant for NS (**Fig. 15A**). Anti-Crb2 IgG titres within the rCrb2-immunized hybrid mice remained high (**Fig. 15B**), indicating that there may be risk factors associated with the C3H mice not present in the BL/6 mice. Our attention then turned to the BALB/c mouse strain, which possesses various genetic models that can be utilized for future experimentation. After immunizing against rCrb2, nephrotic-range proteinuria and high levels of anti-Crb2 IgG serum titres 6-weeks post-initial immunization was successfully induced (**Fig. 15A-B**). However, it was noticed that disease progression in BALB/c mice appeared to be slower than in the standard EANS model with C3H mice, as levels of IgG production were considerably lower in the BALB/c mice than in hybrid (**Fig. 15B**).

Since proteinuria was detected in rCrb2-immunized BALB/c mice, immunophenotyping analysis was conducted using flow cytometry 6-weeks post-initial immunization. Fortunately, adequate events were recoded from rLN from both PBS- and rCrb2-immunized BALB/c mice and were reported (**Fig. 15 C-E and 16**). Six-weeks post-initial immunization, within the B cell compartment like the C3H, there were no differences in SM B cells expressing IgG⁺ BCRs in the draining iLN of rCrb2-immunized BALB/c mice. However, within the rLN a significant increase in IgG⁺ B cell numbers was detected (**Fig. 15D**), but we did not detect any difference in MHC-II expression within both LNs (**Fig. 15E**). In the T cell compartment, there was an increase in overall memory and ICOS-expressing memory CD4⁺ T_{EFF} cells in the rLN of rCrb2-immunized BALB/c mice, whereas in the iLN there we not observable changes (**Fig. 16A-B**). Lastly, no differences were detected in FoxP3⁺ T_{REG} cell populations nor Helios expression within the iLN and rLN's 6-weeks post-immunization (**Fig. 16C-D**). As a final note, immunophenotyping within the kidneys showed no evidence of memory CD4⁺ T cell or FoxP3⁺ T_{REG} cells population fluctuation (**Fig. 17**). Overall, these preliminary results suggest that the use of BALB/c may be an attractive alternative to the C3H strain to develop the EANS model. It was made clear that additional studies are required to fully understand the potential limitations and benefits of using different mouse strains for

characterizing the individual aspects of the cellular and humoral responses mediating podocyte injury in the EANS model.

Chapter 4: DISCUSSION

4.1 SUMMARY AND DISCUSSION

Adjuvant supplemented vaccines can promote the generation of immune responses against a chosen target [308], presenting an elegant model to investigate the involvement of podocyte-specific B and T cell responses. In the modified novel EANS model [249], we were able to induce nephrotic-range proteinuria while maintaining glomerular structure integrity. Importantly, we observed no noticeable immune cell infiltration in the kidney or tissue-injuring pro-inflammatory responses, replicating some of the key hallmarks of MCD disease. This validated the use of the EANS model for the study of the immunological events leading to MCD. Of significance was the detection of high serum titres of anti-Crb2 IgG correlating with proteinuria severity and the presence of glomerular deposition with podocyte binding as it 1) provides additional evidence for MCD as an autoimmune disorder, and 2) suggests a potential involvement of humoral responses in podocyte injury. While the data supports the hypothesis of causation, it is important to note that they have not definitively proven causation currently and further research is required. While the function(s) of pathogenic SM B cells have yet to be determined, we hypothesized that peripheral auto-reactive CD4⁺ T cells from GC reactions are involved in their activation and maturation. Moreover, T cells may be involved in the deposition of auto-Abs to the glomeruli by generating factor that increase GBM permeability and access to the podocytes, as it was observed that auto-Abs alone do not have the immunogenic capacity to induce proteinuria. This model provided convincing evidence that activated T and B cells are communicating during GC reactions to produce high-affinity podocyte-targeting auto-Abs and effector responses leading to the induction of NS. Importantly, it showed that this EANS model can be transposed in alternative mice strains which allow to characterize the complex mechanisms involved in the breakdown of immune tolerance.

4.1.1 How does this model recapitulates key humoral responses and clinical aspects of human MCD?

Much of the pathogenesis of MCD remained unclear, particularly when it was initially perceived to be non-immune mediated. The lack of observable tissue- or podocyte-targeting immune responses (such as infiltrating immune cells or inflammatory responses) during peak disease led to the perception that abnormal peripheral immune cell activity may be responsible

[4, 7, 8]. However, the use of immunosuppressant drugs (especially with the success of RTX to mediate long-term remission), in addition to Ab detection assays and optimized IF staining techniques on renal biopsies, have provided strong evidence of immune involvement, most recently by humoral responses [5-7, 10, 239-241]. While there are animal models of proteinuria and podocyte injury (see **Table 1**), the common caveat shared amongst them is they do not fully recapitulate clinical parameters of human MCD and fail to elicit anti-podocyte immunity. Instead, chemical and some biological agents (e.g. LPS and anti-nephrin Abs) were relied on to induce podocyte injury directly, though not without their downfalls such as adverse toxicity or additional responses (e.g. complement activation, etc.) not related to MCD pathogenesis [252]. Consequently, to be able to characterize how immune mechanisms influenced by the CD4⁺ T-B cell crosstalk induced disease onset and progression, the development of a novel experimental autoimmune model of NS was critical. This was especially prudent as these interactions are unobservable from patient PBMCs. We presented the EANS immunization model induced nephrotic-range proteinuria and developed histological features of MCD-like injury such as podocyte foot effacement, glomerular structural integrity, anti-podocyte auto-Ab production and deposition. This was significant as this was the first instance, to our knowledge, depicting an association of autoimmunity to MCD.

The model utilized throughout this Thesis work does replicate key humoral and clinical aspects of human MCD. Within the kidneys, no detectable changes in renal immune cell infiltration or activation were detected during EANS onset and progression. This reassured that this model 1) recapitulated key aspects of MCD-like injury and 2) suggests that pathological effects occur peripheral to the kidneys, most likely in the rLN. The migration of activated auto-reactive immune cells to the rLN has been implicated in renal disease, though their function in inflammatory kidney disease is still poorly understood [309]. In the context of renal autoimmune disorders, rLN could be an important site where loss of tolerance to self-Ags may occur. With expansion of activated cytokine secreting CD4⁺ T_{EFF} cells, they could potentially be caught in a local pro-inflammatory feedback loop, recruiting more APC's with self-Ags which in turn maintains CD4⁺ T and B cell activity and interactions [310]. For the EANS model utilizing C3H mice throughout this Thesis, we were unable to track the progression of effector responses from CD4⁺ T and B cells from the

draining iLN to the peripheral rLN during nephrotic-range proteinuria due to insufficient cell numbers. Thus, to determine if there are other strains in which the rLN are more easily accessible and known to expand during renal auto-reactivity, BALB/c mice were immunized. Subsequently, sufficient cell events from BALB/c rLN provided preliminary results of increased SM IgG⁺ B cells and memory CD4⁺ T_{EFF} cells.

FoxP3⁺ T_{REG} cells, that are specialized CD4⁺ T cells in preserving immune tolerance, have also been implicated in break in tolerance, particularly with reports of an imbalance in the Th17/T_{REG} cell subsets in adult MCD patients [231, 234-236]. Using the EANS model, no changes in FoxP3⁺ Helios⁺ T_{REG} cells were reported during the development of nephrotic-range proteinuria while pathogenic CD4⁺ T_{EFF} cells and auto-reactive humoral responses still occurred. We suspect there are irregularities in the suppressor function of the FoxP3⁺ T_{REG} cells in the EANS model. Future studies are necessary to identify and characterize the FoxP3⁺ T_{REG} cell suppressor function and their possible dysregulation in MCD, as current knowledge remains limited.

In autoimmunity, HLA-II alleles have been strongly associated with autoimmune disease susceptibility [311]. Recently, single-cell RNA sequencing analysis of BCRs from B cells isolated from relapsing pediatric MCD patients conducted in our lab, discovered a clustering of a particular HLA-type associated with relapsing MCD (**data not released**). These results collaborated with genome-wide association studies noting strong association of MCD susceptibility and HLA gene expression [253]. By challenging distinct allo-incompatible murine strains, it was observed that not all strains were susceptible to develop proteinuria, possibly recapitulating the role of MHC-II in the presentation of the Crb2 Ag. As described previously, extracellular Ags are uptaken within APCs through receptor-mediated endocytosis, processed, and presented onto MHC-II molecules for CD4⁺ TCR ligation [118, 312]. During this process, only a small peptide of the original Ag is presented. Additionally, the polymorphic variant of the MHC-II gene influences which peptide portion of a given Ag is presented to the TCR [312, 313]. However, this could influence the *immunogenicity* of the presented Ag. Immunogenicity and antigenicity are distinct concepts within the realm of immunology [314]. Immunogenicity refers to the ability of an Ag to provoke a humoral and/or cellular immune responses, stimulating the production of Abs and/or the activation of immune cells. Antigenicity, on the other hand, pertains to the ability of an Ag to specifically bind

to immune system components, such as Abs or TCRs, leading to immune recognition and response [315]. This does not necessarily mean that the Ag will induce a robust immune response; it merely signifies that the immune system can detect and interact with the Ag [314]. In essence, immunogenicity focuses on the ability of an Ag to initiate immune reactions, while antigenicity emphasizes the capacity of an Ag to be recognized and bound by components of the immune system [315]. An Ag can possess antigenicity without being highly immunogenic, and an immunogenic Ag will inherently exhibit antigenicity due to its ability to trigger immune responses [314]. Therefore, we theorize the inability to induced proteinuria in BL/6 or the B6C3F1 hybrid mice may be due to the antigenic portion of the rCrb2 Ag presented was not inducing immunogenically strong effector CD4⁺ T cells responses to induce podocyte injury as they express a different MHC-II haplotype. This is especially relevant since there was still strong Ab production. Thus, the next strain we attempted to transpose this EANS model was the BALB/c strain. Much like the BL/6 mice, immunizations against a podocyte-specific Ag have not been previously conducted to our knowledge. While BLAB/c also contains a differing MHC-II haplotype than C3H [316], what made this mouse strain appealing is BALB/c mice tend to have a Th2-biased immune reaction, in comparison to the BL/6 which skewed towards Th1-like reactions [317]. In the end, preliminary results from rCrb2-immunization in BALB/c reported success in proteinuria development and serum anti-Crb2 IgG secretion, and therefore is a promising candidate in the further development of the EANS model.

4.1.2 How are germinal centre reactions key in determining auto-antibody generations?

GC reactions play a critical role in the interactions between B and T cells, as well as the maturation of Abs. Occurring in the secondary lymphoid organs, they are initiated by the activation of Ag-specific B cells by CD4⁺ Th cells; B cells then undergo rapid proliferation and SHM, resulting in the production of high-affinity Abs [138]. Ultimately, the outcome of these interactions and the cytokines secreted by differentiated CD4⁺ Th cells determined the quality and specificity of the Abs produced [95]. The affinity maturation process during this T-B cell interaction ensure the selection of B cells with high-affinity BCRs, providing signals for survival further cellular differentiation; B cells with low-affinity BCRs undergo apoptosis [147, 148]. Our model demonstrated active GC reactions were occurring with the presence of SM B cells and IgG production. In autoimmunity, B

cell maturation in GCs can lead to the production of auto-Abs, which contributed to the development and progression disease [81], reminiscent to what was observed in our EANS model and anti-Crb2 IgG production and glomerular disposition.

The increased expression of MHC-II on IgG⁺ B cells and ICOS expression on CD4⁺ memory T_{EFF} cells within the draining iLN of Crb2-immunized mice during early phases of EANS suggested T-B cells interaction occurred in the GC for IgG-secreting PC differentiation. These interactions with memory B cells can enhance cellular responses of primed-CD4⁺ Th cells through selection of auto-reactive CD4⁺ T cells (observed *in vitro*), the promotion of T cell activity through co-stimulatory molecules binding (e.g. ICOS), and proliferation of specific lineage-differentiated CD4⁺ T_{EFF} cells during re-challenge [302, 318]. Additionally, cytokines such as IL-4 have strong associations with humoral responses by influences affinity maturation and class-switching fate [108]. It has also been implicated in the breaking of peripheral immune tolerance, giving rise to auto-reactive B cells and auto-Ab production by making the B cells resistant to BCR-mediated negative selection in the GC [319]. When comparing the immunopathology of MN, FSGS, and MCD recorded in human patients across different studies, evidence suggested a skewing of CD4⁺ Th2 cell activation and cytokine production. Additionally, an imbalance in the Th17/T_{REG} cell axis was observed, with up-regulation in Th17 differentiation and IL-17A secretion, and the concomitant down-regulation of FoxP3⁺ T_{REG} cell proportion and/or suppressor functions [225, 229, 231, 234, 235, 320-322]. While we are unable to currently observe Th17-associated cytokines in the EANS model, we suspect a higher sensitive analysis (**Section 4.2.2**) may depict IL-17A production as IL-17A is a vital B cell helper for strong proliferation, Ab production with class switching to IgG *in vivo*, and mediator of GC formation in autoimmune disorders [109].

GC reactions is described when Abs undergo SHM and CSR to increase affinity maturation. The increased affinity developed has several important functional implications, with the ability to carry out their effector functions (i.e. neutralization, Fc-mediated function, etc.) being the focus [323]. With FTY720-treatment, we observed an overall suppression of GC reactivity and an eventual decline in anti-Crb2 IgG. Regarding the serum titres, the average anti-Crb2 IgG was still relatively high even when the titres observed in PBS-immunized C3H from previous immunizations were considered. The question remains, if we were still able to detect serum auto-Abs, why are we not

able to detect even faint signals of deposition in the glomeruli? It is possible that the initial anti-Crb2 auto-Abs are not able to cause disease and the FTY720-treatment stunned the maturation of high-affinity auto-Ab development against Crb2. Short-lived PCs are terminally differentiated PC that arise during early phases of both follicular and extrafollicular responses [324]. Found in the extrafollicular site of secondary lymphoid organs, they secreted intense levels of Abs for a brief period prior to cell death [325, 326]. This provides much needed time for Ab affinity optimization and the development of long-lived PCs. Short-lived PCs can be derived from T cell-dependent B cell activation and differentiated from memory B cells from previous reactions and consequently secrete class-switched Igs such as IgG [327, 328]. The Abs that were secreted may not have undergone additional SHM or class-switching maturation to enhance binding affinity, and therefore may not have been capable of critically contributing to podocytopathy [329].

In the early case studies of MCD, when observing incidences of MCD pathogenic was mediated by pathogenic T cells, some cases have indicated atopic diseases, allergic reactions, and viral infections such as human respiratory syncytial virus (RSV) [7, 208, 229, 330] may have triggered auto-reactive T cell responses through molecular mimicry or bystander activation when engrossed in a pro-inflammatory environment [67, 86, 117]. With the proximity of Crb2 and nephrin within the podocyte slit diaphragm, we hypothesize epitope spreading may have occurred as disease progresses in the EANS model, prompting the production of anti-nephrin auto-Abs. Unfortunately, the presence of anti-nephrin serum IgG was not analyzed as the extracellular domain of mouse nephrin is not commercially available but is currently being produced in-house at the time of this Thesis writing for future experiments.

The high-affinity maturation of Abs was evident with the presence of anti-Crb2 IgG preceding proteinuria detection. This was significant as the time between anti-Crb2 IgG detection and the development of nephrotic-range proteinuria was 2-3 weeks which is ample time for the maturation of high-affinity auto-Abs. Moreover, in some organ-specific autoimmune disorders, including some recent MCD cases, auto-Abs could be detected prior to appearance of clinical symptoms [245] and could reflect the presence, nature and intensity of the immune responses occurring and the overall severity of disease for which we reported. The serum auto-Abs, however, did not have the capacity to mediate disease onset individually (passive transfer), which suggested

the aid of peripheral effectors functions (i.e. cytokines, T cells interaction, etc.) is essential for this model. Experimental passive transfer studies conducted from other groups with serum from INS patients (annexin A₂ auto-Abs) or purified anti-nephrin IgG were successful in inducing proteinuria in rodent models [247, 261]. A possible caveat of this experiment was the serum Ab titres were insufficient to induce proteinuria. Another possibility of the unsuccessful serum transfer could be that the auto-Abs were transferred into healthy naïve C3H mice with non-active adaptive immune responses. We hypothesize that for the initiation of NS, an initial injury to the kidneys needs to occur to prime auto-reactive CD4⁺ T_{EFF} cells and B cells. It has been suspected pro-inflammatory responses arising from viral infections, atopic or allergic reactions, or from accidental bystander activation from inflammatory responses not associated with the kidneys, would expose and prime pathogenic CD4⁺ T cells and B cells with podocyte auto-Ags or epitopes resembling podocyte [7, 67, 86, 117, 208, 229]. While it is possible that auto-Abs are not the cause of podocyte injury, they may be maintaining injury and the high titres production needed to maintain that level of injury are influenced by the CD4⁺ T-B cell crosstalk.

The selection of the adjuvant utilized in an immunization can have defining effects on GC formation and B cell maturation. It can also influence the properties of the Ab response generated, including its affinity, specificity, and functional characteristics. [331]. Additionally, responses directed against an Ag are strongly dependent on the adjuvant used to orchestrate the type of effector (e.g. CD4⁺ Th1/Th2 cells, CD8⁺ T cells, etc.) and memory responses [308]. For example, CFA and IFA tend to be biased towards a Th1-mediated response, while Alum favors Th2-mediated responses, and TMG have been suggested to have mixed Th1/Th2 response and produce high IgG titres [282, 332, 333]. Nonetheless, with the successful induction of EANS in C3H mice after rCrb2-immunization with CFA and IFA with high auto-Ab serum titres, we are confident that the current immunization model accurately portrays immunological responses mediating clinical outputs observed.

Newly arising data reveals podocyte-targeting auto-Abs are secreted and detected in the serum of MCD patients during active disease [10, 245]. After RTX treatment, MCD patients who have established remission have a depletion in CD20⁺ B cells phenotypes, which includes the pathogenic SM and non-switched memory (NSM) B cells and naïve B cells [334]. Likewise, auto-

Abs titres decrease in patients in remission [10]. After FTY720-treatment of mice immunized with rCrb2, we reported a reduction in SM B cells and anti-Crb2 IgG serum titres, reminiscent to what is observed in RTX treated MCD patients in remission. It was clear Crb2-specific CD4⁺ T and isotype-switched IgG⁺ B cells were activated prior to the detection of proteinuria in EANS mice along with auto-Ab production. This implied a break in peripheral immune tolerance and/or regulation of the T-B cell crosstalk threshold in this EANS model [329]. Additionally, while the causes of INS remain largely unknown, evidence gathered thus far are in consensus that the pathogenesis of INS is manifested by an imbalance and/or dysfunction of CD4⁺ T cell functions [335]. Based on the results gathered thus far, the biological interpretations make for a strong hypothesis that CD4⁺ T cells auto-reactivity, followed by humoral responses, may be needed to initiate, and then maintain podocyte injury.

4.1.3 How are humoral responses and effector functions linked in the pathogenesis of MCD?

A rise of reports depicting podocyte targeting auto-Abs in patients is giving new light to how auto-Abs are possibly perceived in MCD, yet the role of these Abs remains ill-defined. These reports have described patients at risk of MCD/INS onset or relapse with detectable serum auto-Abs, with podocyte-targeting auto-Abs in serum and glomerular deposition during active disease, which decreased during remission [10, 244, 245, 247-249, 276]. Additionally, in relevance to the SAR-CoV2 (COVID-19) pandemic, there were reports of MCD relapses in patients after long-term remission 10-14 days after exposure to COVID-19 or receiving a COVID-19 vaccination [336, 337]. Overall, the current literature and our results showed that anti-podocyte auto-Abs do have some relevance in proteinuria development, podocyte injury, and clinical consequences associated with MCD. A limitation of this Thesis study is the function of the anti-Crb2 IgG detected within EANS C3H mice with nephrotic proteinuria was not determined and causation yet to be proven. Based on results gathered, we hypothesize binding of auto-Abs to podocytes mediates cytoskeletal rearrangement and protein leakage.

We theorize anti-Crb2 auto-Abs are interacting with podocytes either by 1) directly binding with the extracellular domain of Crb2 activating downstream signals to the actin cytoskeleton, or 2) Crb2-IgG IC's bind to the neonatal FcR (FcRn) thus triggering endocytosis altering cell morphology. In human patients, mutations in Crb2 have been associated with congenital NS with

steroid-resistance [338, 339]. It was also observed in human immortalized podocytes with podocyte-specific Crb2^{KO} showed to have decreased F-actin rich areas [264], suggesting involvement in epithelial homeostasis. Crb2 contains a FERM motif (N-terminal 4.1/ezrin/radixin/moesin) and tyrosine phosphorylation sites in their cytoplasmic domains, allowing for the cross-linking between the PM and the actin cytoskeleton [339]. It was shown by Hada *et al.*, an increase in ezrin phosphorylation in EANS mice with nephrotic-range proteinuria [249]; this increase in ezrin phosphorylation was also observed in preliminary *in vitro* experimentations in our laboratory where human immortalized podocytes expressing mouse Crb2 were incubated with serum from rCrb2-immunized mice (**unpublished data**). The relationship between Crb2 and ezrin has not been fully described, and therefore, it is possible that the auto-Abs produced in the EANS model may be involved in this signaling pathway. The alternative theory for how anti-Crb2 auto-Abs may be mediating podocyte injury is through IC-FcR binding activity. In the case of podocytes, they express surface FcRn to internalize IgG and albumin from the GBM and transport them to the urinary filtrate [172, 340, 341]. As such, the change in podocyte morphology and actin cytoskeleton rearrangement may be due to this interaction between IgG and the FcRn. An example of this would be in the nephrotoxic serum nephritis (NTS) model of GN which is initiated through transfer of anti-GBM Abs, triggering complement pathways and inflammation [342]. Using podocyte-specific FcRn^{KO} NTS mice, it was observed that FcRn^{KO} has significantly reduced symptoms associated with GN including glomerulosclerosis, crescent formation, and albuminuria during the autologous phase of disease (i.e. disease progression rather than induction) [343]. While NS is a group of non-inflammatory renal disorders and our current EANS model have shown little evidence of highly inflammatory responses in the kidney, the persistent high titres of anti-Crb2 IgG in serum of EANS mice makes FcRn-IC interactions of the podocytes a viable avenue of study.

Our overall understanding of the precise role of Crb2 in renal diseases is still rather limited, regardless of growing evidence suggesting Crb2 being involved in the pathogenesis of NS and other renal diseases [263, 264]. Crb2 has been shown to play a role in the polarization and organization of podocytes, which included the trafficking of nephrin to the cell surface for slit diaphragm maintenance [262, 338]. Nephrin is a key component of the slit diaphragm, preventing the leakage

of proteins into the urine. It does so by regulating signalling processes controlling podocyte cell adhesion, cytoskeletal arrangement, survival, lamellipodia formation for cellular migration, and endocytosis. Phosphorylation of nephrin's intracellular domain provided a scaffold for signaling protein recruitment and downstream signalling [198, 199]. It was found that disruption of the Crb2-nephrin interaction leads to defects in podocyte morphology and function, suggesting that this interaction is critical for glomerular filtration [262]. Thus, we hypothesize anti-Crb2 auto-Ab interactions on podocytes exposes nephrin to anti-nephrin auto-Ab development and are enhancing or maintaining podocyte injury in the EANS model. The use of anti-nephrin Abs in a transgenic transfer model showed anti-nephrin has strong immunogenic properties with a link to actin filament rearrangement in podocytes [261]. Significantly noted was the binding of anti-nephrin auto-Abs to podocyte induced MCD injury within 24hrs, prior to immediate progression into FSGS with accompanying immunological factors such as complement activity not associated with MCD [261]. Hence, it would be interesting to determine when the production of anti-nephrin auto-Abs arise in relation to 1) the production of anti-Crb2 auto-Abs and 2) the detection of proteinuria in disease positive mice and correlate to disease severity as observed with anti-Crb2 IgG production.

It was proposed that inflammatory cytokines produced by abnormal CD4⁺ T cell populations can trigger glomerular podocyte injury as serum from nephrotic patients can induce proteinuria in healthy rodents [229, 230]. Specifically, there is evidence describing IL-13 may lead to morphological changes in podocytes, coinciding with case studies of patients in sustained remission showing significant decrease in IL-13 [229, 231]. Increased serum IL-4 levels, along with IL-13, have been connected to pediatric steroid-sensitive NS, with IgE detection during active disease [344]. In a recent case study, two pediatric patients with Atopic Dermatitis (AD, a common pediatric Th2-immune-mediated inflammatory skin disease) complicated with NS were treated with Dupilumab, a monoclonal-Ab dual inhibitor of IL-4 and IL-13 binding to IL-4R α binding. What was reported was a significant relief of NS and AD symptoms [345]. Furthermore, unrelated infections, particularly viral infections, and atopic diseases that generate pro-inflammatory responses, could trigger the onset of MCD in vulnerable individuals [7, 208, 229]. We have observed activated T cells prior detecting proteinuria and the unsuccessful induction of

proteinuria through passive transfer of raw serum from diseased mice. We hypothesize effector factors such as cytokines may work with auto-Abs in combination. This could lead to the binding of auto-Abs to surface cytokine-receptors, which could then cause podocyte restructuring and expose Crb2 for Ab binding. Alternatively, the effector factors may mediate GBM permeability, allowing the passage of auto-Abs for binding to podocytes. As cytokine detection was inconclusive in our study, we propose future experiments (**Section 4.2.2**) using enhanced detection assays on serum samples and *in vitro* co-cultures with rCrb2 reactivation will be necessary to validate this hypothesis.

4.2 EXPLORING THE ROLE OF THE CD4⁺ T-B CELL CROSSTALK IN THE DEVELOPMENT OF MCD AND THE INTERPLAY BETWEEN HUMORAL & CELLULAR FUNCTIONS

The experiments conducted for most of this Thesis centered around the confirmation of the EANS model after modifying the immunization protocol. Once proteinuria and clinical aspects of human MCD injury were confirmed, we then proceeded to characterize initial immune responses to auto-Ag exposure and the development of humoral immunity leading to disease. Additional analysis is necessary to establish EANS as an accurate representation of MCD-like injury. This includes using electron microscopy to confirm podocyte foot process effacement when detecting proteinuria, staining renal sections for complement activity caused by Ig deposition observed in other INS injury types (ex. FSGS) [226], and further developing EANS in BALB/c mice. Moving forward, we propose the following analyses to characterize the consequences of the humoral response and how the CD4⁺ T-B cell crosstalk mediates podocyte injury.

4.2.1 How are humoral responses mediating podocyte cytoskeletal rearrangement and continued podocyte injury?

A principle aim of this Thesis study was to investigate the specificity and characteristics of the auto-Abs produced in response to rCbr2 immunization. While we provided evidence of Crb2-specificity and glomerular binding, we have yet to determine how these auto-Abs are binding to podocytes nor if epitope spreading to nephrin occurred to maintain or enhance disease severity. Additionally, the composition and quality of the IgG subclasses and the presence of other Ab isotypes should be confirmed to better understand the disease pathogenesis. Lastly, while the current findings of high-serum auto-Ab titres correlates with proteinuria severity, we have yet to prove causality of auto-Abs establishing autoimmune etiology of MCD.

First, to investigate the composition of the IgG subclasses of the auto-reactive IgG, an ELISA using the appropriate subclass-specific secondary Abs would determine the relative amounts of IgG1, IgG2a, IgG2b, and IgG3 in the serum. This could also give insight to the type of effector responses occurring during EANS as Ig class-switching and functions are strongly linked to the cytokine milieu secreted by specific CD4⁺ Th cell subsets [95]. In the study released by Hada *et al.*, they characterized the IgG subclasses deposited in the glomerular of EANS C3H mice 5-weeks post-initial immunization when proteinuria and podocyte foot process effacement was first detected. They reported a predominant expression of IgG1, followed by IgG2a and IgG2b, and faint fluorescence from IgG3 [249]. Secreted cytokines also influence CSR during GC reaction to produce IgA and IgE Abs, further influencing the type of humoral response against the target Ag [150, 158-160]. The isotype classification of secreted Abs would be quantified through ELISA and IF glomerular staining. Next, to determine whether there was a difference Ab maturation an ELISA would be performed with a chaotropic agent (ex. urea) present. In the presence of a chaotropic agent, interactions between the anti-Crb2 IgG and fixed rCrb2 would be interrupted; concentration at which the chaotropic agent disrupts this interaction provides value information as low avidity Abs are more sensitive to dissociating effects and therefore their binding decreases drastically compared to high-avidity Abs [346]. The estimated Ab binding avidity of the auto-reactive IgG would then be compared to fluorescent binding intensity from glomerular IgG IF staining to determine if the avidity binding and level of IgG binding correlated to proteinuria levels. Lastly, with regards to the close proximity and interactions between Crb2 and nephrin occurring in the slit diaphragm [262, 264], and the ability of anti-nephrin Abs to induce heavy proteinuria and NS in other mice models [261], an ELISA using a recombinant protein of nephrin's extracellular domain would determine if epitope spreading occurred during EANS disease development with rCrb2-immunization. Since nephrin is a vital slit diaphragm protein, we also wonder if the presence of anti-nephrin Abs would correlate to disease severity.

Although our study provided evidence for the presence of anti-Crb2 auto-Abs and their relation to disease severity, in addition to proposing future experiments to further describe the specificity and characteristics of auto-Abs produced in the EANS model, the functions of these Abs in inducing proteinuria are not yet fully understood. To address this knowledge gap, we propose

the following future experiments which were designed around the hypothesis that podocyte-bound auto-Abs arbitrates cytoskeletal rearrangement, for which we theorized is mediated through one of two main pathways: 1) activating Crb2 signaling to the actin cytoskeleton by directly binding to the extracellular domain, and/or 2) Crb2-IgG IC binding to surface FcRn and inducing endocytosis.

First is that allogenic IgG binding to the extracellular domain of Crb2 activates Crb2 signaling to the actin cytoskeleton. Our proposal is to conduct an *in vitro* study to take serum samples from mice that have a strong response to EANS, and then incubate those samples on immortalized podocytes expressing mouse Crb2. Observation required on the downstream phosphorylation of ezrin, an indicator of Crb2 signaling activation, [339]. If true, we would expect to see an increase in ezrin phosphorylation in podocytes and cytoskeletal rearrangement after phalloidin staining of actin filaments [347]. Although immortalized podocytes do not have same morphology as primary podocyte *in vitro* cell lines or podocytes *in vivo*, we will still be able to assess F-actin arrangement as thick actin bundles or overall disruption [348, 349].

Second, IgG from the GBM is internalized into the podocytes after ligation to the FcRn expressed on the surface of podocyte [172, 340, 341]. It is theorized the removal of soluble GBM- and podocyte-targeting auto-Abs may be a protective measure to reduce the severity of EANS. To test this, serum from EANS mice would be incubated on podocytes after FcRn blocking (e.g. monoclonal Ab treatment) *in vitro*, for which cells will be IF stained to monitor podocyte morphology and mouse IgG internalization. Additionally, we propose to conduct these experiments in a podocyte-specific FcRn^{KO} model to see if missing FcRn can abrogate EANS severity *in vivo*. If this hypothesis is correct, we expect to see an increase in the severity of EANS and a decrease in urinary IgG in the due to the inability of podocytes to remove auto-Abs.

To better understand the direct consequences of podocyte function influenced by bound auto-Abs, we propose two experiments – a wound healing assay to assess motility and a permeability assay to evaluate the capacity of podocytes. Podocyte motility is a crucial aspect of the normal glomerular function and is coordinated by the Rho GTPases and ezrin [350]. To assay motility, in a confluent plate of podocytes a wound is created by scratching down the middle and

the podocytes are allowed to migrate towards the wound. The rate of gap closure would correlate to the motility of podocytes. It is known that motility is associated with nephrosis [351], and therefore, by adding serum containing auto-Abs which help mediate cytoskeletal rearrangement we theorize an increase in podocyte motility would be observed. Simultaneously being the specialized filtration cells of the kidneys, podocyte permeability is an incredibly important aspect of the glomerular filtration barrier. The permeability assay would involve growing a layer of primary podocytes cells between two chambers, for which slit diaphragms would develop between adjacent podocytes. After the incubation of serum from disease positive EANS mice, podocyte permeability would be assessed. If the podocyte slit diaphragm is compromised leading to increase permeability, that would suggest auto-Abs produced from rCrb2-immunization and after immune activation mediate cytoskeletal rearrangement and loss of slit diaphragm connections.

A question that still needs to be answered is whether the auto-Abs produced after rCrb2-immunization can enter healthy glomerular and bind to podocytes or do they require initial access mediated by pro-inflammatory responses? This is in response in anti-Crb2 serum's inability to induce proteinuria in healthy mice in addition to the flow cytometry analysis revealing activation of CD4⁺ memory T_{EFF} cells within the draining iLN of EANS mice. We hypothesize an initial injury to the podocytes will allow podocyte auto-Ags to be released and be presented to pathogenic T cells, breaking immune tolerance, and initiating podocyte injury. To test this, serum from disease positive EANS mice would be incubated on renal sections from healthy mice (control) and various renal injury models, including but not limited to NTS (inflammation), ischemia reperfusion injury (physical injury), LN (auto-Ab mediated), RVS-mediated renal injury, and analysed via IF staining.

Prior to these inquiries, it would be prudent to ascertain whether auto-Abs play an intrinsic role in the autoimmune etiology of MCD-like injury in this EANS model, and therefore we need to prove the causative link between anti-Crb2 auto-Ab production to disease severity. The initial work done thus far do demonstrate a notable correlation between the levels of auto-Abs and the severity of proteinuria, particularly in the early stages within the EANS model. However, attempts to establish a causal relationship encountered challenges. Efforts involving passive serum transfer and the FTY720-treatment experiment failed to provide conclusive evidence for causality; the

latter experiment requires revisiting while ensuring prevention of B cell activation and differentiation suppression. Furthermore, a prospective strategy entails the creation of genetically modified mice to impede serum Ab secretion. One avenue for investigation could utilize the versatile Cre-Lox KO model. For example, researchers explored the role of B cell-specific B-lymphocyte-induced maturation protein-1 (BLIMP1) expression by creating $p38^{fl/fl}CD19^{cre}$ KO mice to hinder the differentiation of B cells to PC during T cell-dependent and -independent activation [352]. A second strategy could involve a transgenic mouse model, as utilized in a murine SLE study, where a mutant transgene encoded surface IgM expression while restricting Ig secretion. For there, they crossbred these mice with B cell deficient counterparts to yield offspring with functional B cells incapable of substantial serum Ig production [353]. Regardless of the methods described, both studies reported a significant depletion of serum Abs while maintaining robust cellular responses including B cell activation and APC functionality, and auto-reactive T cell responses [352, 353], and therefore could allow us to observe if the absence of anti-podocyte target auto-Abs alleviates EANS disease severity in our model. As an added bonus, with the integrity of cellular responses and memory B cell subsets conserved with these genetic mouse model, it could allow additional exploration of their individual roles in autoimmune processes during disease onset independent of humoral responses.

4.2.2 How is the T-B cell crosstalk mechanistically involved in podocyte injury and MCD pathogenesis in the murine EANS model?

Further investigations are needed to understand the complex interplay between the $CD4^+$ T-B cell crosstalk, secreted cytokines, and auto-Abs in the development and progression of NS in our model. Multiplex cytokine assays would be performed to determine if there are differences in $CD4^+$ Th cell-associated cytokines at early, peak, and at late stages of EANS progression. These cytokines could be correlated with the type of Abs produced during those times, which could be linked to the maturation of these auto-Abs. In addition, it is essential to investigate the potential influence of the $CD4^+$ T-B cell crosstalk on the class-switching of Ig during B cell activation and differentiation into PCs. To achieve this, cytokine assays of the serum and supernatants of cultured $CD4^+$ T cells isolated from immunized mice should be performed. The cytokines measured would include $IFN\gamma$, IL-4, IL-13, and IL-17A, as they have a role in the regulation of B cell activation, proliferation, and differentiation and are associated with specific $CD4^+$ Th cell subsets [92, 95].

While the results presented in this work have shown GC responses occurred with the presence of activated CD4⁺ T_{EFF} cells and SM IgG⁺ B cells during EANS development EANS, the actual interaction between these cell types has yet to be demonstrated. To understand the role of the CD4⁺ T-B cell crosstalk in EANS onset and progression, the next step would be to investigate what happens if these interactions were disrupted. To disrupt T-B cell interaction, CD20⁺ B cells in C3H mice will be depleted with a single dose of a mouse anti-CD20 mAb prior to immunization with rCrb2. We aim to 1) demonstrate a shift in B cell phenotypes results in protection from EANS, 2) observe if inhibiting pathogenic B cell activation dampens CD4⁺ T_{EFF} cell responses, and 3) reinforce the role anti-podocyte auto-Abs in EANS as SM B cell activation and PC differentiation will be abolished. While this experiment will provide valuable insight into the role of pathogenic SM B cells in EANS, supplementary studies will need to be conducted. To gain a better understanding of the role B cells play in EANS induction and to characterize how CD4⁺ T-B cell interactions lead to podocyte injury in this model, two approaches can be employed: Firstly, adoptive transfer of primed re-activated SM B cells from rCrb2-immunized mice to naïve mice can be done. Secondly, target-specific genetic models such as H2-Ab1^{tm1Koni} x CD19^{creERT2} mice, which specifically remove MHC-II from B cells, can be used. Likewise, Crb2-primed CD4⁺ T cells could be transferred into αβTCR deficient mice (ex. Tcrb^{tm1Mom}), thus depleting T cells, prior to rCrb2-immunization. Responses of the transferred CD4⁺ T cells and B cells would then be measured. A direct approach in observing the CD4⁺ T-B cell crosstalk during EANS onset would be to observe GC responses occurring in the secondary lymphoid organs via flow cytometry and confocal microscopy [148]. Finally, a co-culturing experiment where rCrb2-loaded B cells are cultured with isolated rCrb2-primed CD4⁺ T cells for 96-hrs *in vitro* could assess CD4⁺ T_{EFF} cell activation, CD4⁺ Th cell lineage differentiation, and cytokine production using flow cytometry. This approach could help to determine CD4⁺ T_{EFF} cell responses influencing EANS onset and progression.

Lastly, while some nephrotic diseases are mediated by podocyte protein mutations, particularly those associated with the foot process and slit diaphragm such as *NPHS1* [200, 201], reports of familial MCD or gene mutations associated with disease susceptibility have not been identified to date [354]. Recently, some mutations have been described to influence responses to treatment as described in steroid-resistant NS with Crb2 mutations or recently mutations found

in the kidney ankyrin repeat-controlling (KANK) regulating Rho GTPase activity [237, 263]. To better understand molecular mechanisms underlying disease onset, numerous groups looked at HLA risk alleles of steroid-sensitive NS patients and identified HLA-DQB, HLA-DBA, HLA-DRB1, HLA-DQB1, HLA-DQW2, and HLA-DR7 regions to be significantly associated with childhood steroid-sensitive NS in MCD and FSGS [253, 355]. While attempting to transpose the EANS model from C3H to other mice strains, we theorized that the failure to induce proteinuria in particular strains such as BL/6 was linked to differing MHC-II alleles expressed between strains. It led us to inquire if an immunogenic epitope of Crb2 Ag was being presented on particular HLA-alleles to CD4⁺ T cells to induce stronger auto-reactive responses mediating podocytopathy. To determine the immunogenic epitope, APC's isolated from rCrb2-immunized EANS mice would be loaded with the full rCrb2 Ag (control) or pre-cleaved peptides of the rCrb2 Ag. The loaded APCs would then be co-cultured with isolated Crb2-primed CD4⁺ T cells for which T cell activation and proliferation (i.e. CTV staining) would be observed. Epitopes able to activate T cells would be the immunogenic portion of rCrb2 inducing disease.

Overall, the proposed experiments aim to investigate the specificity and characteristics of the anti-Crb2 IgG auto-Abs produced in response to rCbr2 immunization. By understanding the composition, quality, and function of the auto-Abs, as well as the potential influence of T-B cell interactions and their effector functions in the development and progression of EANS, we could better understand the mechanisms of podocyte injury and potentially develop targeted therapies to prevent or treat NS.

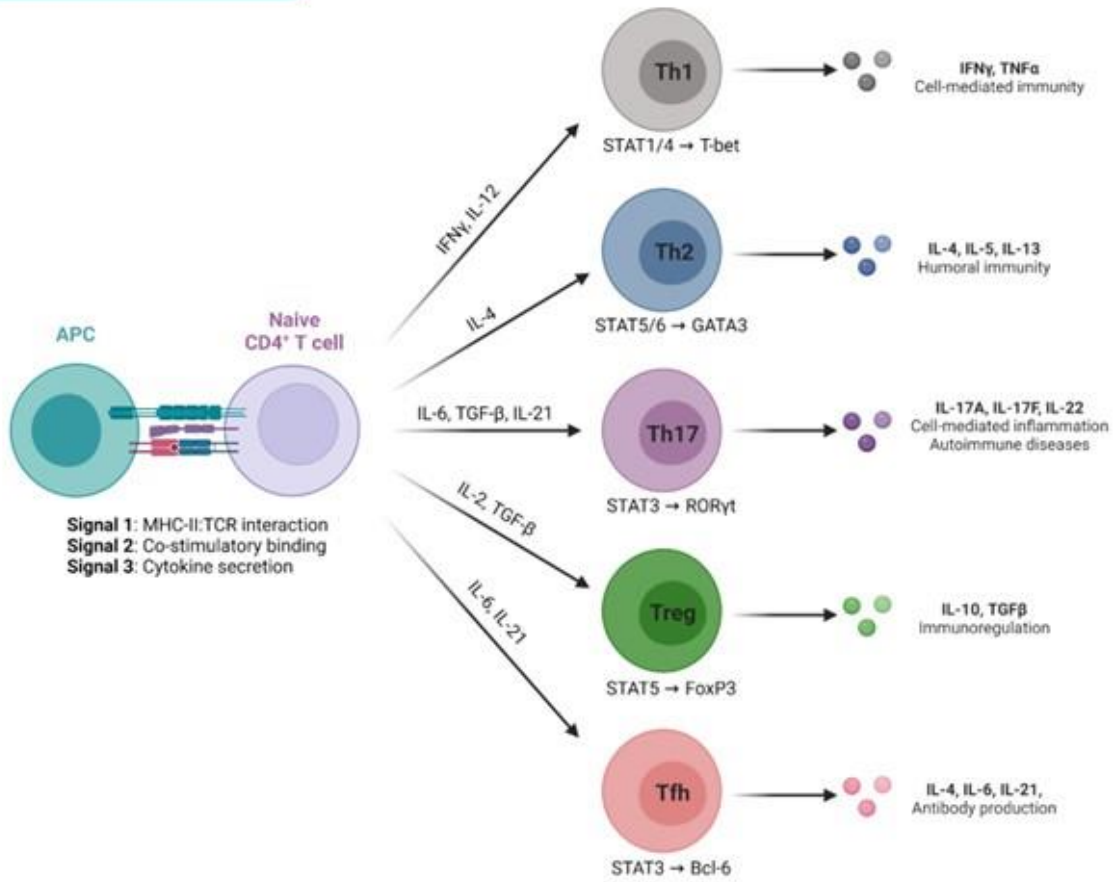
Chapter 5: CONCLUSION

An initial glomerular assault is thought to occur to patients who develop INS/MCD, leading to the release of auto-Ags after podocyte injury. With cumulating evidence that both cellular and humoral immunity influence INS injury and MCD [208, 229, 230, 239, 240], we hypothesize anti-podocyte auto-Ab production sustained by activated cellular responses after auto-Ag exposure, mediate glomerular deposition and podocyte binding leading to proteinuria and MCD-like NS injury. The successful establishment of this immunization model to immunologically induce NS resembling human MCD with anti-podocyte auto-Ab production provides the medium for in-depth analysis into INS immunopathology. Particularly, the presence of serum auto-Abs, deposition into the glomeruli with podocyte binding, and a positive correlation to severity of disease has demonstrated auto-Abs may have more important role in MCD than previously believed. While early activation of peripheral IgG⁺ SM B cells and memory CD4⁺ T_{EFF} cells was observed, further characterization of these cellular responses and their role in the mechanism of podocyte injury in the EANS model still needs to be conducted. The significance of these current and discussed future analyses are not to be understated. They begin to fill in the knowledge gap of immune responses potentially responsible for inducing and influencing humoral responses observed in conjunction with podocyte injury in patients with INS and MCD and guide future functional studies of podocytopathy and potentially more targeted treatment options.

Conflict of interest disclosure: The authors declare no competing financial interests.

FIGURES & TABLES

CD4⁺ T cell differentiation



B cell differentiation

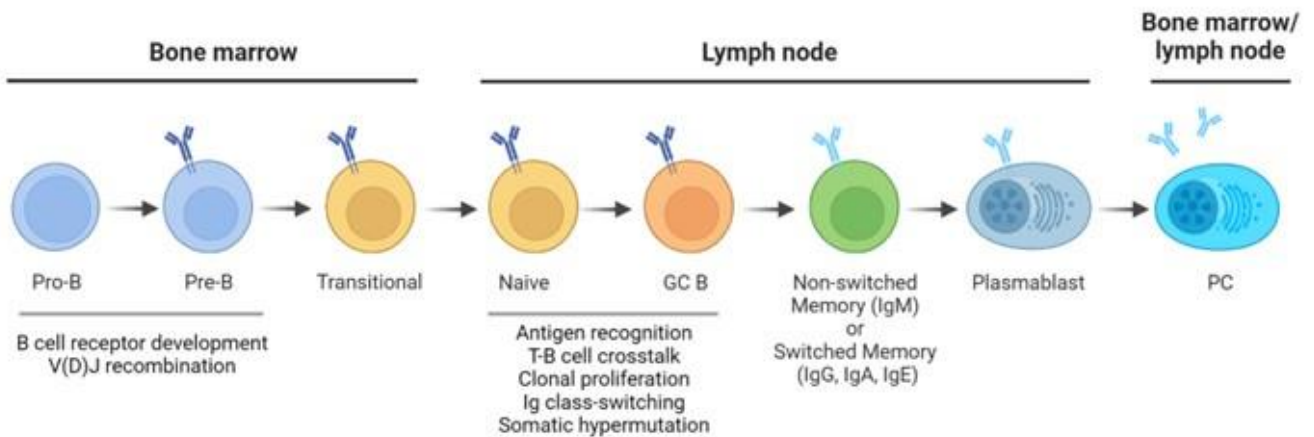


Figure 1. Activation and differentiation of CD4⁺ T cells and B cells.

(TOP) Full activation of naïve CD4⁺ T cells to CD4⁺ T_{EFF} cells requires 3 major signals: 1) MHC-II:TCR interaction, 2) co-stimulatory molecule activation, and 3) cytokine secretion. Differentiation of activated CD4⁺ T cell into specific helper T cell subsets is determined by the environment cytokine milieu, inducing expression of lineage-specific transcription factors T-bet (Th1), GATA3 (Th2), RORγt (Th17), FoxP3 (T_{REG}), and Bcl-6 (Tfh). Each Th cell lineage produce particular pro- and anti-inflammatory cytokines to respond against different pathogen types and to mediated humoral responses by B cells. **(BOTTOM)** Cellular stages of B cell development and differentiation. Within the BM, BCR develop on immature B cells through V(D)J rearrangements, giving rise to a highly diverse repertoire of membrane-bound Ig's. Naïve B cells that have migrated to secondary lymphoid organs are activated upon Ag-BCR ligation and additional interactions/signals from CD4⁺ T cells (T cell-dependent activation), allowing them to clonally proliferate, and undergo CSR and SHM. B cells will then differentiate into memory B cells and long-lived PCs that secrete high-affinity Abs. B cell differentiation to PC's can be followed by the expression of surface markers CD20 and CD138 from naïve to SM and NSM memory B cells (CD20⁺CD138⁻), to plasmablasts (CD20^{int}CD138⁺), finally to terminally differentiated long-lived PC's (CD20⁻CD138⁺). Figure created with BioRender.

T cell-dependent antigen response

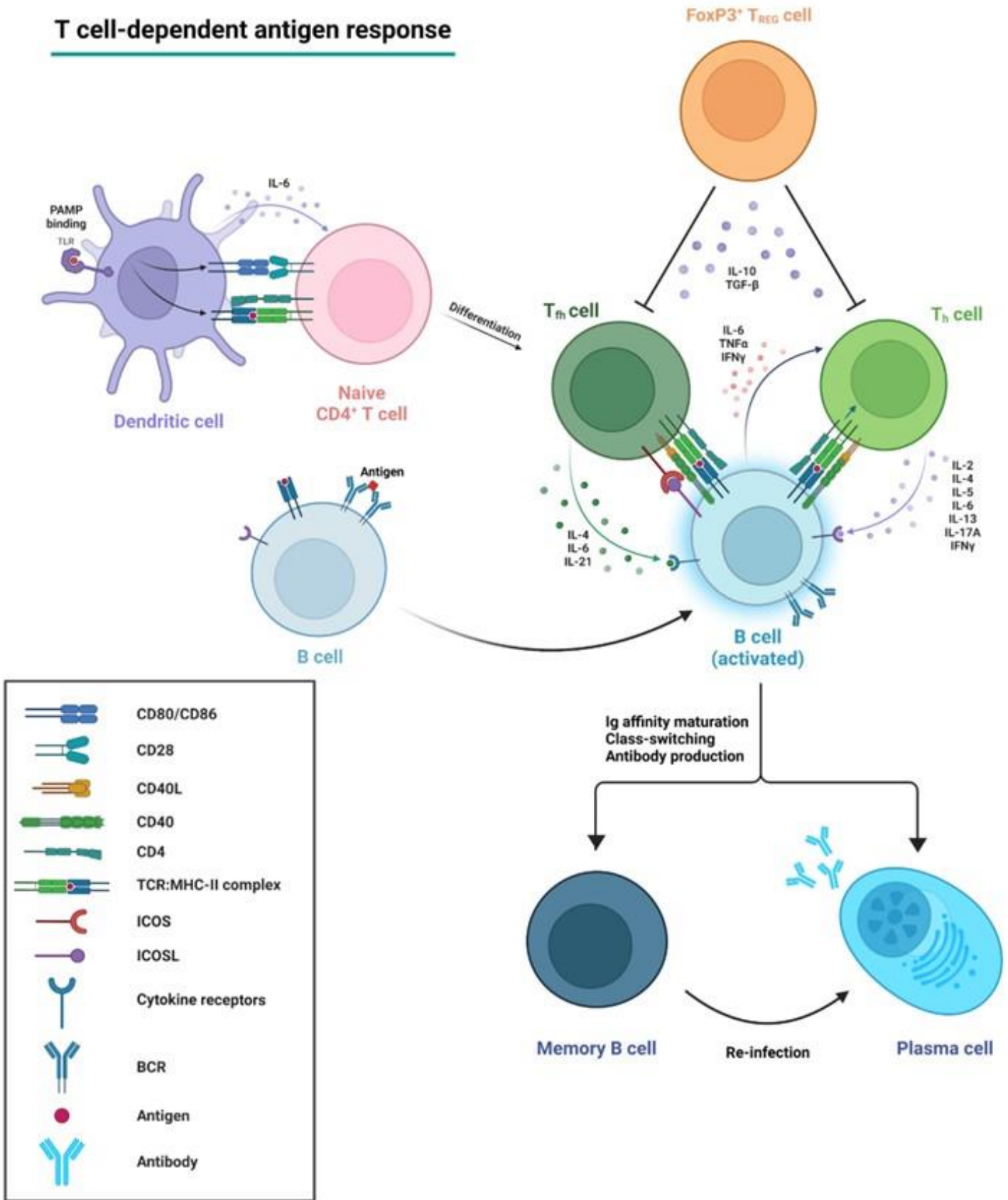


Figure 2. The T-B cell crosstalk is critical for protective immunity and represents a key junction in the development of autoimmunity.

Naïve B cells recognize specific Ags through their BCR and internalize the Ag to present on MHC-II complex. Activated B cells first interact with CD4⁺ Tfh cell in the GC of secondary lymphoid organs and provide signals to B cells for their maturation into Ab-secreting PCs or memory B cells. Activated B cells also interact with pre-activated CD4⁺ Th cells responsive to compatible Ag through TCR:MHC-II ligation. Activated Th cells produce cytokines that promote B-cell proliferation, differentiation, and Ab production. B cells can also produce cytokines to influence and enhance effector responses by CD4⁺ Th cells. FoxP3⁺ T_{REG} cells can suppress interaction and therefore downstream differentiation and secretion of Abs. The interactions between T and B cells are crucial for the development of a robust immune response to pathogens. Various autoimmune disorders have been associated with dysfunction and dysregulation of the T-B cell crosstalk at various points of this interaction. Figure created with BioRender.

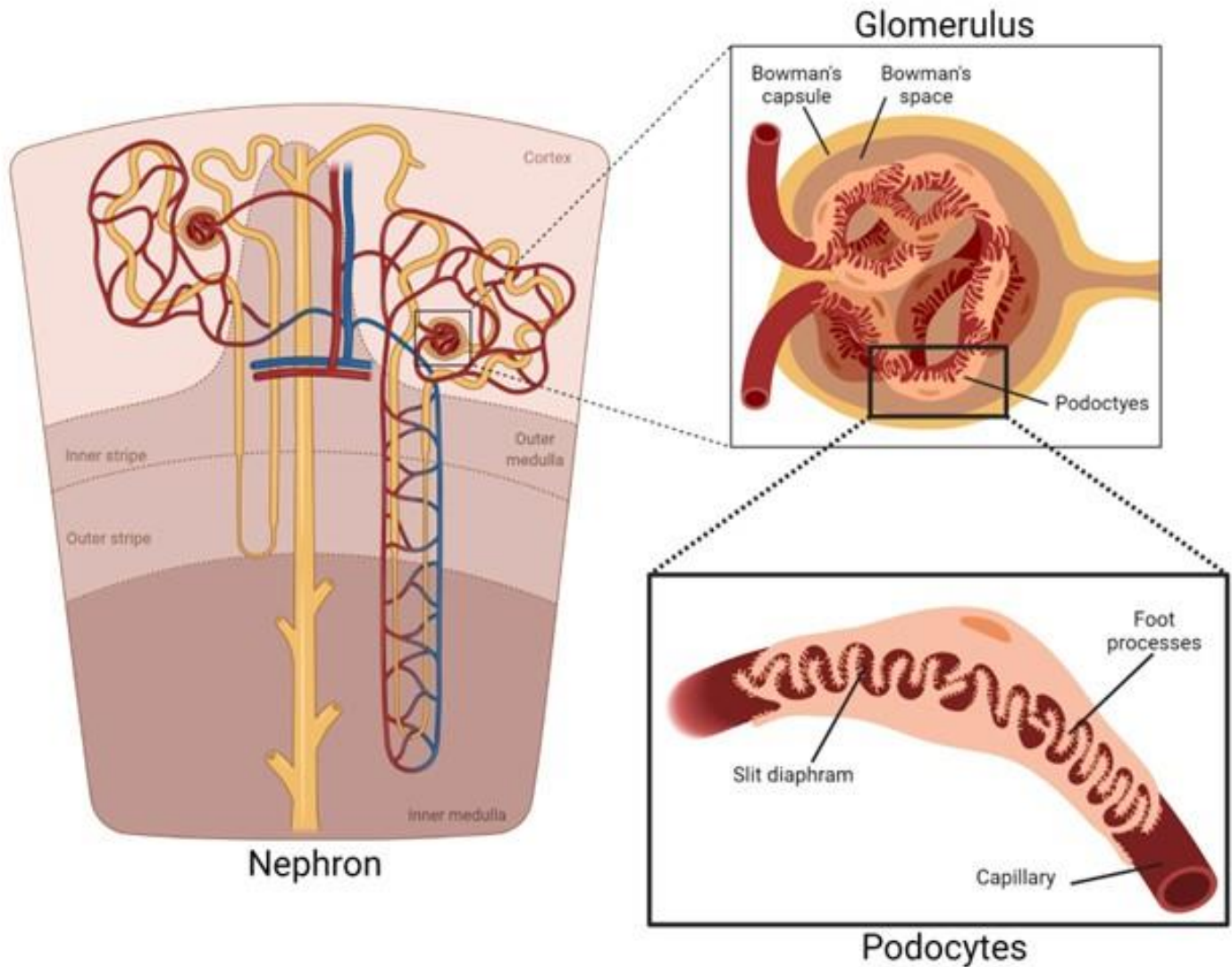


Figure 3. Glomerular filtration is the renal process where ultrafiltrate from the blood is filtered through the podocytes.

Glomeruli are the filtration unit of the kidneys located at the head of the nephron. They comprise of a cluster of capillaries surrounded by a Bowman's capsule, which collects the filtered fluid, called filtrate, and channels it to the rest of the kidney for further processing. Podocytes are specialized epithelial cells essential for kidney filtration. Using their foot processes to wrap around the glomerular capillary, adjacent podocytes make interlocking slit diaphragms for ultrafiltration. Figure created with BioRender.

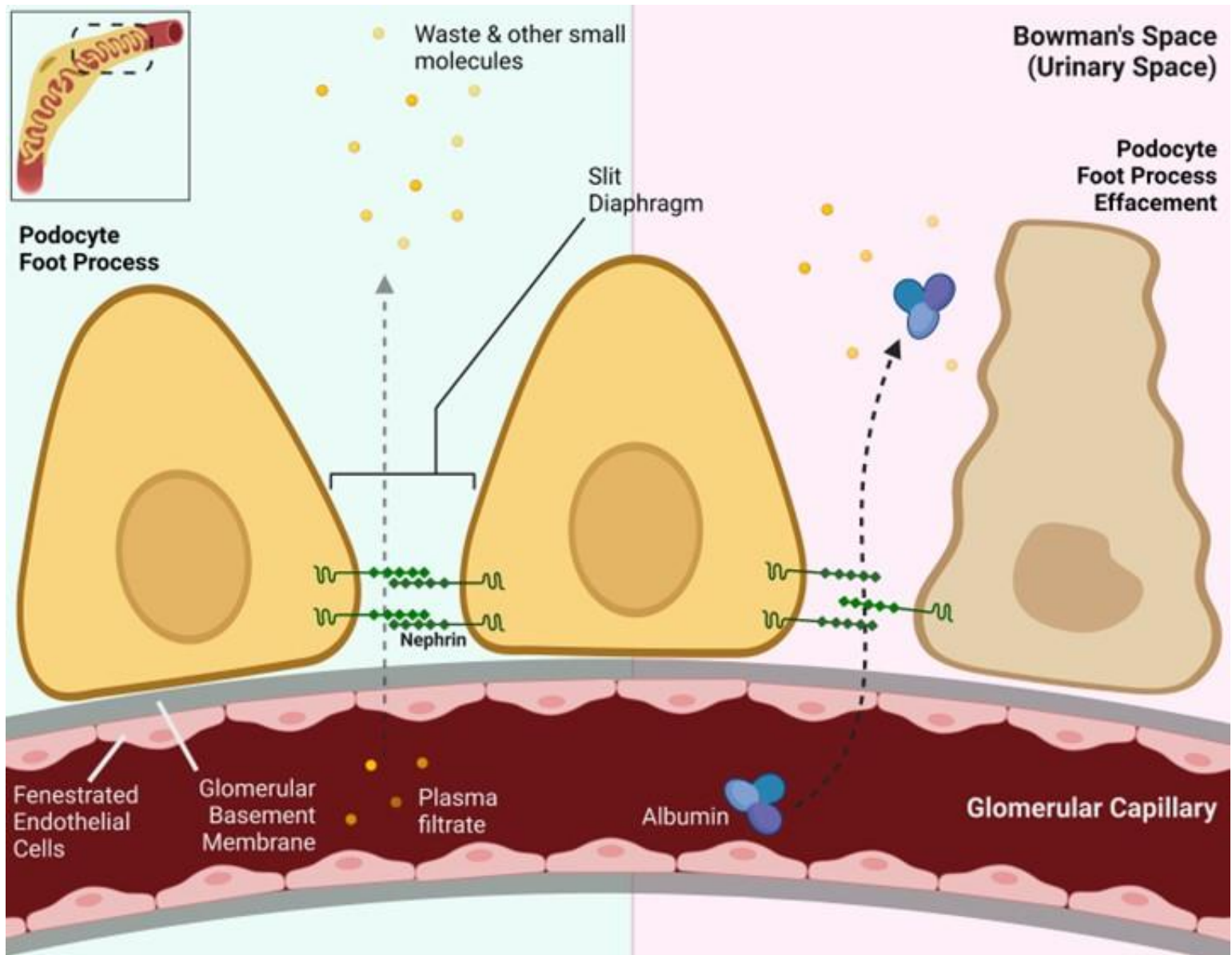


Figure 4. Podocyte foot process effacement causes proteinuria – a common symptom in nephrotic syndrome.

Glomerular capillaries are lined by a thin layer of porous fenestrated endothelial cells, surrounded by a charged layer of GBM, and then by the podocytes. Podocytes form a complex network of interdigitating foot processes with each other and wrap around the glomerular capillaries. The foot processes are separated from each other by narrow spaces bridged together by a series of intercellular junctions called slit diaphragms. Nephrin is essential for the formation and maintenance of the slit diaphragms, which help to regulate the selective permeability of the glomerular filtration barrier. Dysfunction or damage to the foot processes and slit diaphragms, known as podocyte foot process effacement, can lead to kidney disease as the filtration barrier becomes compromised and allows the loss of important molecules from the blood. Figure created with BioRender.

T cell Involvement

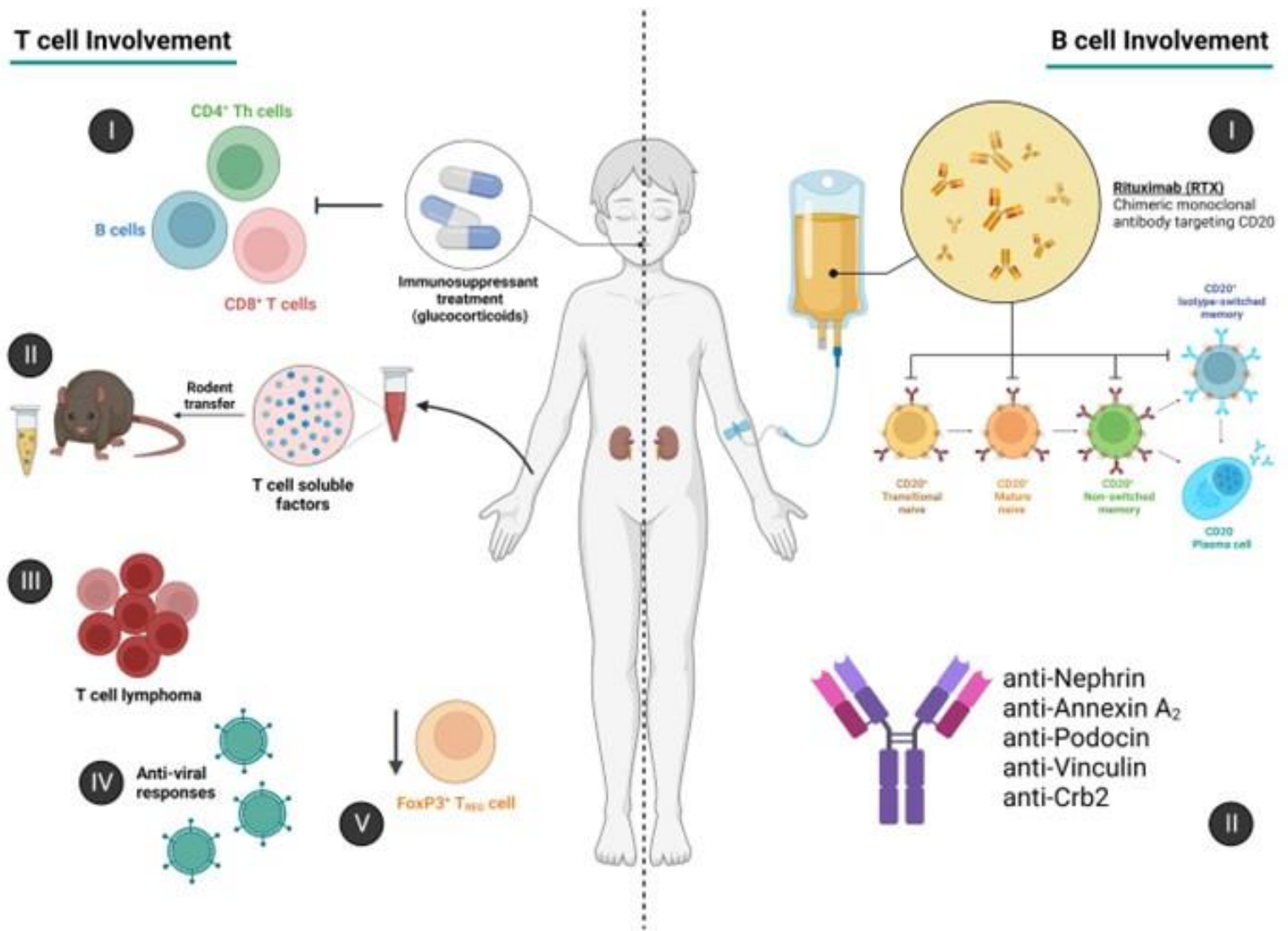


Figure 5. Evidence of immune cell involvement in MCD pathology.

(LEFT) Classical evidence of T cell involvement in MCD pathology. (I) Patient responsiveness to immunosuppressive drugs. (II) The ability of passively transferred T cell cultured supernatants inducing proteinuria in rodents. (III) MCD may occur in cases of T cell hyperproliferation such as T cell lymphomas. (IV) Relapse and remission occurring following viral infections. (V) Dysregulation of FoxP3⁺ T_{REG} cell suppressor function observed during MCD. (RIGHT) Emerging evidence of B cell involvement in MCD pathology. (I) Prolonged remission following treatment with B cell-specific monoclonal anti-CD20 Ab depicted the elimination of pathogenetic isotype switched memory B cells. (II) Detection of auto-Abs in serum of relapsing MCD patients targeting podocyte-specific Ags. Figure created with BioRender.

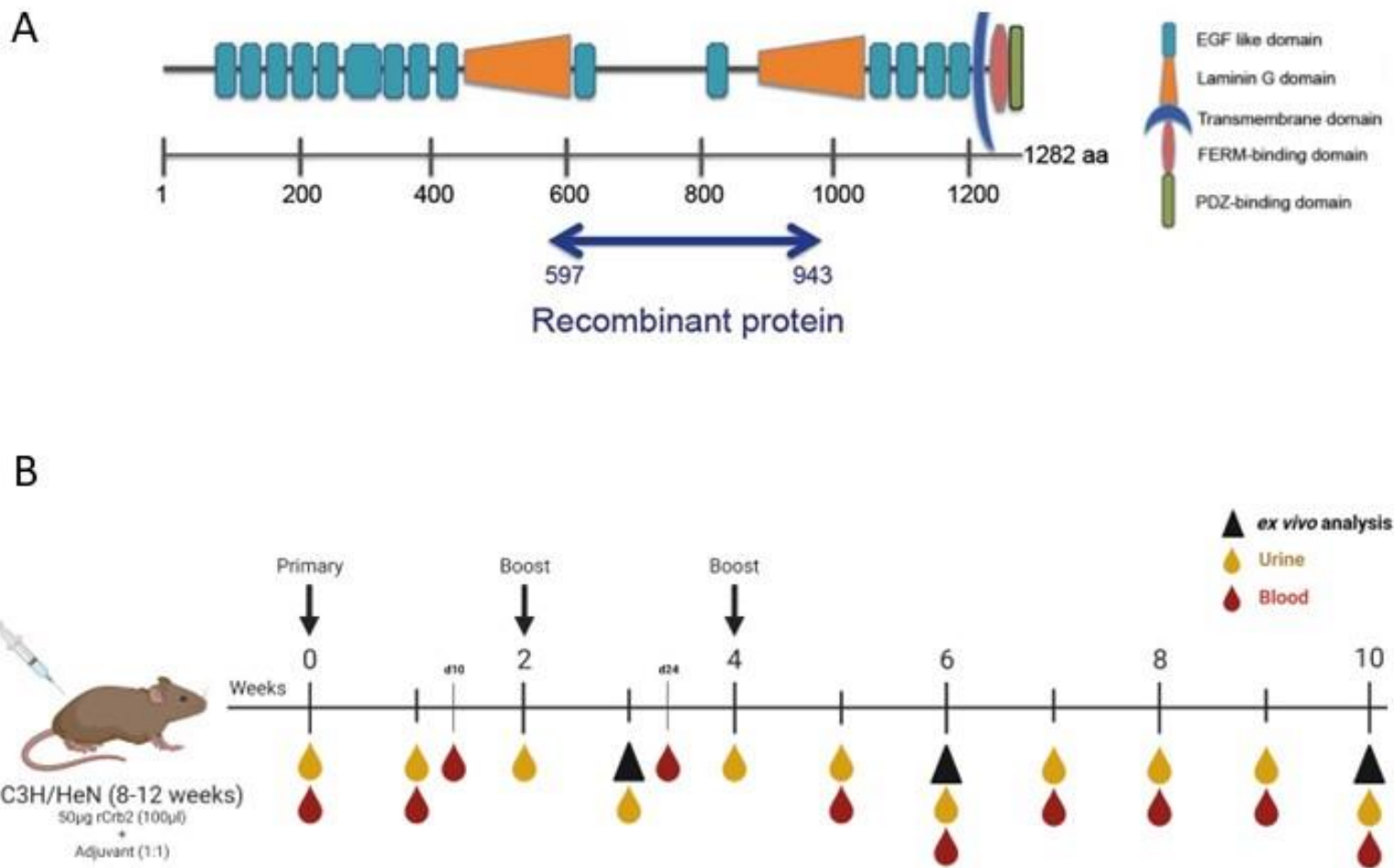
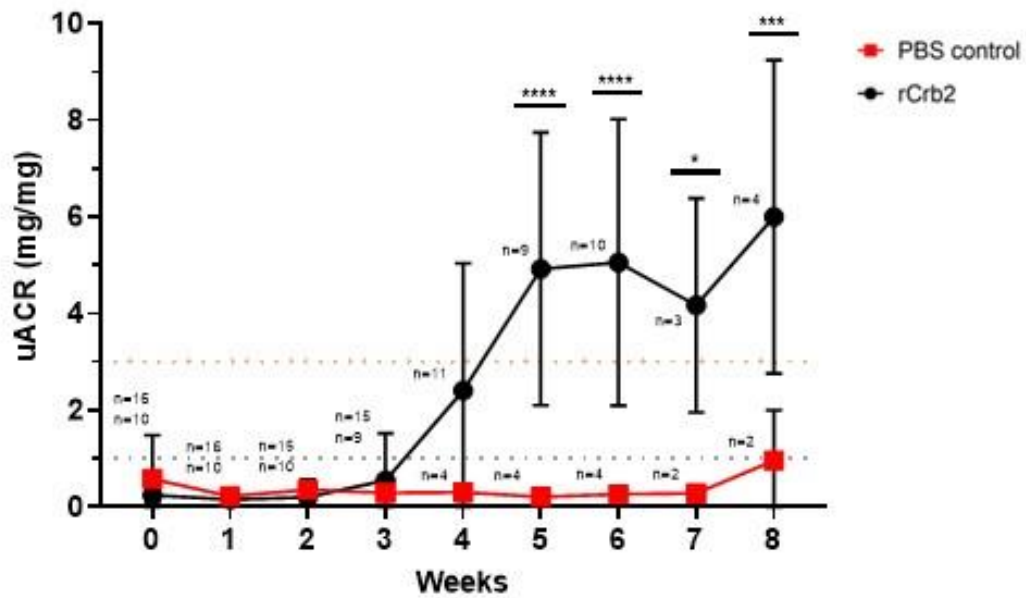


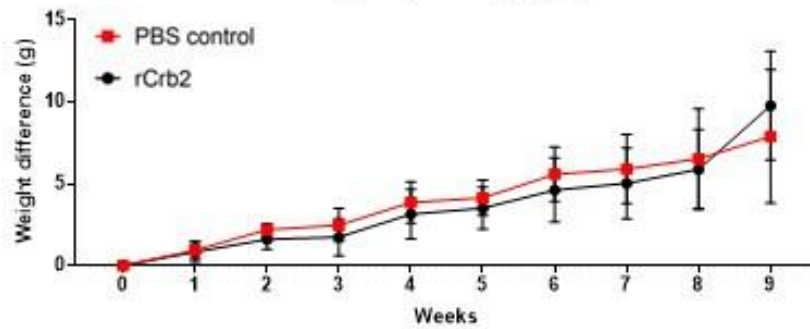
Figure 6. Immunization protocol of C3H/HeN mice with podocyte-specific Crb2.

(A) Structure of recombinant mouse Crb2 protein (extracellular domain) injected in mice during the immunization process. Figure provided and modified from [Hada *et al.*, 2022](#). (B) Schematic timeline of the rCrb2-immunization to induce proteinuria and EANS in male C3H mice and timepoints of urine and blood collection. The immunization protocol was adapted from [Hada *et al.*, 2022](#); subcutaneously injected mice biweekly with 200µl emulsified 50µg purified rCrb2 (or PBS) in a 1:1 emulsification with CFA (primary immunization) and IFA (boosters) bilaterally. Urine and serum samples were collected approximately weekly for ELISA quantification of Ig titres and albumin/creatinine levels (proteinuria severity). Mice were sacrificed at weeks 3, 6, and 10 where kidneys, spleen, and draining iLN were collected for various physical, biochemical, and *ex vivo* immunophenotyping analysis. Figure created with BioRender.

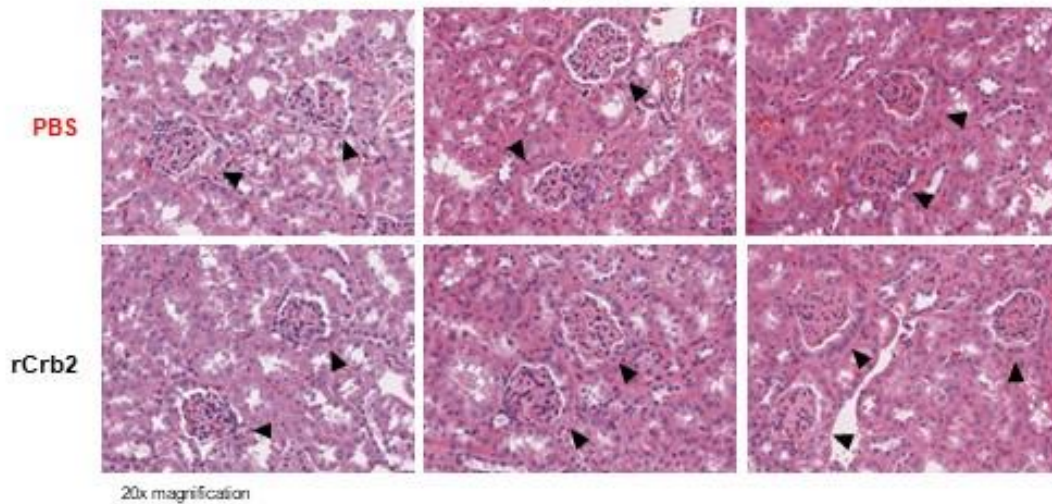
A Proteinuria



B Body weight change (avg)



C 3 weeks 6 weeks 10 weeks



D iLN Kidneys

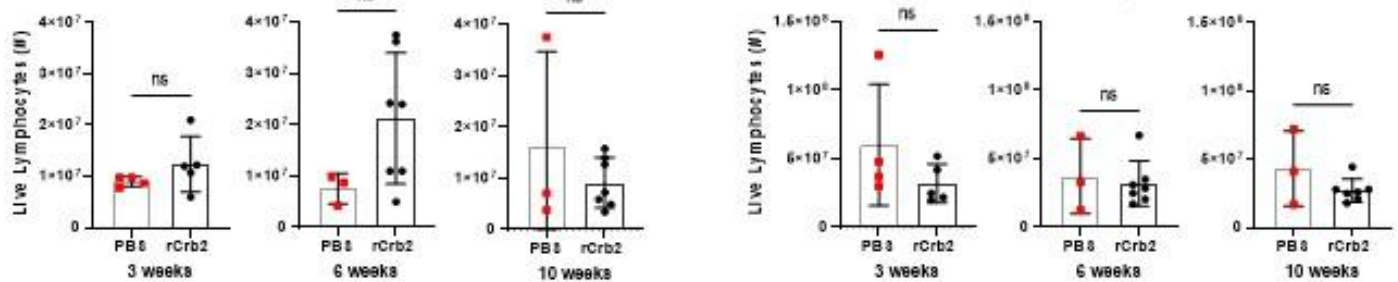


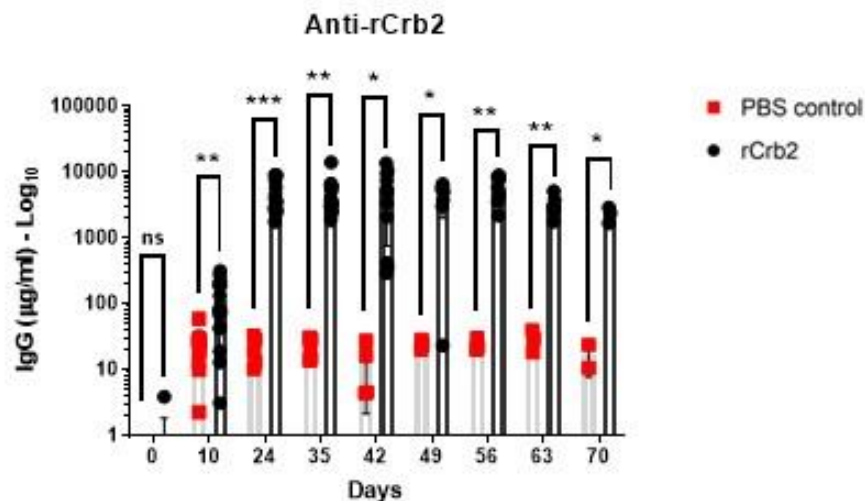
Figure 7. rCrb2-immunized mice developed nephrotic injury with histological features resembling MCD.

(A) uACR were analyzed from spot urine samples collected weekly during immunization and quantified by ELISA. C3H mice immunized against rCrb2 begin developing proteinuria 4-weeks post initial immunization. Mean uACRs displayed. Grey dotted line references minimal range uACR for nephrotic-range proteinuria; pink reference minimal threshold for uACR analysis at past endpoint.

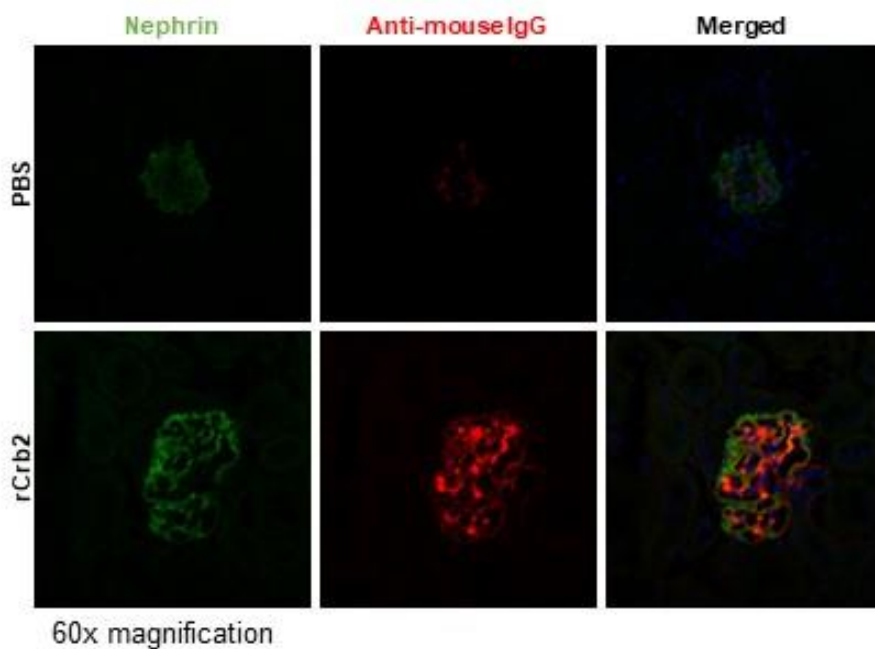
(B) Mice were regularly weighed during the immunization timeframe and weekly after the last boost. Displayed ratio change in weight in relation to day 0. **(C)** Kidney sections for histology were collected 3-, 6-, & 10-weeks post-initial injection. Tissues sections were cut to 4 μ m thickness and stained with H&E to reveal any infiltrating mononuclear cells. No detectable change in glomeruli structure were observed or infiltrating immune cells detected. Representative images of control and high proteinuric rCrb2 mice at 20x magnification with black arrows pointing towards glomeruli.

(D) Live cell counts from draining iLN, spleens, and kidneys of immunized mice prior to analysis. Statistical significance was tested using 2-way ANOVA Tukey multiple comparisons test. $p \geq 0.05$ (ns), $p < 0.05$ (*), $p < 0.01$ (**), $p < 0.001$ (***), $p < 0.0001$ (****).

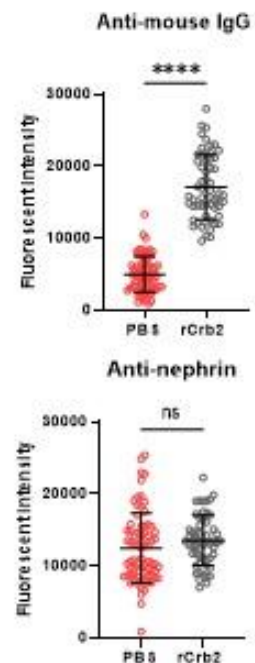
A



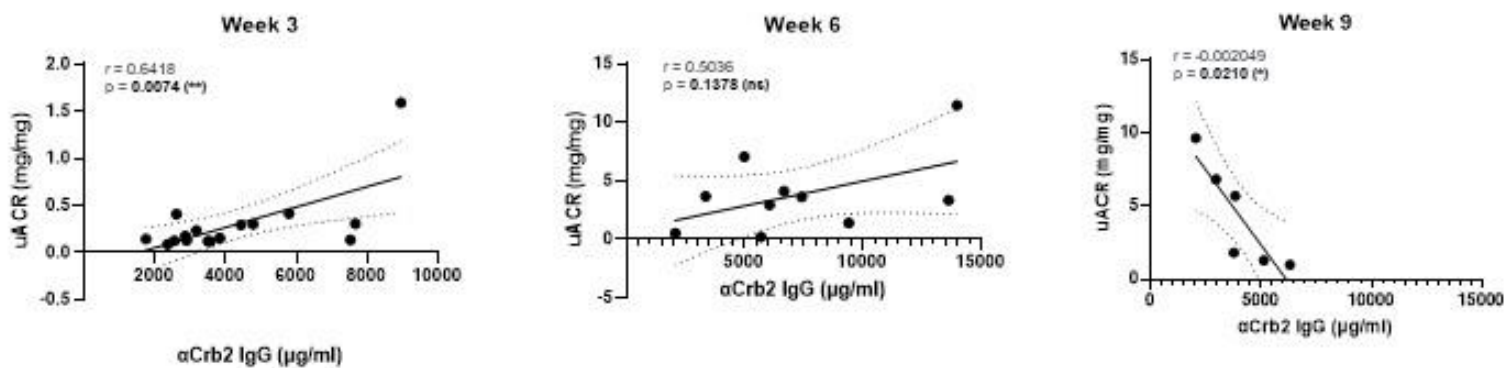
B



C



D



E

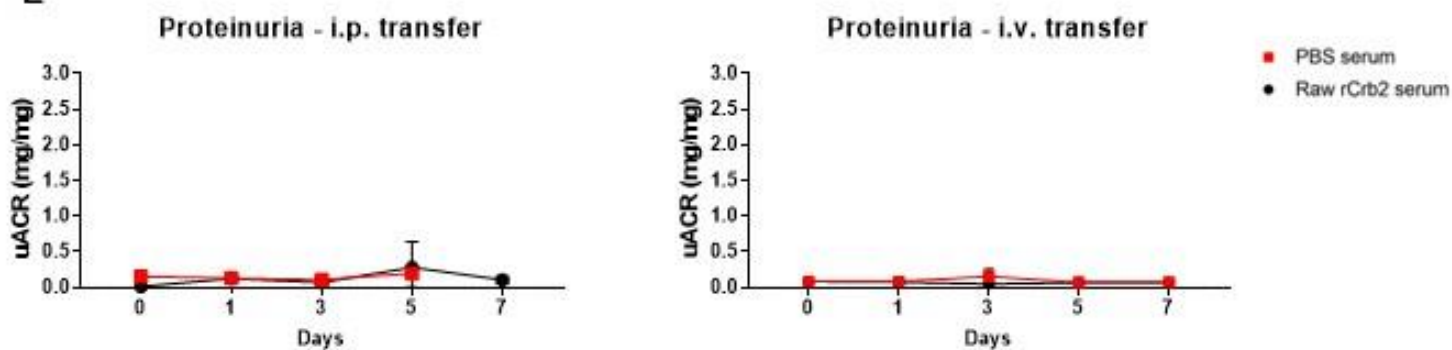


Figure 8. Anti-Crb2 antibody responses were increased in rCrb2-immunized mice with glomerular deposition and podocyte binding.

Serum pIgG concentration titres specifically targeting rCrb2 were quantified with ELISA. Serum was diluted 1:1000 or 1:5000, incubated on 1µg rCrb2, and bound pIgG were targeted by mouse anti-IgG-HRP. pIgG concentrations (µg/ml) were calculated from the detected absorbance values at wavelength 450nm with λ reference at 570nm. **(A)** Blood serum samples collected on day 0, 10, 24, 35, 42, 49, 56, 63, & 70 from mice immunized against rCrb2 (or PBS) in 1:1 adjuvant. Mean pIgG concentrations displayed. **(B&C)** Frozen kidney sections from rCrb2- & PBS-immunized mice were fixed and primarily stained with guinea pig anti-nephrin Ab overnight. Slides were co-stained with secondary reported Abs anti-guinea pig IgG-448 (**nephrin**), anti-mouse IgG-555 (**mouse IgG**), and **Dapi**. Fluorescence was captured by Zeiss LSM780 confocal microscopy, which displayed the podocytes within the glomeruli and glomerular IgG deposition. Representative images of glomeruli 6-weeks post-initial immunization at 60x magnification. Mean fluorescent intensity was quantified for nephrin and mouse IgG by obtaining intensity values from 40-80 pooled glomeruli. **(D)** Correlation analysis on serum anti-Crb2 IgG titres vs. proteinuria uACRs of individual mice sacrificed on weeks 3, 6, and 9 post-initial immunization with simple linear regression with 95% confidence intervals displayed. Significant positive correlation was observed during early stages (3-weeks) of EANS, but showed non-significant positive and significant negative correlation at weeks 6 and 9, respectively. **(E)** Spot urine samples collected on day 0, 1, 3, 5, & 7 from naïve mice passively transferred with raw serum from diseased mice either intraperitoneally (left) or intravenously (right). Y-axis limit to 3.0mg/mg for the minimal uACR indicating nephrotic-range proteinuria in mice. Statistical significance was tested using unpaired parametric two-tailed t test **(A,C,E)** and Pearson correlation coefficients analysis with 95% confidence interval **(D)**. $p \geq 0.05$ (ns), $p < 0.05$ (*), $p < 0.01$ (**), $p < 0.001$ (***), $p < 0.0001$ (****).

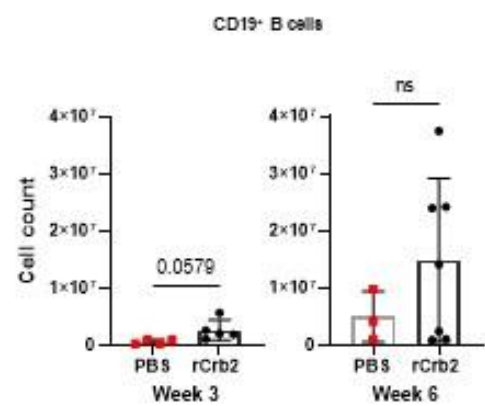
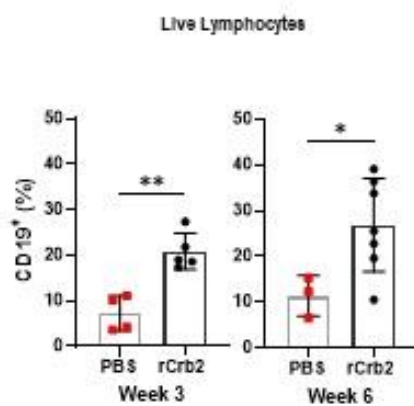
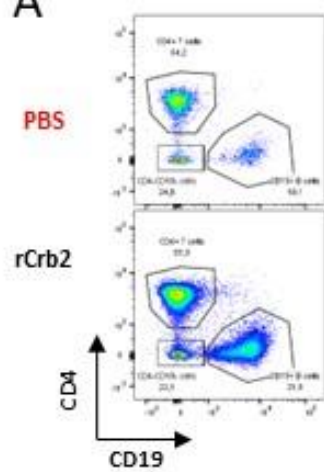
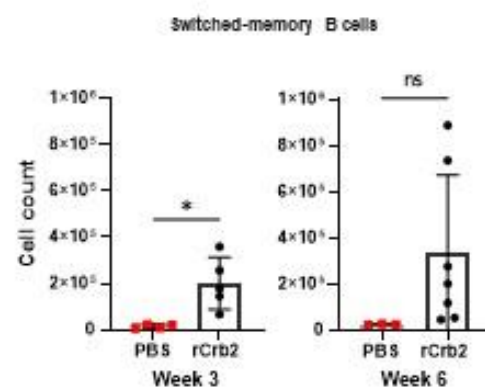
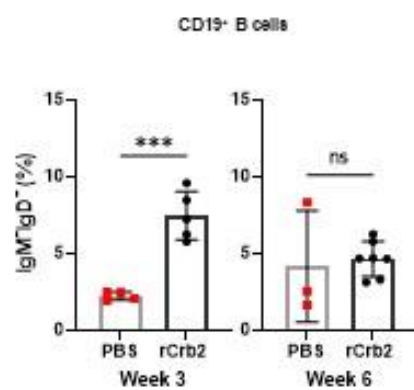
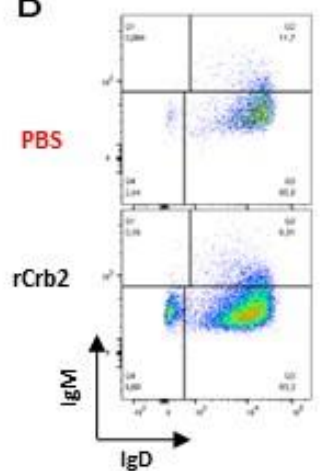
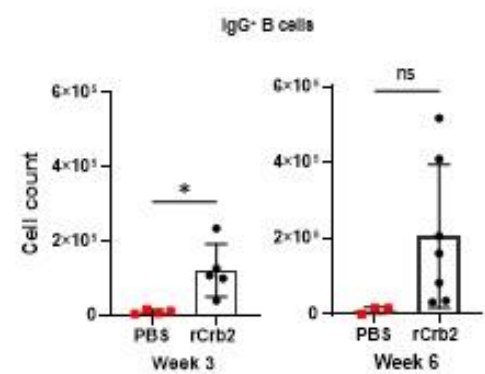
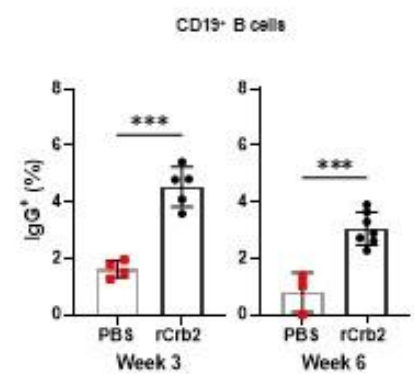
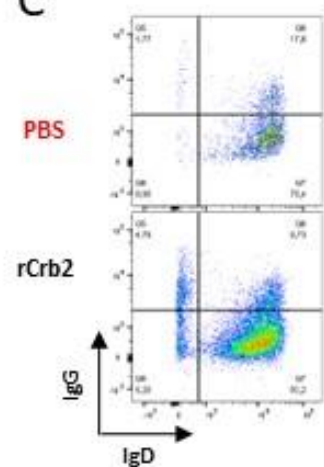
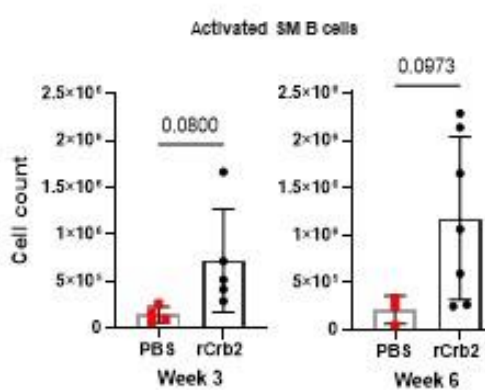
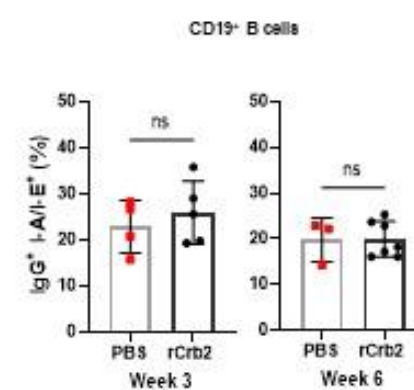
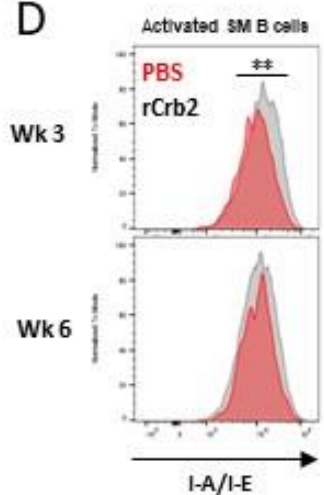
A**B****C****D**

Figure 9. Switch-memory B cells with IgG BCR and increase MHC-II expression preceded proteinuria development in EANS.

Immune cells were stained for viability (v506), CD19 (BUV737), CD4 (AF700), IgD (BUV395), IgM (FitC), IgG (APC), and I-A/I-E (BV711). Representative raw parametric flow cytometry plots obtained from immune cells isolated from draining iLN displayed on the left and quantified analysis graphically on the right. Each point on the graphs represents an individual mouse. **(A)** Live CD4⁺ T cells and CD19⁺ B cells frequencies and calculated live cell count from raw data are graphically displayed. **(B)** Frequencies and cell numbers of isotype switched memory (SM, IgM⁻IgD⁻) responses in iLN of immunized mice were gated on CD19⁺ B cells. **(C)** IgG⁺ CD19⁺ B cells gated on IgG⁺IgD⁻ CD19⁺ B cells frequencies and counts displayed. **(D)** Active B cell frequencies, cell counts obtained from IgG⁺ gated CD19⁺ B cells in iLN. MHC II expression quantified via BV711 mean fluorescent intensity (gMFI) and graphically displayed in histogram. Y-axis of I-A/I-E histograms normalized to mode. Statistical significance was tested using unpaired parametric two-tailed t test. $p \geq 0.05$ (ns), $p < 0.05$ (*), $p < 0.01$ (**), $p < 0.001$ (***), $p < 0.0001$ (****).

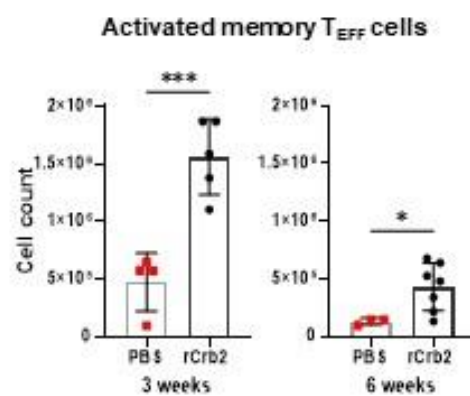
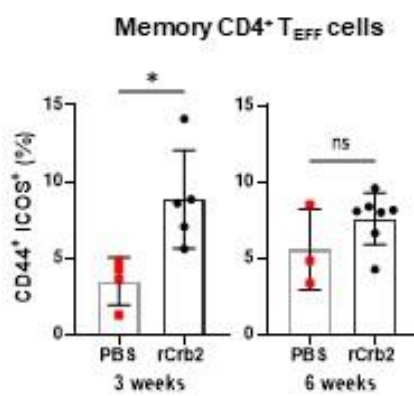
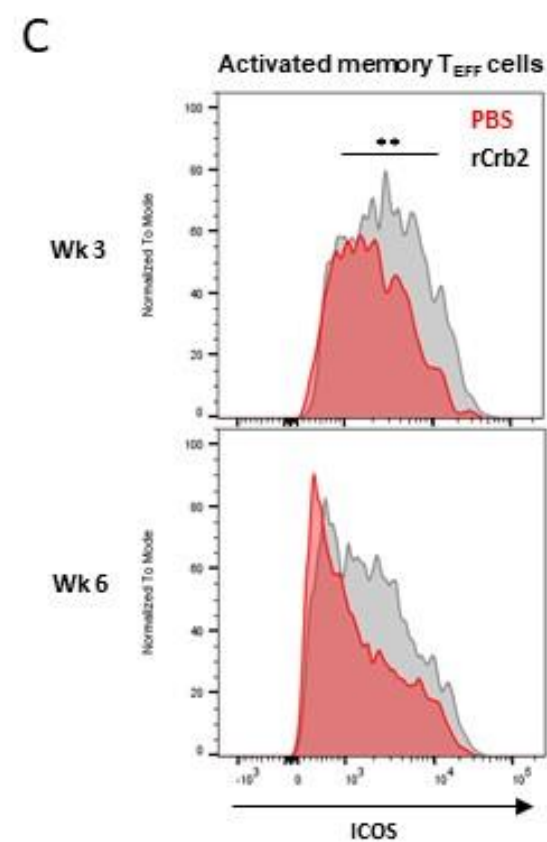
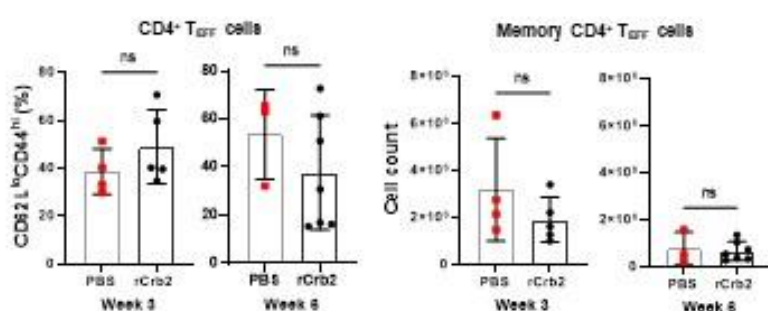
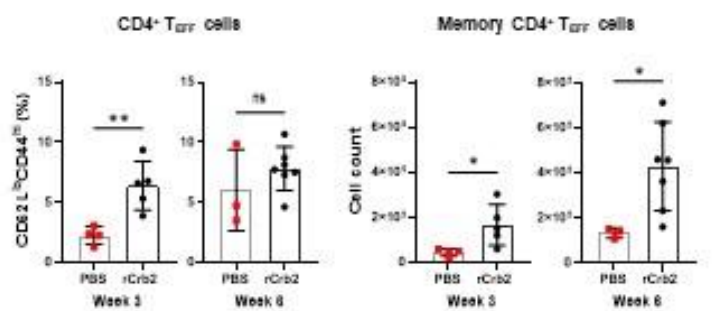
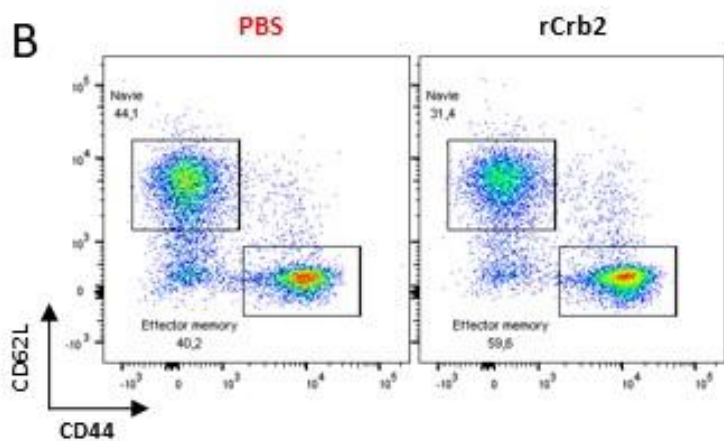
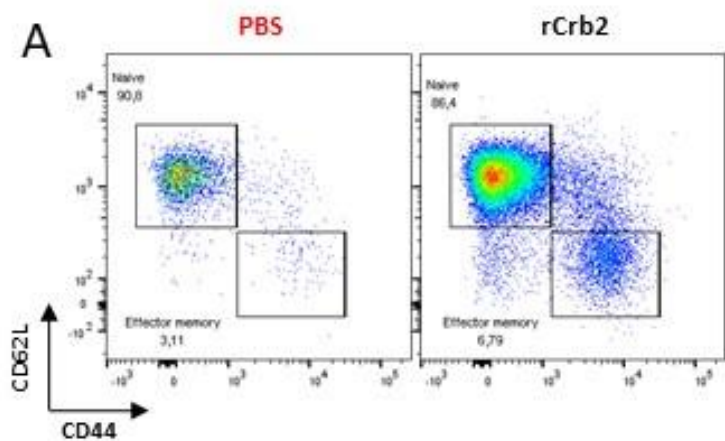


Figure 10. Memory CD4⁺ T_{EFF} cells expressing the co-stimulatory activator molecule accumulated in iLN of EANS mice prior to proteinuria detection.

Immune cells were stained for viability (v780), CD45.2 (PerCP for kidneys), differentiation makers CD3 (BUV737), CD4 (AF700), CD8b (BV510), FoxP3 (FitC), maturity status markers CD44 (APC) and CD62L (PE) & co-stimulatory marker ICOS (v450 for iLN). Representative raw parametric flow cytometry plots displayed on top and quantified analysis graphically below. **(A)** On CD4⁺ T_{EFF} cell subset (see gating in [Figure 11A](#)) in iLN, CD44⁺CD62L⁻ memory T_{EFF} cells were gated, and the frequencies and calculated cell counts were displayed. **(B)** Immune cells were targeted in kidney samples after cells were gated from live CD45.2 cells, then CD3⁺ T cells, and finally differentiated between CD4⁺ and CD8⁺ T cells. Within CD4⁺ T_{EFF} cells (see gating in [Figure 11B](#)), CD44⁺CD62L⁻ memory T_{EFF} cells were gated, and the frequencies and calculated cell counts were displayed. **(C)** T cell activation depicted by ICOS expression of gated memory T_{EFF} cell in iLN. Frequencies, cell count, and surface expression (v450 gMFI) displayed. ICOS expression displayed in histogram, with y-axis normalized to mode. Statistical significance was tested using unpaired parametric two-tailed t test. p≥0.05 (ns), p<0.05 (*), p<0.01 (**), p<0.001 (***), p<0.0001 (****).

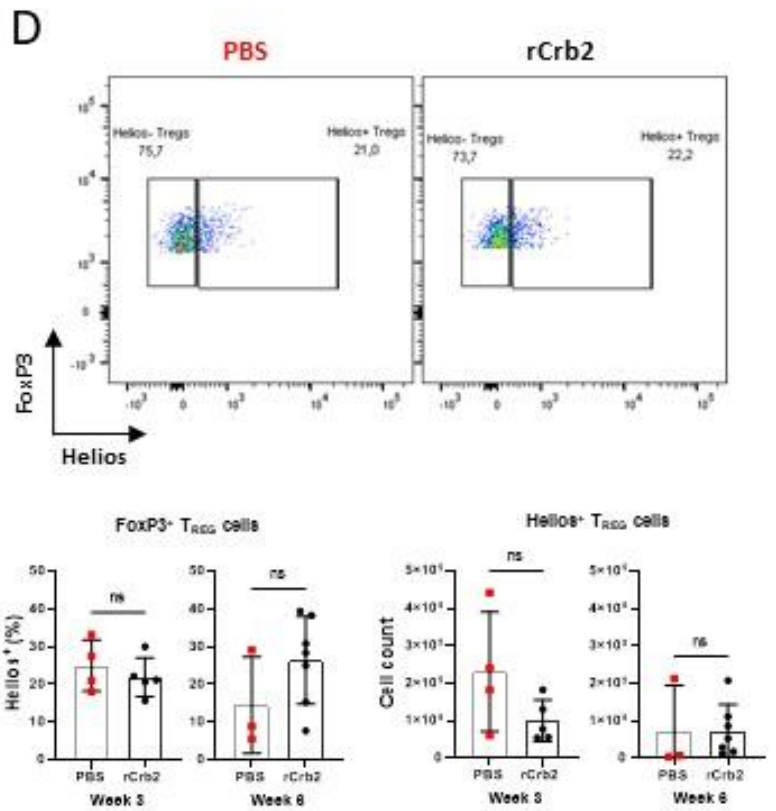
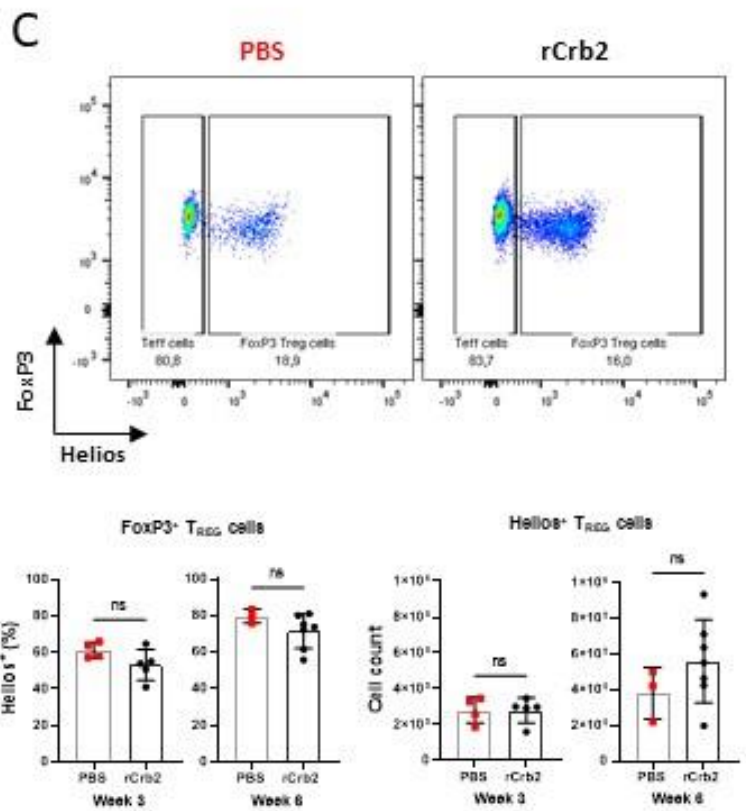
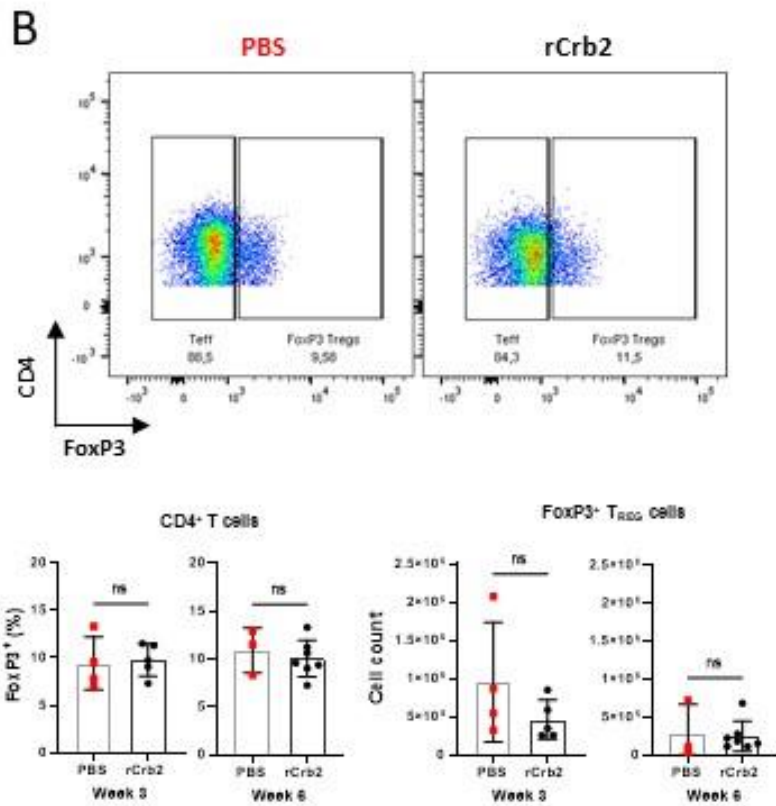
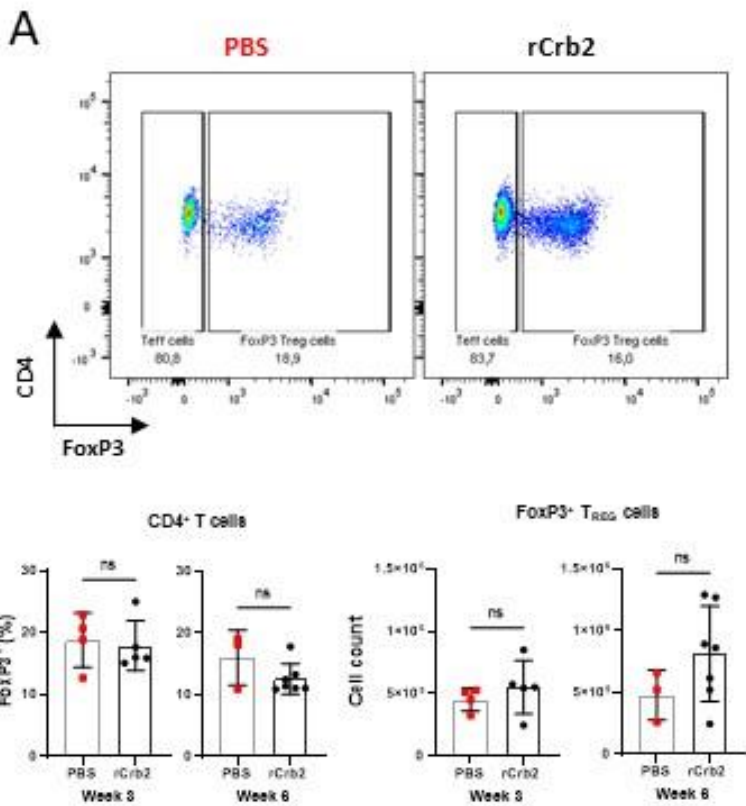


Figure 11. FoxP3⁺ T_{REG} cell frequencies showed no changes in iLN and kidneys in EANS.

Immune cells were stained for viability (v780), CD45.2 (PerCP for kidneys), differentiation makers CD3 (BUV737), CD4 (AF700), CD8b (BV510), FoxP3 (FitC), and Helios (PE/Cy7). Representative raw parametric flow cytometry plots displayed on the top and quantified analysis graphically below. FoxP3⁺ T_{REG} cells in iLN **(A)** and kidneys **(B)** were gated from CD4⁺ T cells, frequencies and cells counts were quantified. Further differentiation of the FoxP3⁺ T_{REG} cell subset was conducted by gating on Helios expression and frequencies of the T_{REG} cell subsets are displayed within the draining iLN **(C)** and kidneys **(D)**. Statistical significance was tested using unpaired parametric two-tailed t test. p \geq 0.05 (ns), p<0.05 (*), p<0.01 (**), p<0.001 (***), p<0.0001 (****).

Figure 12. Increased proliferation in vitro following restimulation with rCrb2 denotes expansion of rCrb2-specific CD4⁺ T cells.

(A) Schematic timeline of the rCrb2- and PBS-immunization, lymphocyte isolation from draining iLN along with control ax/brLN, and culturing conditions for re-activation of Crb2-specific CD4⁺ T cells (image created with BioRender). After co-culturing and cytokine stimulation, CD4⁺ T cells were washed and stained against viability (v780), CD3 (BUV737), CD4 (AF700), CD8 β (BV510), FoxP3 (Fitc), IL-2 (APC), Ki67 (BUV395), IFN γ (PerCP-Cy5.5), IL-4 (PE), IL-13 (PE-Cy7), and IL-17A (v450). Representative flow plots from iLN displayed. **(B)** Ki67 and IL-2 staining determine rCrb2-primed CD4⁺ T_{EFF} cells re-activation from rCrb2 in media. Ki67⁺ frequency and cell counts were quantified and displayed. Representative raw parametric flow cytometry plots and graphical visualization of the frequencies of IFN γ -producing and IL-4-producing **(C)**, IL-13-producing **(D)**, and IL-17A-producing **(E)** CD4⁺ T_{EFF} cells displayed. Statistical significance was tested using unpaired parametric two-tailed t test. p \geq 0.05 (ns), p<0.05 (*), p<0.01 (**), p<0.001 (***), p<0.0001 (****).

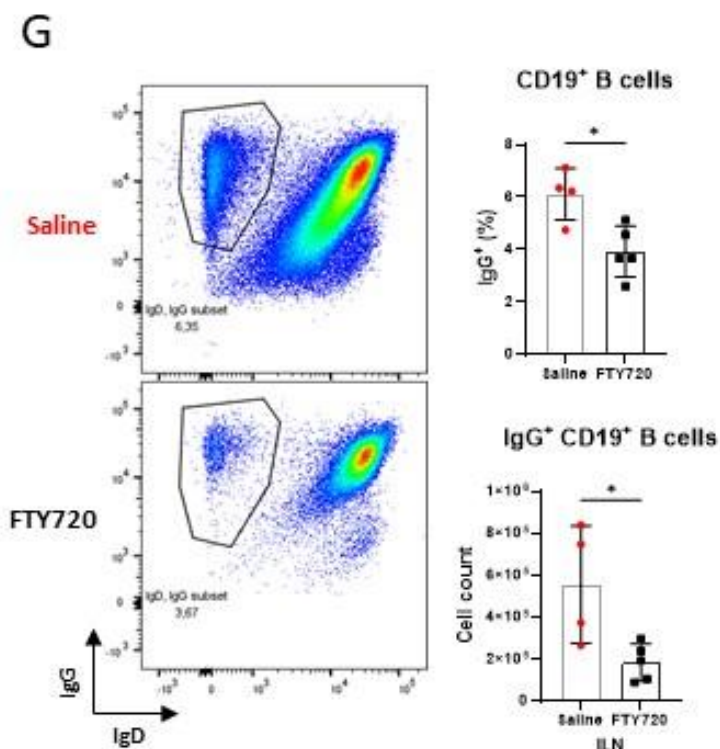
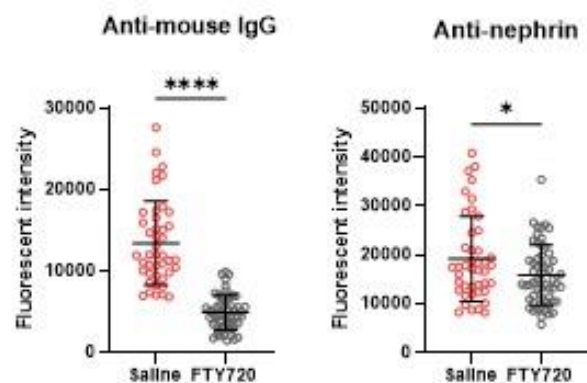
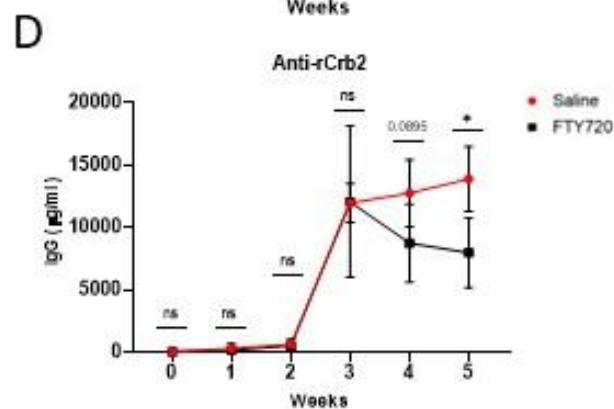
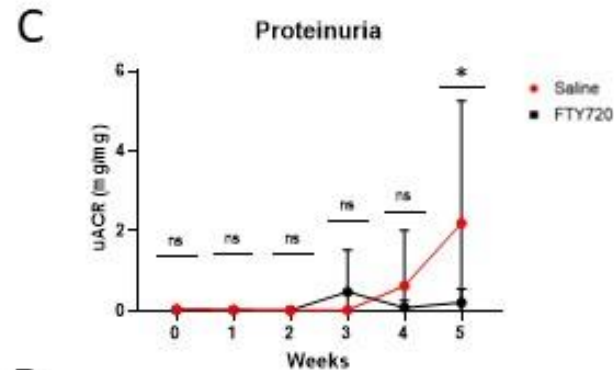
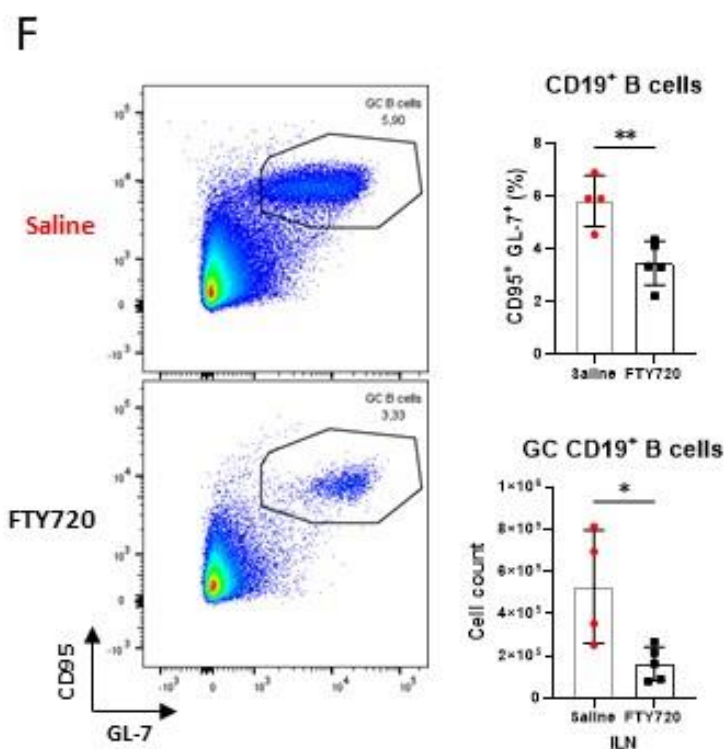
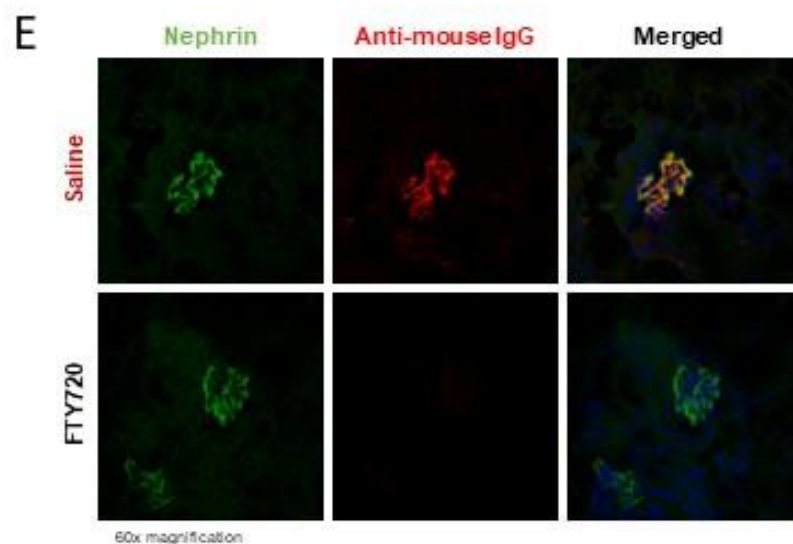
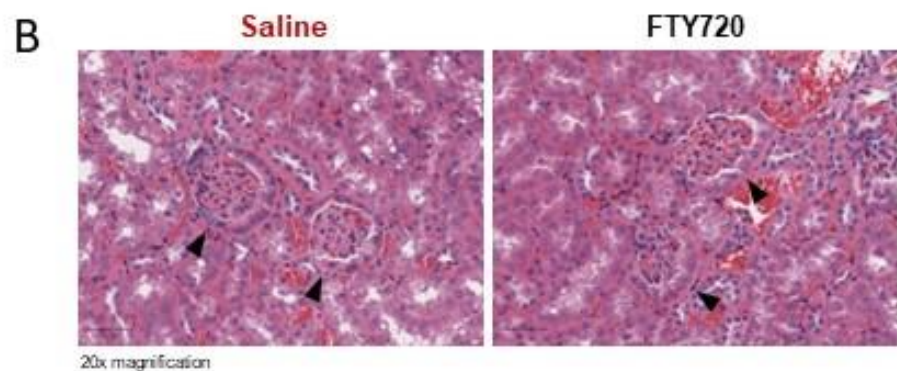
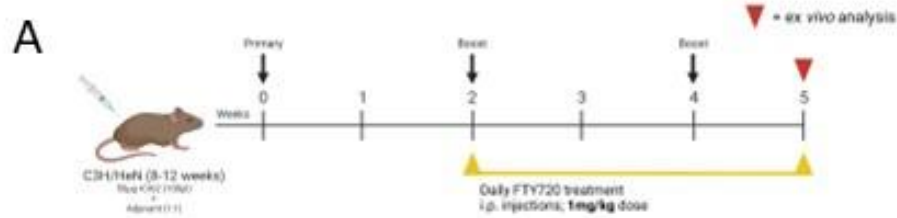


Figure 13. FTY720-treatment attenuated auto-antibody production and inhibited proteinuria development in rCrb2-immunized mice.

(A) Schematic timeline of the rCrb2-immunization to induce proteinuria and EANS in male C3H mice. Mice were treated with daily i.p. injections of FTY720 (1mg/kg dose) starting 2-weeks post-initial immunization. Control mice were treated with saline. **(B)** Kidney sections for histology were collected 5-weeks post-initial injection. Tissue sections were cut to 4 μ m thickness and stained with H&E to reveal any infiltrating mononuclear cells. No detectable change in glomeruli structure were observed or infiltrating immune cells detected. Representative images of saline- and FTY720-treated rCrb2-immunized mice at 20x magnification are displayed with black arrows pointing towards glomeruli. **(C)** uACR was analyzed from spot urine samples collected weekly during immunization and quantified by ELISA. Mean uACRs displayed. **(D)** Weekly blood serum samples were collected from rCrb2-immunized mice treated with FTY720 or saline. Mean pIgG concentrations displayed. **(E)** Frozen kidney sections from FTY720- & saline-treated mice were fixed and primarily stained with guinea pig anti-nephrin Ab overnight. Slides were co-stained with secondary reported Abs anti-guinea pig IgG-448 (**nephrin**), anti-mouse IgG-555 (**mouse IgG**), and **Dapi**. Fluorescence was captured by Zeiss LSM780 confocal microscopy, which displayed the podocytes within the glomeruli and glomerular IgG deposition. Representative images of glomeruli 5-weeks post-initial immunization at 60x magnification. Mean fluorescent intensity was quantified for nephrin and mouse IgG by obtaining intensity values from 40-80 pooled glomeruli. **(F&G)** Immune cells were stained for viability (v506), CD19 (BUV737), CD4 (AF700), GC markers GL-7 (PerCP-Cy5.5) and CD95 (PE-CF594) **(F)**, and BCR expression markers IgD (BUV395), IgM (FitC), and IgG (APC) **(G)**. Representative raw parametric flow cytometry plots obtained from immune cells isolated from draining iLN displayed on the left and quantified analysis graphically on the right. Each point on the graphs represents an individual mouse. Statistical significance was tested using unpaired parametric two-tailed t test. $p \geq 0.05$ (ns), $p < 0.05$ (*), $p < 0.01$ (**), $p < 0.001$ (***), $p < 0.0001$ (****).

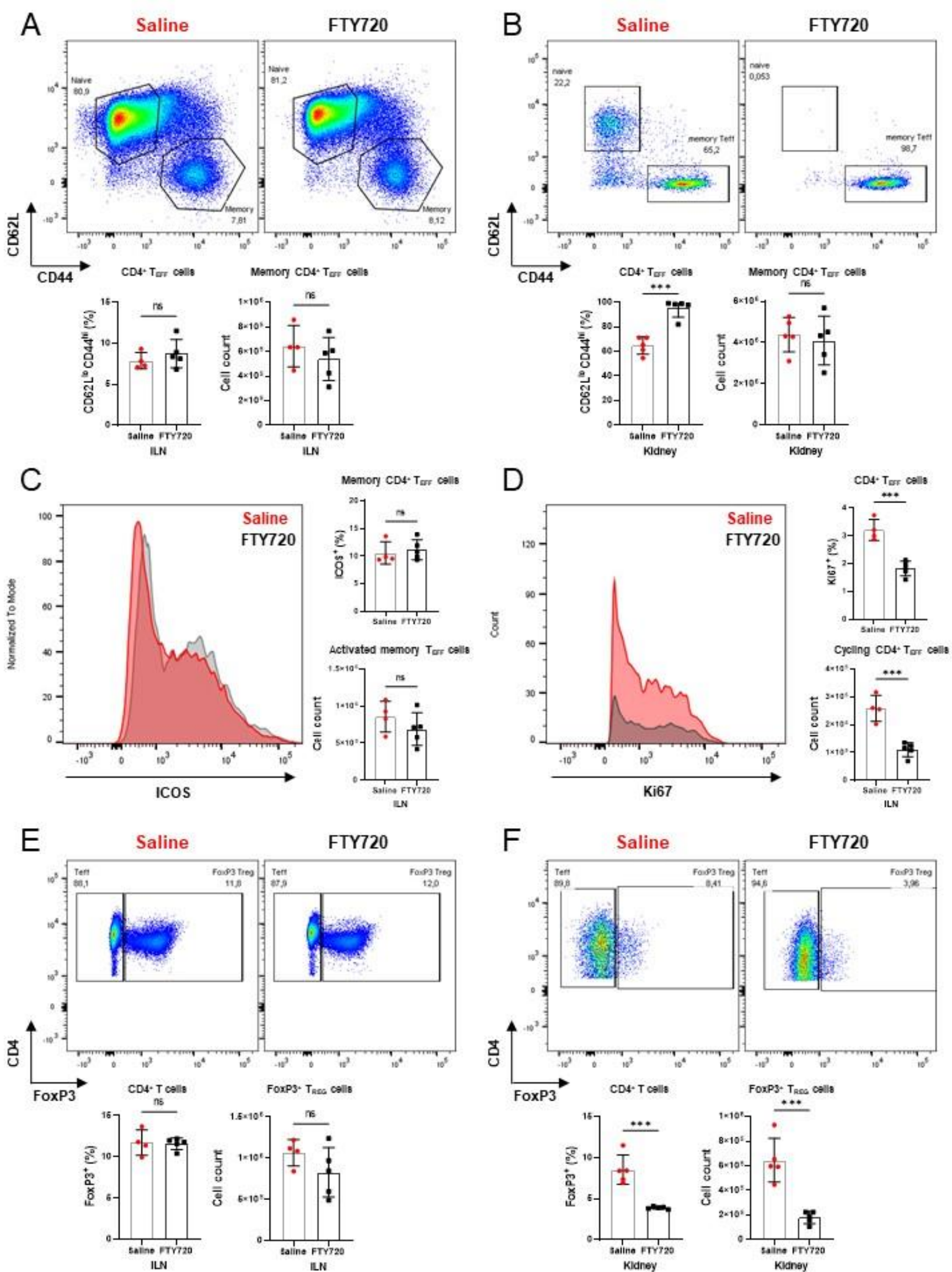


Figure 14. Prolonged FTY720-treatment significantly reduced proliferation responses in CD4⁺ T_{EFF} cells within iLN of EANS mice.

Immune cells were stained for viability (v780), CD45.2 (PerCP for kidneys), differentiation makers CD3 (BUV737), CD4 (AF700), CD8b (BV510), and FoxP3 (FitC), maturity status markers CD44 (APC) and CD62L (PE) & co-stimulatory marker ICOS (v450 for iLN). Representative raw parametric flow cytometry plots displayed on top and quantified analysis graphically below. Frequencies and cells counts were quantified. On CD4⁺ T_{EFF} cell subset (FoxP3⁻ subset in **E&F**) in iLN (**A**) and kidneys (**B**), CD44⁺CD62L⁻ memory T_{EFF} cells were gated, and the frequencies and calculated cell counts were displayed. (**C**) T cell activation depicted by ICOS expression of gated memory T_{EFF} cell in iLN. Frequencies, cell count, and surface expression (v450 gMFI) displayed. ICOS expression displayed in histogram, with y-axis normalized to mode. (**D**) Proliferation status of CD4⁺ T_{EFF} cells in iLN were examined via Ki67 staining. Frequencies, cell count, and surface expression (BUV395 gMFI) displayed. Ki67 expression displayed in histogram. No significant changes in Ki67 gMFI were observed between saline- and FTY720-treated mice. FoxP3⁺ T_{REG} cells in iLN (**E**) and kidneys (**F**) were gated from CD4⁺ T cells. Statistical significance was tested using unpaired parametric two-tailed t test. p \geq 0.05 (ns), p<0.05 (*), p<0.01 (**), p<0.001 (***), p<0.0001 (****).

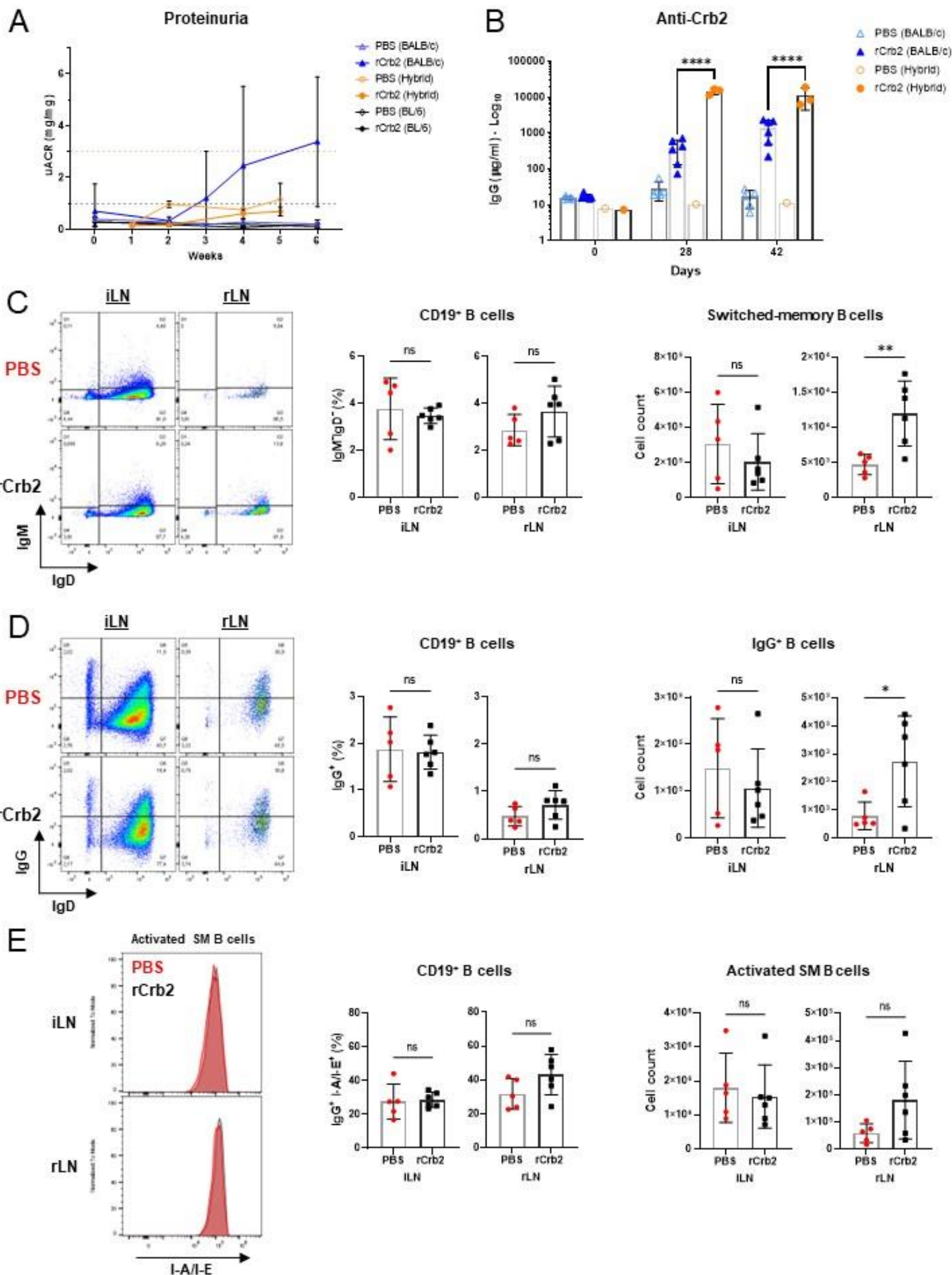


Figure 15. Migrating the EANS immunization model into the BALB/c mouse strain.

Male BALB/c, C3B6F1 hybrid, and BL/6 mice (8-12 weeks of age) subcutaneously injected biweekly with 200 μ l emulsified 50 μ g purified rCrb2 (or PBS) in a 1:1 emulsification with CFA (primary injection) and IFA (boosters) bilaterally. Mice were sacrificed 6-weeks post-immunization where kidneys, spleen, draining iLN, and rLN were collected for *ex vivo* immunophenotyping analysis. **(A)** uACR were analyzed from spot urine samples collected weekly during immunization and quantified by ELISA. Mean uACRs displayed. Grey dotted line references minimal range uACR for nephrotic-range proteinuria; pink reference minimal threshold for uACR analysis at experimental endpoint. No statistics available due to low sample size in some strain cohorts. **(B)** Blood serum samples collected on days 0, 28, & 42 from BALB/c and C3B6F1 hybrid mice immunized against rCrb2 (or PBS) in 1:1 adjuvant. Serum pIgG concentration titres specifically targeting rCrb2 were quantified with ELISA. Serum was diluted 1:1000 or 1:5000, incubated on 1 μ g rCrb2, and bound pIgG were targeted with mouse anti-IgG-HRP. pIgG concentrations (μ g/ml) calculated from detected absorbance values at wavelength 450nm with λ refence at 570nm. Mean pIgG concentrations displayed. Immune cells were stained for viability (v506), CD19 (BUV737), CD4 (AF700), IgD (BUV395), IgM (FitC), IgG (APC), and I-A/I-E (BV711). Representative raw parametric flow cytometry plots obtained from immune cells isolated from draining iLN and rLN displayed on the left and quantified analysis graphically on the right. Each point on the graphs represents an individual mouse. **(C)** Frequencies and cell numbers of isotype switched memory (SM,IgM⁻IgD⁻) responses were gated on CD19⁺ B cells. **(D)** IgG⁺ CD19⁺ B cells gated on IgG⁺IgD⁻ CD19⁺ B cells frequencies and counts displayed. **(E)** Active B cell frequencies, cell counts obtained from IgG⁺ gated CD19⁺ B cells. MHC II expression quantified via BV711 mean fluorescent intensity (gMFI) and graphically displayed in histogram. Y-axis of I-A/I-E histograms normalized to mode. Statistical significance was tested using Two-way ANVOA Šídák multiple comparisons test for serum anti-Crb2 IgG titres (B) and unpaired parametric two-tailed t test (C-E). $p \geq 0.05$ (ns), $p < 0.05$ (*), $p < 0.01$ (**), $p < 0.001$ (***), $p < 0.0001$ (****).

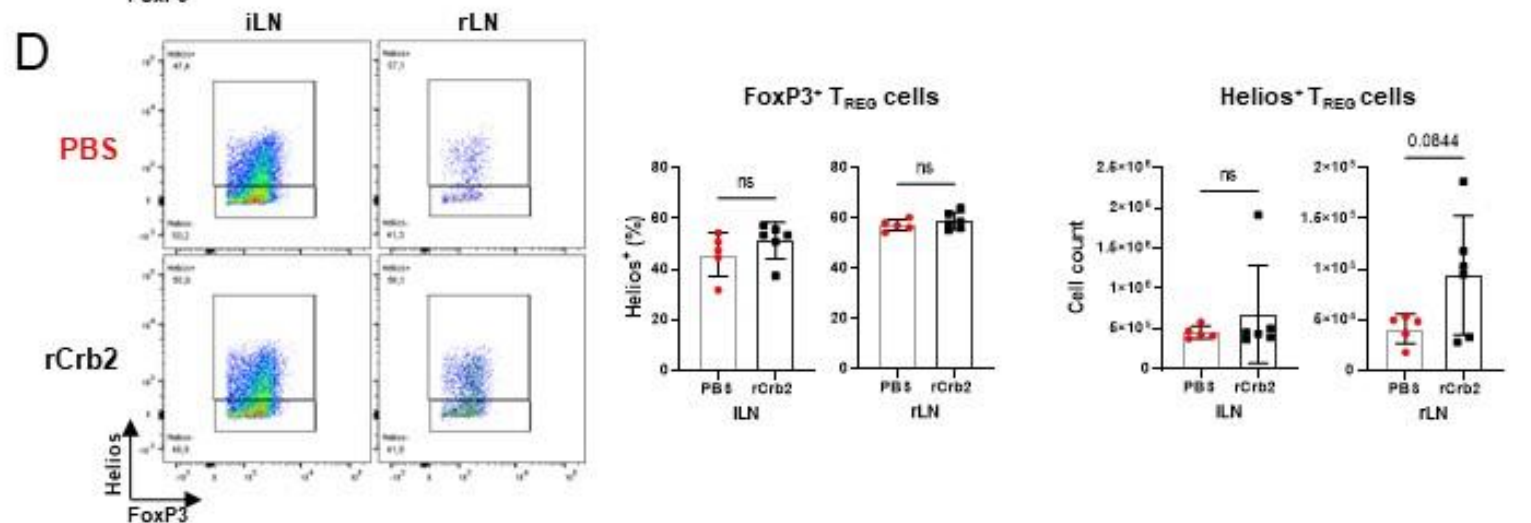
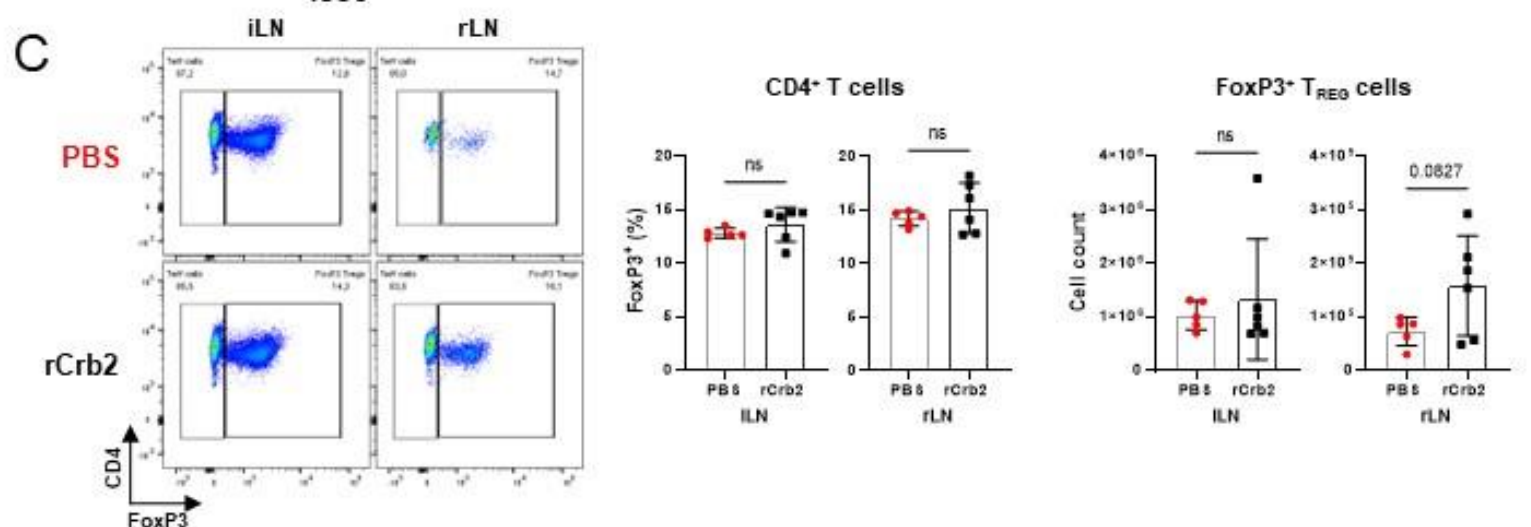
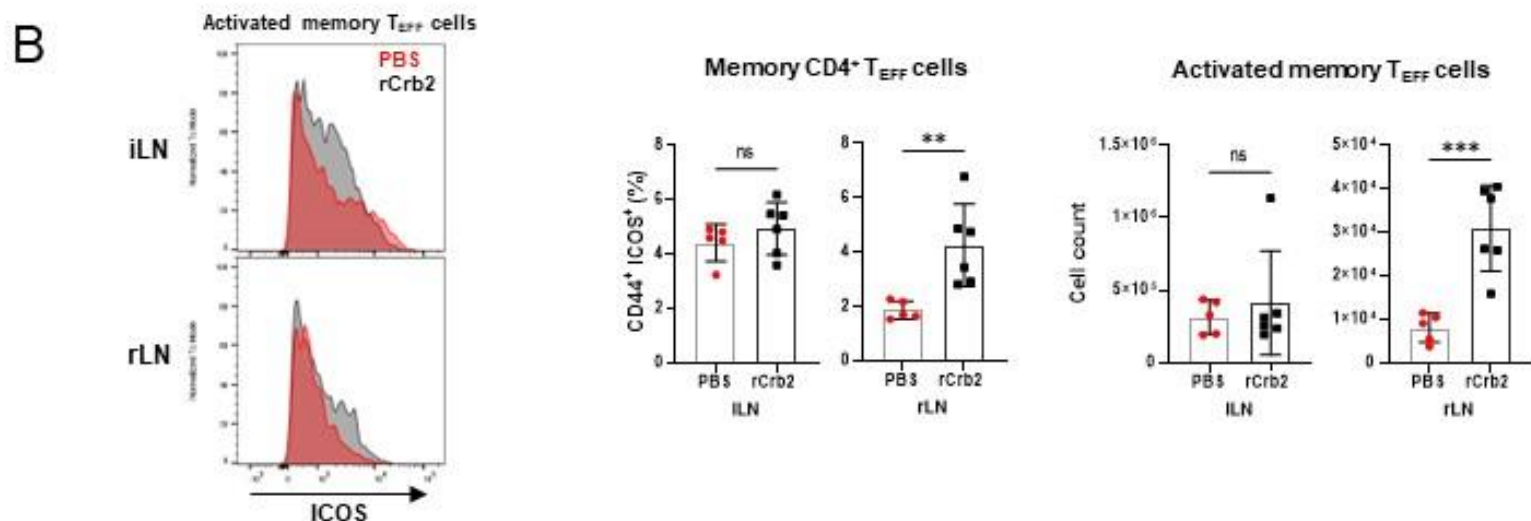
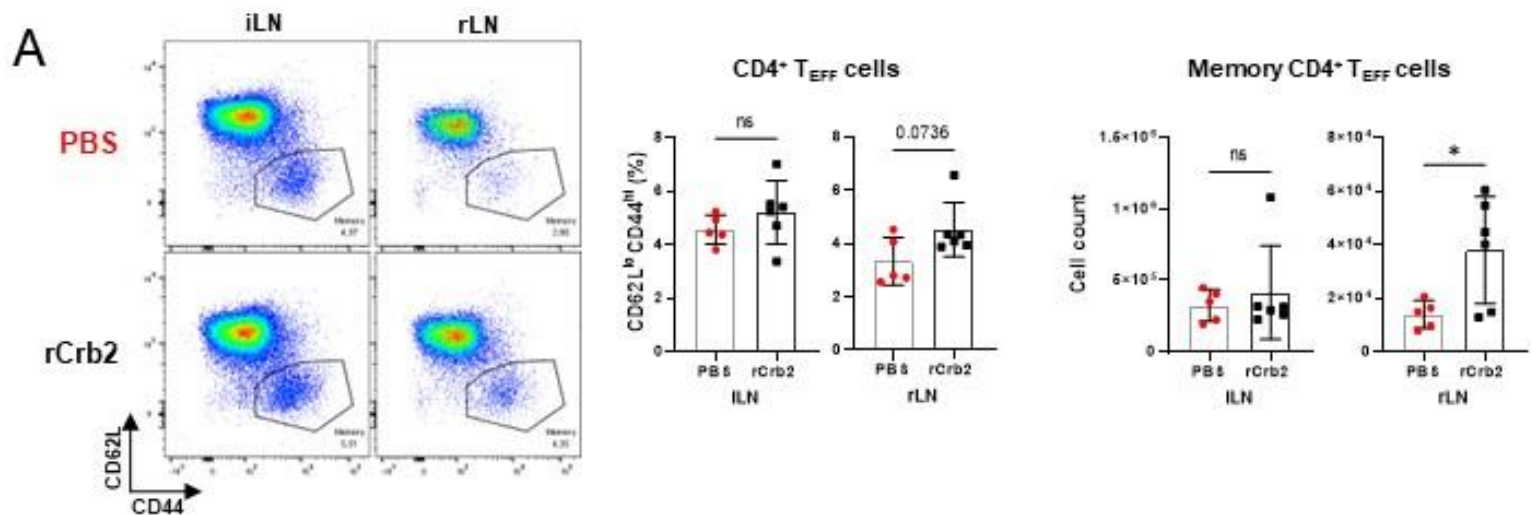


Figure 16. Renal LN acquisition from rCrb2-immunized BALB/c mice revealed accumulation of activated CD4⁺ T_{EFF} cells.

Immune cells isolated from iLN and rLN of rCrb2- and PBS-immunized BALB/c sacrificed 6-weeks post-initial immunized were stained for viability (v780), phenotyping makers CD3 (BUV737), CD4 (AF700), CD8b (BV510), FoxP3 (FitC), Helios (PE-Cy7), maturity status markers CD44 (APC) and CD62L (PE), & co-stimulatory marker ICOS (v450). Representative raw parametric flow cytometry plots displayed on the left and quantified analysis graphically on the right. **(A)** On CD4⁺ T_{EFF} cell subset, CD44⁺CD62L⁻ memory T_{EFF} cells were gated, and the frequencies and calculated cell counts were displayed. **(B)** T cell activation depicted by ICOS expression of gated memory T_{EFF} cell in iLN. Frequencies, cell count, and surface expression (v450 gMFI) displayed. ICOS expression displayed in histogram, with y-axis normalized to mode. **(C)** FoxP3⁺ T_{REG} cells were gated from CD4⁺ T cells, frequencies and cells counts were quantified. Further differentiation of the FoxP3⁺ T_{REG} cell subset was conducted by gating on Helios expression and frequencies of the T_{REG} cell subsets are displayed within the draining iLN **(D)**. Statistical significance was tested using unpaired parametric two-tailed t test. p≥0.05 (ns), p<0.05 (*), p<0.01 (**), p<0.001 (***), p<0.0001 (****).

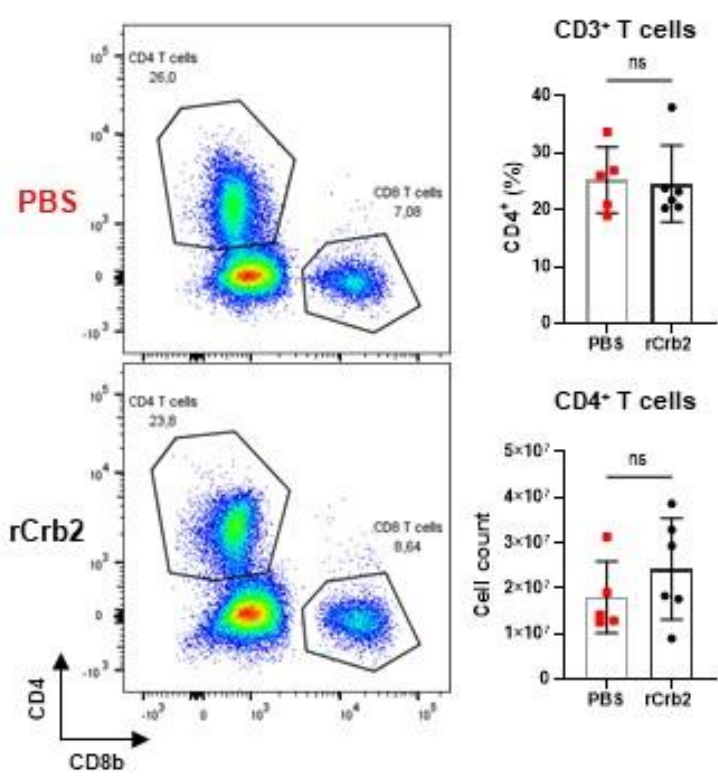
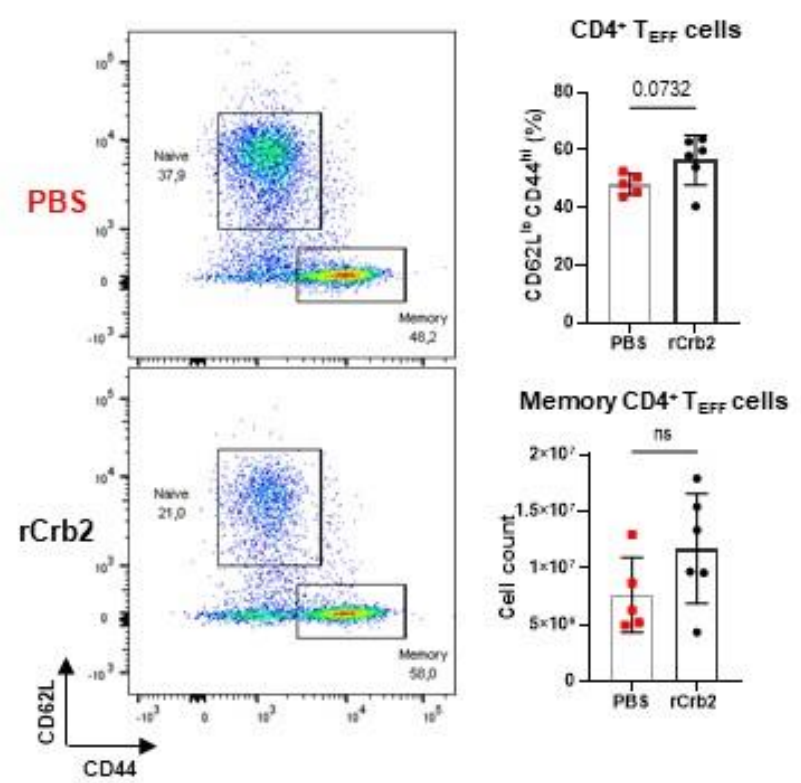
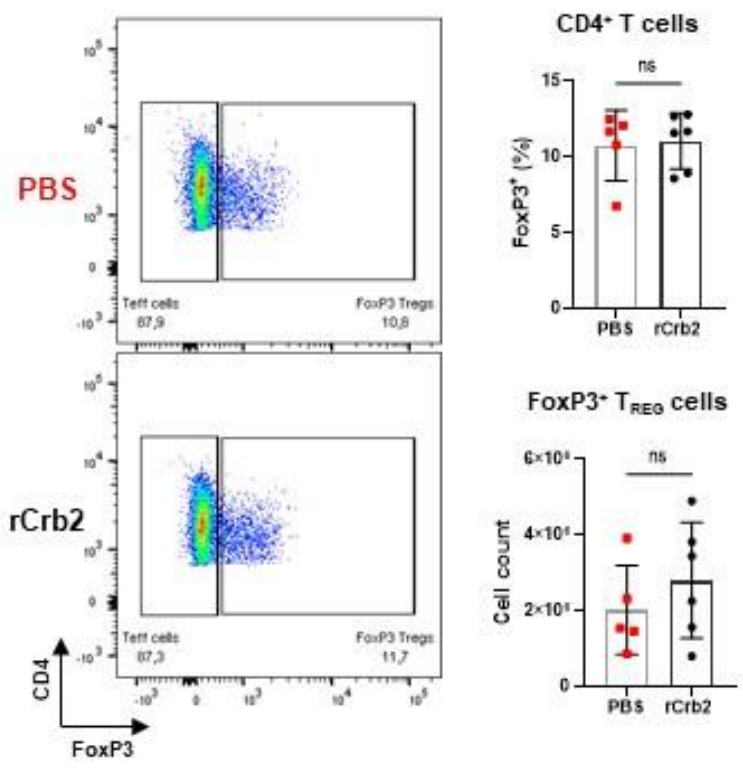
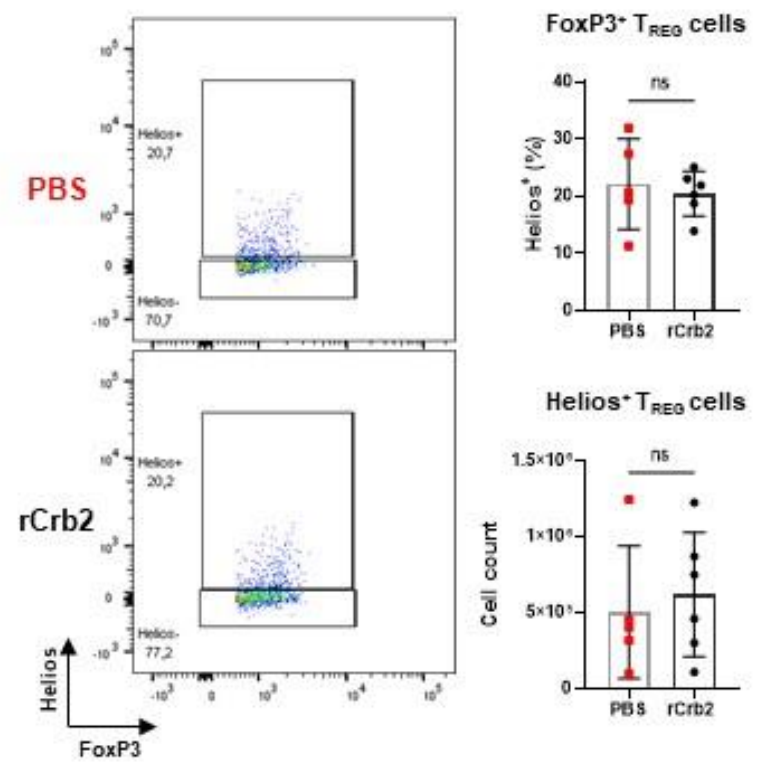
A**B****C****D**

Figure 17. Induction of EANS in BALB/c with rCrb2-immunization showed no changes in renal CD4⁺ T_{EFF}⁺ and FoxP3⁺ T_{REG} cell proportions.

Immune cells isolated from kidneys 6-weeks post-initial immunization of rCrb2- and PBS-injected BALB/c were stained for viability (v780), phenotyping makers CD45.2 (PerCP), CD3 (BUV737), CD4 (AF700), CD8b (BV510), FoxP3 (FitC), Helios (PE-Cy7), maturity status markers CD44 (APC) and CD62L (PE). Representative raw parametric flow cytometry plots displayed on the left and quantified analysis graphically on the right. **(A)** From whole kidney cells, CD3⁺ T cells were gated from live CD45.2 lymphocytes which was further differentiated between CD4⁺ and CD8⁺ T cells. **(B)** On CD4⁺ T_{EFF} cell subset, CD44⁺CD62L⁻ memory T_{EFF} cells were gated, and the frequencies and calculated cell counts were displayed. **(C)** FoxP3⁺ T_{REG} cells were gated from CD4⁺ T cells, frequencies and cells counts were quantified. Further differentiation of the FoxP3⁺ T_{REG} cell subset was conducted by gating on Helios expression and frequencies of the T_{REG} cell subsets are displayed within the draining iLN **(D)**. Statistical significance was tested using unpaired parametric two-tailed t test. p≥0.05 (ns), p<0.05 (*), p<0.01 (**), p<0.001 (***), p<0.0001 (****).

Table 1. Historically used animal models of podocyte injury.

Model Type	Induction	Animal Model	Proteinuria & podocyte injury?	Limitations
Chemical	Puromycin aminonucleoside nephrosis	Rat	Yes	Dose-dependent effect on GC-sensitivity
Chemical	Protamine sulfate	Rat	Yes	Dose-dependent effect on GC-sensitivity
Chemical	Adriamycin	Rat Mouse	Yes	Dose-dependent toxicity. Mechanism of podocyte injury is non-specific
Biological	LPS	Mouse	Yes	Mild proteinuria development(non-nephrotic-range). Systemic or septic effects with the use of LSP
Transgenic/passive transfer	Polyclonal rabbit anti-mouse nephrin antibody	Mouse	Yes	MCD-like injury progressing into FSGS-like injury immediately

Table 2. List of antibodies.

Antibody	Analysis	Catalog No.	Company	Address
Goat pAb to Ms IgG (HRP) 500µg/ml	ELISA	ab97040	Abcam	Cambridge, United Kingdom
Moues anti-Crb2 poly-IgG 1mg/ml	ELISA IF	Hada <i>et al</i> , 2022	Dr. Kunimasa Yan (Kyorin University)	Tokyo, Japan
Goat anti-Mouse Albumin Antibody HRP Conjugated	ELISA	A90-134P	Bethyl	Waltham, Massachusetts, United States
Affinity Purified Goat anti- Mouse Albumin Coating Antibody	ELISA	A90-134A	Bethyl	Waltham, Massachusetts, United States
Alexa Fluor® 700 anti-mouse CD4 Antibody	Flow cytometry	100536	BioLegend	San Diego, California, United States
APC Goat anti-mouse IgG (minimal x-reactivity) Antibody	Flow cytometry	405308	BioLegend	San Diego, California, United States
APC Rat Anti-Mouse CD44	Flow cytometry	559250	BD Bioscience	Franklin Lakes, New Jersey, United States

APC Rat Anti-Mouse IL-2	Flow cytometry	554429	BD Bioscience	Franklin New United States	Lakes, Jersey,
APC-Cy™7 Mouse Anti-Bcl-6	Flow cytometry	563581	BD Bioscience	Franklin New United States	Lakes, Jersey,
Biotin Rat Anti-Mouse CD40	Flow cytometry	553789	BD Bioscience	Franklin New United States	Lakes, Jersey,
BUV395 Mouse Anti-Ki-67	Flow cytometry	564071	BD Bioscience	Franklin New United States	Lakes, Jersey,
BUV395 Rat Anti-Mouse IgD	Flow cytometry	564274	BD Bioscience	Franklin New United States	Lakes, Jersey,
BUV737 Rat Anti-Mouse CD19	Flow cytometry	612781	BD Bioscience	Franklin New United States	Lakes, Jersey,
BUV737 Rat Anti-Mouse CD3 Molecular Complex	Flow cytometry	612803	BD Bioscience	Franklin New United States	Lakes, Jersey,
BV510 Rat Anti-Mouse CD8b	Flow cytometry	740155	BD Bioscience	Franklin New United States	Lakes, Jersey,
BV711 Rat Anti-Mouse I-A/I-E	Flow cytometry	563414	BD Bioscience	Franklin New United States	Lakes, Jersey,

CD278 (ICOS) Monoclonal Antibody (7E.17G9), PE, eBioscience™	Flow cytometry	12-9942-82	eBioscience, ThermoFisher Scientific	Waltham, Massachusetts, United States
CD278 (ICOS) Monoclonal Antibody (C398.4A), Super Bright™ 436, eBioscience™	Flow cytometry	62-9949-82	Invitrogen	Waltham, Massachusetts, United States
CD279 (PD-1) Monoclonal Antibody (J43), Super Bright™ 436, eBioscience™	Flow cytometry	62-9985-82	Invitrogen	Waltham, Massachusetts, United States
CD62L (L-Selectin) Monoclonal Antibody (MEL-14), PerCP-Cyanine5.5, eBioscience™	Flow cytometry	45-0621-82	Invitrogen	Waltham, Massachusetts, United States
eBioscience™ Fixable Viability Dye eFluor™ 506	Flow cytometry	65-0866-18	Invitrogen	Waltham, Massachusetts, United States
eBioscience™ Fixable Viability Dye eFluor™ 780	Flow cytometry	65-0865-14	Invitrogen	Waltham, Massachusetts, United States
eBioscience™ Streptavidin PE Conjugate	Flow cytometry	12-4317-87	eBioscience, ThermoFisher Scientific	Waltham, Massachusetts, United States
FITC anti-mouse IgM Antibody	Flow cytometry	406506	BioLegend	San Diego, California, United States

FOXP3 Monoclonal Antibody (FJK-16s), FITC, eBioscience™	Flow cytometry	11-5773-82	Invitrogen	Waltham, Massachusetts, United States
FOXP3 Monoclonal Antibody (FJK-16s), PE-Cyanine7, eBioscience™	Flow cytometry	25-5773-82	eBioscience, ThermoFisher Scientific	Waltham, Massachusetts, United States
HELIOS Monoclonal Antibody (22F6), PE-Cyanine7, eBioscience™	Flow cytometry	25-9883-42	Invitrogen	Waltham, Massachusetts, United States
IFN gamma Monoclonal Antibody (XMG1.2), PE-Cyanine7, eBioscience™	Flow cytometry	25-7311-82	Invitrogen	Waltham, Massachusetts, United States
IFN gamma Monoclonal Antibody (XMG1.2), PerCP-Cyanine5.5, eBioscience™	Flow cytometry	45-7311-82	Invitrogen	Waltham, Massachusetts, United States
IL-13 Monoclonal Antibody (eBio13A), eFluor™ 450, eBioscience™	Flow cytometry	48-7133-82	Invitrogen	Waltham, Massachusetts, United States
IL-13 Monoclonal Antibody (eBio13A), PE-Cyanine7, eBioscience™	Flow cytometry	25-7133-82	Invitrogen	Waltham, Massachusetts, United States
IL-17A Monoclonal Antibody (eBio17B7), APC, eBioscience™	Flow cytometry	17-7177-81	Invitrogen	Waltham, Massachusetts, United States

PE Rat Anti-Mouse CD62L			Flow cytometry	553151	BD Bioscience	Franklin Lakes, New Jersey, United States
PE Rat Anti-Mouse IL-4			Flow cytometry	554435	BD Bioscience	Franklin Lakes, New Jersey, United States
PE/Cyanine7 CD138 (Syndecan-1) Antibody	anti-mouse		Flow cytometry	142513	BioLegend	San Diego, California, United States
PE-CF594 Mouse CD95	Hamster Anti-		Flow cytometry	562499	BD Bioscience	Franklin Lakes, New Jersey, United States
PE-Cy™7 CD25	Rat Anti-Mouse		Flow cytometry	552880	BD Bioscience	Franklin Lakes, New Jersey, United States
PerCP Antibody	anti-mouse	CD45.2	Flow cytometry	109826	BioLegend	San Diego, California, United States
PerCP/Cyanine5.5 mouse/human GL7 Antigen (T and B cell Activation Marker) Antibody	anti-		Flow cytometry	144609	BioLegend	San Diego, California, United States
V450 Rat Anti-Mouse IL-17A			Flow cytometry	560522	BD Bioscience	Franklin Lakes, New Jersey, United States

Anti-mouse IgG (H+L), F(ab') ₂ Fragment (Alexa Fluor® 555 Conjugate)	IF	4409S	Cell Signaling Technology	Danvers, Massachusetts, United States
Goat anti-Guinea Pig IgG (H+L) Highly Cross-Adsorbed Secondary Antibody, Alexa Fluor™ 488	IF	A-11073	Invitrogen	Waltham, Massachusetts, United States
Nephrin (NPHS1) (1243-1256) Guinea Pig Polyclonal Antibody	IF	BP5030	OriGene	Rockville, Maryland, United States
AffiniPure Fab Fragment Donkey Anti-Mouse IgG (H+L)	IF	715-007-003	Jackson ImmunoResearch Laboratories, Inc.	West Grove, PA, USA

REFERENCES

1. Wang, C.S. and L.A. Greenbaum, *Nephrotic Syndrome*. *Pediatr Clin North Am*, 2019. **66**(1): p. 73-85.
2. Downie, M.L., et al., *Nephrotic syndrome in infants and children: pathophysiology and management*. *Paediatr Int Child Health*, 2017. **37**(4): p. 248-258.
3. Noone, D.G., K. Iijima, and R. Parekh, *Idiopathic nephrotic syndrome in children*. *Lancet*, 2018. **392**(10141): p. 61-74.
4. Eddy, A.A. and J.M. Symons, *Nephrotic syndrome in childhood*. *Lancet*, 2003. **362**(9384): p. 629-39.
5. Durkan, A.M., et al., *Immunosuppressive agents in childhood nephrotic syndrome: a meta-analysis of randomized controlled trials*. *Kidney Int*, 2001. **59**(5): p. 1919-27.
6. Koskimies, O., et al., *Long-term outcome of primary nephrotic syndrome*. *Arch Dis Child*, 1982. **57**(7): p. 544-8.
7. Vivarelli, M., et al., *Minimal Change Disease*. *Clin J Am Soc Nephrol*, 2017. **12**(2): p. 332-345.
8. Yang, E.M., *Pathogenesis of Minimal Change Nephrotic Syndrome: A Review of the Underlying Molecular Mechanisms*. *Child Kidney Dis.*, 2019. **23**(1): p. 1-6.
9. Hsiao, C.-C., et al., *Immunoglobulin E and G Levels in Predicting Minimal Change Disease before Renal Biopsy*. *BioMed Research International*, 2018. **2018**: p. 3480309.
10. Watts, A.J.B., et al., *Autoantibodies against nephrin elucidate a novel autoimmune phenomenon in proteinuric kidney disease*. *medRxiv*, 2021.
11. Hong, S., et al., *B Cells Are the Dominant Antigen-Presenting Cells that Activate Naive CD4(+) T Cells upon Immunization with a Virus-Derived Nanoparticle Antigen*. *Immunity*, 2018. **49**(4): p. 695-708 e4.
12. Kroeger, D.R., C.D. Rudulier, and P.A. Bretscher, *Antigen presenting B cells facilitate CD4 T cell cooperation resulting in enhanced generation of effector and memory CD4 T cells*. *PLoS One*, 2013. **8**(10): p. e77346.
13. Gorenjak, M., *4. Kidneys and Autoimmune Disease*. *EJIFCC*, 2009. **20**(1): p. 28-32.
14. Hocking, A.M. and J.H. Buckner, *Genetic basis of defects in immune tolerance underlying the development of autoimmunity*. *Front Immunol*, 2022. **13**: p. 972121.
15. Seifert, M. and R. Kuppers, *Human memory B cells*. *Leukemia*, 2016. **30**(12): p. 2283-2292.
16. Sakaguchi, S., et al., *Regulatory T cells and immune tolerance*. *Cell*, 2008. **133**(5): p. 775-87.
17. Pugliese, A., *Central and peripheral autoantigen presentation in immune tolerance*. *Immunology*, 2004. **111**(2): p. 138-46.
18. Hardy, R.R. and K. Hayakawa, *B cell development pathways*. *Annu Rev Immunol*, 2001. **19**: p. 595-621.
19. Hofer, T. and H.R. Rodewald, *Differentiation-based model of hematopoietic stem cell functions and lineage pathways*. *Blood*, 2018. **132**(11): p. 1106-1113.
20. Seo, W. and I. Taniuchi, *Transcriptional regulation of early T-cell development in the thymus*. *Eur J Immunol*, 2016. **46**(3): p. 531-8.
21. Xing, Y. and K.A. Hogquist, *T-cell tolerance: central and peripheral*. *Cold Spring Harb Perspect Biol*, 2012. **4**(6).
22. Tsai, D.Y., et al., *Regulatory mechanisms of B cell responses and the implication in B cell-related diseases*. *J Biomed Sci*, 2019. **26**(1): p. 64.
23. Teh, Y.M. and M.S. Neuberger, *The immunoglobulin (Ig)alpha and Igbeta cytoplasmic domains are independently sufficient to signal B cell maturation and activation in transgenic mice*. *J Exp Med*, 1997. **185**(10): p. 1753-8.
24. Treanor, B., *B-cell receptor: from resting state to activate*. *Immunology*, 2012. **136**(1): p. 21-7.

25. Dong, Y., et al., *Structural principles of B cell antigen receptor assembly*. Nature, 2022. **612**(7938): p. 156-161.
26. Winkler, T.H. and I.L. Martensson, *The Role of the Pre-B Cell Receptor in B Cell Development, Repertoire Selection, and Tolerance*. Front Immunol, 2018. **9**: p. 2423.
27. Giltiay, N.V., C.P. Chappell, and E.A. Clark, *B-cell selection and the development of autoantibodies*. Arthritis Res Ther, 2012. **14 Suppl 4**(Suppl 4): p. S1.
28. Nguyen, T.V., et al., *V(D)J recombination process and the Pre-B to immature B-cells transition are altered in Fanca(-/-) mice*. Sci Rep, 2016. **6**: p. 36906.
29. Nemazee, D., *Mechanisms of central tolerance for B cells*. Nat Rev Immunol, 2017. **17**(5): p. 281-294.
30. Kondelkova, K., et al., *Regulatory T cells (TREG) and their roles in immune system with respect to immunopathological disorders*. Acta Medica (Hradec Kralove), 2010. **53**(2): p. 73-7.
31. van Parijs, L., V.L. Perez, and A.K. Abbas, *Mechanisms of peripheral T cell tolerance*. Novartis Found Symp, 1998. **215**: p. 5-14; discussion 14-20, 33-40.
32. Piccirillo, C.A., *Transcriptional and translational control of Foxp3(+) regulatory T cell functional adaptation to inflammation*. Curr Opin Immunol, 2020. **67**: p. 27-35.
33. Bin Dhuban, K., et al., *Coexpression of TIGIT and FCRL3 identifies Helios+ human memory regulatory T cells*. J Immunol, 2015. **194**(8): p. 3687-96.
34. Kumar, B.V., T.J. Connors, and D.L. Farber, *Human T Cell Development, Localization, and Function throughout Life*. Immunity, 2018. **48**(2): p. 202-213.
35. Santamaria, J.C., A. Borelli, and M. Irla, *Regulatory T Cell Heterogeneity in the Thymus: Impact on Their Functional Activities*. Front Immunol, 2021. **12**: p. 643153.
36. Caramalho, I., et al., *Regulatory T-Cell Development in the Human Thymus*. Front Immunol, 2015. **6**: p. 395.
37. Attias, M., T. Al-Aubodah, and C.A. Piccirillo, *Mechanisms of human FoxP3(+) T(reg) cell development and function in health and disease*. Clin Exp Immunol, 2019. **197**(1): p. 36-51.
38. Deng, G., et al., *Foxp3 Post-translational Modifications and Treg Suppressive Activity*. Front Immunol, 2019. **10**: p. 2486.
39. Liao, W., J.X. Lin, and W.J. Leonard, *IL-2 family cytokines: new insights into the complex roles of IL-2 as a broad regulator of T helper cell differentiation*. Curr Opin Immunol, 2011. **23**(5): p. 598-604.
40. Okeke, E.B. and J.E. Uzonna, *The Pivotal Role of Regulatory T Cells in the Regulation of Innate Immune Cells*. Front Immunol, 2019. **10**: p. 680.
41. Bettini, M. and D.A. Vignali, *Regulatory T cells and inhibitory cytokines in autoimmunity*. Curr Opin Immunol, 2009. **21**(6): p. 612-8.
42. Klein, M. and T. Bopp, *Cyclic AMP Represents a Crucial Component of Treg Cell-Mediated Immune Regulation*. Front Immunol, 2016. **7**: p. 315.
43. Ohta, A. and M. Sitkovsky, *Extracellular adenosine-mediated modulation of regulatory T cells*. Front Immunol, 2014. **5**: p. 304.
44. Schmidt, A., N. Oberle, and P.H. Krammer, *Molecular mechanisms of treg-mediated T cell suppression*. Front Immunol, 2012. **3**: p. 51.
45. Gertel, S., et al., *Lymphocyte activation gene-3 (LAG-3) regulatory T cells: An evolving biomarker for treatment response in autoimmune diseases*. Autoimmun Rev, 2022. **21**(6): p. 103085.
46. Puccetti, P. and U. Grohmann, *IDO and regulatory T cells: a role for reverse signalling and non-canonical NF-kappaB activation*. Nat Rev Immunol, 2007. **7**(10): p. 817-23.
47. Baban, B., et al., *IDO activates regulatory T cells and blocks their conversion into Th17-like T cells*. J Immunol, 2009. **183**(4): p. 2475-83.

48. Cashman, K.S., et al., *Understanding and measuring human B-cell tolerance and its breakdown in autoimmune disease*. Immunol Rev, 2019. **292**(1): p. 76-89.
49. Rice, J.S., et al., *Receptor editing in peripheral B cell tolerance*. Proc Natl Acad Sci U S A, 2005. **102**(5): p. 1608-13.
50. Schwartz, R.H., *T cell anergy*. Annu Rev Immunol, 2003. **21**: p. 305-34.
51. Sckisel, G.D., et al., *Out-of-Sequence Signal 3 Paralyzes Primary CD4(+) T-Cell-Dependent Immunity*. Immunity, 2015. **43**(2): p. 240-50.
52. Crespo, J., et al., *T cell anergy, exhaustion, senescence, and stemness in the tumor microenvironment*. Curr Opin Immunol, 2013. **25**(2): p. 214-21.
53. Cambier, J.C., et al., *B-cell anergy: from transgenic models to naturally occurring anergic B cells?* Nat Rev Immunol, 2007. **7**(8): p. 633-43.
54. Brooks, J.F., et al., *Peripheral Tolerance Checkpoints Imposed by Ubiquitous Antigen Expression Limit Antigen-Specific B Cell Responses under Strongly Immunogenic Conditions*. J Immunol, 2020. **205**(5): p. 1239-1247.
55. Wells, A.D., et al., *Requirement for T-cell apoptosis in the induction of peripheral transplantation tolerance*. Nat Med, 1999. **5**(11): p. 1303-7.
56. Waring, P. and A. Mullbacher, *Cell death induced by the Fas/Fas ligand pathway and its role in pathology*. Immunol Cell Biol, 1999. **77**(4): p. 312-7.
57. Schattner, E. and S.M. Friedman, *Fas expression and apoptosis in human B cells*. Immunol Res, 1996. **15**(3): p. 246-57.
58. Rothstein, T.L., *Inducible resistance to Fas-mediated apoptosis in B cells*. Cell Res, 2000. **10**(4): p. 245-66.
59. Hao, Z., et al., *Fas receptor expression in germinal-center B cells is essential for T and B lymphocyte homeostasis*. Immunity, 2008. **29**(4): p. 615-27.
60. Madley, R., et al., *Negative selection of human T cells recognizing a naturally-expressed tissue-restricted antigen in the human thymus*. J Transl Autoimmun, 2020. **3**: p. 100061.
61. Kishimoto, H. and J. Sprent, *A defect in central tolerance in NOD mice*. Nat Immunol, 2001. **2**(11): p. 1025-31.
62. Shum, A.K., et al., *Identification of an autoantigen demonstrates a link between interstitial lung disease and a defect in central tolerance*. Sci Transl Med, 2009. **1**(9): p. 9ra20.
63. Zhao, B., et al., *The Role of Autoimmune Regulator (AIRE) in Peripheral Tolerance*. J Immunol Res, 2018. **2018**: p. 3930750.
64. Chen, Z., C. Benoist, and D. Mathis, *How defects in central tolerance impinge on a deficiency in regulatory T cells*. Proc Natl Acad Sci U S A, 2005. **102**(41): p. 14735-40.
65. Mathis, D. and C. Benoist, *Back to central tolerance*. Immunity, 2004. **20**(5): p. 509-16.
66. Mackay, I.R., *Tolerance and autoimmunity*. Western Journal of Medicine, 2001. **174**(2): p. 118-123.
67. Ring, G.H. and F.G. Lakkis, *Breakdown of self-tolerance and the pathogenesis of autoimmunity*. Semin Nephrol, 1999. **19**(1): p. 25-33.
68. Yamada, A., A.D. Salama, and M.H. Sayegh, *The role of novel T cell costimulatory pathways in autoimmunity and transplantation*. J Am Soc Nephrol, 2002. **13**(2): p. 559-575.
69. Bijl, M., et al., *Expression of costimulatory molecules on peripheral blood lymphocytes of patients with systemic lupus erythematosus*. Ann Rheum Dis, 2001. **60**(5): p. 523-6.
70. Marken, J., S. Muralidharan, and N.V. Giltiay, *Anti-CD40 antibody KPL-404 inhibits T cell-mediated activation of B cells from healthy donors and autoimmune patients*. Arthritis Res Ther, 2021. **23**(1): p. 5.
71. Karnell, J.L., et al., *Targeting the CD40-CD40L pathway in autoimmune diseases: Humoral immunity and beyond*. Adv Drug Deliv Rev, 2019. **141**: p. 92-103.

72. Wikenheiser, D.J. and J.S. Stumhofer, *ICOS Co-Stimulation: Friend or Foe?* Front Immunol, 2016. **7**: p. 304.
73. Taams, L.S., et al., *Regulatory T cells in human disease and their potential for therapeutic manipulation.* Immunology, 2006. **118**(1): p. 1-9.
74. Murguia-Favela, L., et al., *IPEX syndrome caused by a novel mutation in FOXP3 gene can be cured by bone marrow transplantation from an unrelated donor after myeloablative conditioning.* LymphoSign Journal, 2014. **2**(1): p. 31-38.
75. Barzaghi, F. and L. Passerini, *IPEX Syndrome: Improved Knowledge of Immune Pathogenesis Empowers Diagnosis.* Front Pediatr, 2021. **9**: p. 612760.
76. Danikowski, K.M., S. Jayaraman, and B.S. Prabhakar, *Regulatory T cells in multiple sclerosis and myasthenia gravis.* J Neuroinflammation, 2017. **14**(1): p. 117.
77. Viglietta, V., et al., *Loss of functional suppression by CD4+CD25+ regulatory T cells in patients with multiple sclerosis.* J Exp Med, 2004. **199**(7): p. 971-9.
78. Ishigame, H., et al., *Excessive Th1 responses due to the absence of TGF-beta signaling cause autoimmune diabetes and dysregulated Treg cell homeostasis.* Proc Natl Acad Sci U S A, 2013. **110**(17): p. 6961-6.
79. Dejaco, C., et al., *Imbalance of regulatory T cells in human autoimmune diseases.* Immunology, 2006. **117**(3): p. 289-300.
80. Mizui, M. and G.C. Tsokos, *Targeting Regulatory T Cells to Treat Patients With Systemic Lupus Erythematosus.* Front Immunol, 2018. **9**: p. 786.
81. Petersone, L., et al., *T Cell/B Cell Collaboration and Autoimmunity: An Intimate Relationship.* Front Immunol, 2018. **9**: p. 1941.
82. Arkatkar, T., et al., *B cell-derived IL-6 initiates spontaneous germinal center formation during systemic autoimmunity.* J Exp Med, 2017. **214**(11): p. 3207-3217.
83. Nepom, G.T. and H. Erlich, *MHC class-II molecules and autoimmunity.* Annu Rev Immunol, 1991. **9**: p. 493-525.
84. Tsai, S. and P. Santamaria, *MHC Class II Polymorphisms, Autoreactive T-Cells, and Autoimmunity.* Front Immunol, 2013. **4**: p. 321.
85. Matzaraki, V., et al., *The MHC locus and genetic susceptibility to autoimmune and infectious diseases.* Genome Biol, 2017. **18**(1): p. 76.
86. Rojas, M., et al., *Molecular mimicry and autoimmunity.* J Autoimmun, 2018. **95**: p. 100-123.
87. Magee, C.N., O. Boenisch, and N. Najafian, *The role of costimulatory molecules in directing the functional differentiation of alloreactive T helper cells.* Am J Transplant, 2012. **12**(10): p. 2588-600.
88. Sansom, D.M., *CD28, CTLA-4 and their ligands: who does what and to whom?* Immunology, 2000. **101**(2): p. 169-77.
89. Mayer, C.T., et al., *An apoptosis-dependent checkpoint for autoimmunity in memory B and plasma cells.* Proc Natl Acad Sci U S A, 2020. **117**(40): p. 24957-24963.
90. Francisco, L.M., P.T. Sage, and A.H. Sharpe, *The PD-1 pathway in tolerance and autoimmunity.* Immunol Rev, 2010. **236**: p. 219-42.
91. Gronski, M.A. and M. Weinem, *Death pathways in T cell homeostasis and their role in autoimmune diabetes.* Rev Diabet Stud, 2006. **3**(2): p. 88-95.
92. Geginat, J., et al., *Plasticity of human CD4 T cell subsets.* Front Immunol, 2014. **5**: p. 630.
93. Meng, X.T., et al., *The Role of Th17 Cells and IL-17 in Th2 Immune Responses of Allergic Conjunctivitis.* J Ophthalmol, 2020. **2020**: p. 6917185.
94. Lin, Y.J., A. Goretzki, and S. Schulke, *Immune Metabolism of IL-4-Activated B Cells and Th2 Cells in the Context of Allergic Diseases.* Front Immunol, 2021. **12**: p. 790658.

95. Stavnezer, J., J.E. Guikema, and C.E. Schrader, *Mechanism and regulation of class switch recombination*. Annu Rev Immunol, 2008. **26**: p. 261-92.
96. Luckheeram, R.V., et al., *CD4(+)T cells: differentiation and functions*. Clin Dev Immunol, 2012. **2012**: p. 925135.
97. Zhu, J., H. Yamane, and W.E. Paul, *Differentiation of effector CD4 T cell populations (*)*. Annu Rev Immunol, 2010. **28**: p. 445-89.
98. Seif, F., et al., *The role of JAK-STAT signaling pathway and its regulators in the fate of T helper cells*. Cell Commun Signal, 2017. **15**(1): p. 23.
99. O'Shea, J.J. and R. Plenge, *JAK and STAT signaling molecules in immunoregulation and immune-mediated disease*. Immunity, 2012. **36**(4): p. 542-50.
100. Matsumoto, Y., et al., *Expression of Master Regulators of T-cell, Helper T-cell and Follicular Helper T-cell Differentiation in Angioimmunoblastic T-cell Lymphoma*. Intern Med, 2017. **56**(21): p. 2851-2856.
101. Liu, X., et al., *Bcl6 expression specifies the T follicular helper cell program in vivo*. J Exp Med, 2012. **209**(10): p. 1841-52, S1-24.
102. Clay, S.L., et al., *Regulatory T cells control the dynamic and site-specific polarization of total CD4 T cells following Salmonella infection*. Mucosal Immunol, 2020. **13**(6): p. 946-957.
103. Dardalhon, V., et al., *Role of Th1 and Th17 cells in organ-specific autoimmunity*. J Autoimmun, 2008. **31**(3): p. 252-6.
104. Kamali, A.N., et al., *A role for Th1-like Th17 cells in the pathogenesis of inflammatory and autoimmune disorders*. Mol Immunol, 2019. **105**: p. 107-115.
105. Skapenko, A., et al., *The role of the T cell in autoimmune inflammation*. Arthritis Res Ther, 2005. **7 Suppl 2**(Suppl 2): p. S4-14.
106. Jackson, S.W., et al., *B cell IFN-gamma receptor signaling promotes autoimmune germinal centers via cell-intrinsic induction of BCL-6*. J Exp Med, 2016. **213**(5): p. 733-50.
107. Meng, X.-T., et al., *The Role of Th17 Cells and IL-17 in Th2 Immune Responses of Allergic Conjunctivitis*. Journal of Ophthalmology, 2020. **2020**: p. 6917185.
108. Tangye, S.G., et al., *Isotype switching by human B cells is division-associated and regulated by cytokines*. J Immunol, 2002. **169**(8): p. 4298-306.
109. Mitsdoerffer, M., et al., *Proinflammatory T helper type 17 cells are effective B-cell helpers*. Proc Natl Acad Sci U S A, 2010. **107**(32): p. 14292-7.
110. Zhang, S., *The role of transforming growth factor beta in T helper 17 differentiation*. Immunology, 2018. **155**(1): p. 24-35.
111. Lee, G.R., *The Balance of Th17 versus Treg Cells in Autoimmunity*. Int J Mol Sci, 2018. **19**(3).
112. Eisenstein, E.M. and C.B. Williams, *The T(reg)/Th17 cell balance: a new paradigm for autoimmunity*. Pediatr Res, 2009. **65**(5 Pt 2): p. 26R-31R.
113. Crotty, S., *T follicular helper cell differentiation, function, and roles in disease*. Immunity, 2014. **41**(4): p. 529-42.
114. Laidlaw, B.J., J.E. Craft, and S.M. Kaeck, *The multifaceted role of CD4(+) T cells in CD8(+) T cell memory*. Nat Rev Immunol, 2016. **16**(2): p. 102-11.
115. Wieczorek, M., et al., *Major Histocompatibility Complex (MHC) Class I and MHC Class II Proteins: Conformational Plasticity in Antigen Presentation*. Front Immunol, 2017. **8**: p. 292.
116. Riedhammer, C. and R. Weissert, *Antigen Presentation, Autoantigens, and Immune Regulation in Multiple Sclerosis and Other Autoimmune Diseases*. Front Immunol, 2015. **6**: p. 322.
117. Bachmann, M.F. and M. Kopf, *On the role of the innate immunity in autoimmune disease*. J Exp Med, 2001. **193**(12): p. F47-50.
118. Ruiz-Argüelles, A., *Chapter 7, T lymphocytes in autoimmunity*. Autoimmunity: From Bench to Bedside, 2013.

119. Jogdand, G.M., S. Mohanty, and S. Devadas, *Regulators of Tfh Cell Differentiation*. Front Immunol, 2016. **7**: p. 520.
120. Olatunde, A.C., J.S. Hale, and T.J. Lamb, *Cytokine-skewed Tfh cells: functional consequences for B cell help*. Trends Immunol, 2021. **42**(6): p. 536-550.
121. Nurieva, R.I. and Y. Chung, *Understanding the development and function of T follicular helper cells*. Cell Mol Immunol, 2010. **7**(3): p. 190-7.
122. Gensous, N., et al., *T Follicular Helper Cells in Autoimmune Disorders*. Front Immunol, 2018. **9**: p. 1637.
123. Akkaya, M., K. Kwak, and S.K. Pierce, *B cell memory: building two walls of protection against pathogens*. Nat Rev Immunol, 2020. **20**(4): p. 229-238.
124. Forthal, D.N., *Functions of Antibodies*. Microbiol Spectr, 2014. **2**(4): p. AID-0019-2014.
125. MacConmara, M. and J.A. Lederer, *B cells*. Crit Care Med, 2005. **33**(12 Suppl): p. S514-6.
126. Schroeder, H.W., Jr. and L. Cavacini, *Structure and function of immunoglobulins*. J Allergy Clin Immunol, 2010. **125**(2 Suppl 2): p. S41-52.
127. Horns, F., et al., *Signatures of selection in the human antibody repertoire: Selective sweeps, competing subclones, and neutral drift*. Proc Natl Acad Sci U S A, 2019.
128. Kuri-Magana, H., et al., *Non-coding Class Switch Recombination-Related Transcription in Human Normal and Pathological Immune Responses*. Front Immunol, 2018. **9**: p. 2679.
129. Collins, A.M. and C.T. Watson, *Immunoglobulin Light Chain Gene Rearrangements, Receptor Editing and the Development of a Self-Tolerant Antibody Repertoire*. Front Immunol, 2018. **9**: p. 2249.
130. El Shikh, M.E. and C. Pitzalis, *Follicular dendritic cells in health and disease*. Front Immunol, 2012. **3**: p. 292.
131. van der Poel, C.E., et al., *Follicular Dendritic Cells Modulate Germinal Center B Cell Diversity through FcγRIIB*. Cell Rep, 2019. **29**(9): p. 2745-2755 e4.
132. Powell, A.M. and M.M. Black, *Epitope spreading: protection from pathogens, but propagation of autoimmunity?* Clin Exp Dermatol, 2001. **26**(5): p. 427-33.
133. Bousso, P., *T-cell activation by dendritic cells in the lymph node: lessons from the movies*. Nat Rev Immunol, 2008. **8**(9): p. 675-84.
134. Bajenoff, M. and R.N. Germain, *B-cell follicle development remodels the conduit system and allows soluble antigen delivery to follicular dendritic cells*. Blood, 2009. **114**(24): p. 4989-97.
135. Fan, H., D. Ren, and Y. Hou, *TLR7, a third signal for the robust generation of spontaneous germinal center B cells in systemic lupus erythematosus*. Cell Mol Immunol, 2018. **15**(3): p. 286-288.
136. Ng, Y.H. and G. Chalasani, *Role of secondary lymphoid tissues in primary and memory T-cell responses to a transplanted organ*. Transplant Rev (Orlando), 2010. **24**(1): p. 32-41.
137. Stebbeg, M., et al., *Regulation of the Germinal Center Response*. Front Immunol, 2018. **9**: p. 2469.
138. Gatto, D. and R. Brink, *The germinal center reaction*. J Allergy Clin Immunol, 2010. **126**(5): p. 898-907; quiz 908-9.
139. Allen, C.D., T. Okada, and J.G. Cyster, *Germinal-center organization and cellular dynamics*. Immunity, 2007. **27**(2): p. 190-202.
140. Jellusova, J. and R.C. Rickert, *The PI3K pathway in B cell metabolism*. Crit Rev Biochem Mol Biol, 2016. **51**(5): p. 359-378.
141. Yamazaki, T., et al., *Essential immunoregulatory role for BCAP in B cell development and function*. J Exp Med, 2002. **195**(5): p. 535-45.
142. Duan, L., et al., *Follicular dendritic cells restrict interleukin-4 availability in germinal centers and foster memory B cell generation*. Immunity, 2021. **54**(10): p. 2256-2272 e6.

143. Soni, C., et al., *B cell-intrinsic TLR7 signaling is essential for the development of spontaneous germinal centers*. J Immunol, 2014. **193**(9): p. 4400-14.
144. LeBien, T.W. and T.F. Tedder, *B lymphocytes: how they develop and function*. Blood, 2008. **112**(5): p. 1570-80.
145. Hoffman, W., F.G. Lakkis, and G. Chalasani, *B Cells, Antibodies, and More*. Clin J Am Soc Nephrol, 2016. **11**(1): p. 137-54.
146. Stavnezer, J. and C.E. Schrader, *IgH chain class switch recombination: mechanism and regulation*. J Immunol, 2014. **193**(11): p. 5370-8.
147. Galibert, L., et al., *Negative selection of human germinal center B cells by prolonged BCR cross-linking*. J Exp Med, 1996. **183**(5): p. 2075-85.
148. Nakagawa, R. and D.P. Calado, *Positive Selection in the Light Zone of Germinal Centers*. Front Immunol, 2021. **12**: p. 661678.
149. Liu, X., et al., *Heterogeneous plasma cells and long-lived subsets in response to immunization, autoantigen and microbiota*. Nat Immunol, 2022. **23**(11): p. 1564-1576.
150. Cyster, J.G. and C.D.C. Allen, *B Cell Responses: Cell Interaction Dynamics and Decisions*. Cell, 2019. **177**(3): p. 524-540.
151. Palm, A.E. and C. Henry, *Remembrance of Things Past: Long-Term B Cell Memory After Infection and Vaccination*. Front Immunol, 2019. **10**: p. 1787.
152. Sundling, C., et al., *Positive selection of IgG(+) over IgM(+) B cells in the germinal center reaction*. Immunity, 2021. **54**(5): p. 988-1001 e5.
153. Capolunghi, F., et al., *Why do we need IgM memory B cells?* Immunol Lett, 2013. **152**(2): p. 114-20.
154. Weill, J.C. and C.A. Reynaud, *IgM memory B cells: specific effectors of innate-like and adaptive responses*. Curr Opin Immunol, 2020. **63**: p. 1-6.
155. Khodadadi, L., et al., *The Maintenance of Memory Plasma Cells*. Front Immunol, 2019. **10**: p. 721.
156. Pioli, P.D., *Plasma Cells, the Next Generation: Beyond Antibody Secretion*. Front Immunol, 2019. **10**: p. 2768.
157. Fridman, W.H., *Fc receptors and immunoglobulin binding factors*. FASEB J, 1991. **5**(12): p. 2684-90.
158. Maity, P.C., et al., *Isotype Specific Assembly of B Cell Antigen Receptors and Synergism With Chemokine Receptor CXCR4*. Front Immunol, 2018. **9**: p. 2988.
159. Barnidge, D.R., et al., *Subset of Kappa and Lambda Germline Sequences Result in Light Chains with a Higher Molecular Mass Phenotype*. J Proteome Res, 2015. **14**(12): p. 5283-90.
160. Lightman, S.M., A. Utley, and K.P. Lee, *Survival of Long-Lived Plasma Cells (LLPC): Piecing Together the Puzzle*. Front Immunol, 2019. **10**: p. 965.
161. Liu, J., et al., *Role of the IgM Fc Receptor in Immunity and Tolerance*. Front Immunol, 2019. **10**: p. 529.
162. Vidarsson, G., G. Dekkers, and T. Rispens, *IgG subclasses and allotypes: from structure to effector functions*. Front Immunol, 2014. **5**: p. 520.
163. Woof, J.M. and M.A. Kerr, *The function of immunoglobulin A in immunity*. J Pathol, 2006. **208**(2): p. 270-82.
164. Woof, J.M. and M.W. Russell, *Structure and function relationships in IgA*. Mucosal Immunol, 2011. **4**(6): p. 590-7.
165. Hanson, L.A., et al., *The transfer of immunity from mother to child*. Ann N Y Acad Sci, 2003. **987**: p. 199-206.
166. Sutton, B.J., et al., *IgE Antibodies: From Structure to Function and Clinical Translation*. Antibodies (Basel), 2019. **8**(1).

167. Geisberger, R., M. Lamers, and G. Achatz, *The riddle of the dual expression of IgM and IgD*. Immunology, 2006. **118**(4): p. 429-37.
168. Amendt, T., et al., *Primary Immune Responses and Affinity Maturation Are Controlled by IgD*. Front Immunol, 2021. **12**: p. 709240.
169. Bossie, A. and E.S. Vitetta, *IFN-gamma enhances secretion of IgG2a from IgG2a-committed LPS-stimulated murine B cells: implications for the role of IFN-gamma in class switching*. Cell Immunol, 1991. **135**(1): p. 95-104.
170. Moens, L. and S.G. Tangye, *Cytokine-Mediated Regulation of Plasma Cell Generation: IL-21 Takes Center Stage*. Front Immunol, 2014. **5**: p. 65.
171. Nydegger, U.E., *Immune complex pathophysiology*. Ann N Y Acad Sci, 2007. **1109**: p. 66-83.
172. Akilesh, S., et al., *Podocytes use FcRn to clear IgG from the glomerular basement membrane*. Proc Natl Acad Sci U S A, 2008. **105**(3): p. 967-72.
173. Ben Mkaddem, S., M. Benhamou, and R.C. Monteiro, *Understanding Fc Receptor Involvement in Inflammatory Diseases: From Mechanisms to New Therapeutic Tools*. Front Immunol, 2019. **10**: p. 811.
174. Takai, T., *Roles of Fc receptors in autoimmunity*. Nat Rev Immunol, 2002. **2**(8): p. 580-92.
175. Swanson, J.A. and A.D. Hoppe, *The coordination of signaling during Fc receptor-mediated phagocytosis*. J Leukoc Biol, 2004. **76**(6): p. 1093-103.
176. Mora, N. and C. Rosales, *[Fc receptor functions in host and immune regulation]*. Rev Invest Clin, 2009. **61**(4): p. 313-26.
177. Lioulios, G., et al., *Exhausted but Not Senescent T Lymphocytes Predominate in Lupus Nephritis Patients*. Int J Mol Sci, 2022. **23**(22).
178. Wright, R.D. and M.W. Beresford, *Podocytes contribute, and respond, to the inflammatory environment in lupus nephritis*. Am J Physiol Renal Physiol, 2018. **315**(6): p. F1683-F1694.
179. Icardi, A., et al., *[Kidney involvement in rheumatoid arthritis]*. Reumatismo, 2003. **55**(2): p. 76-85.
180. Mestecky, J., et al., *IgA nephropathy: current views of immune complex formation*. Contrib Nephrol, 2007. **157**: p. 56-63.
181. McAdoo, S.P. and C.D. Pusey, *Anti-Glomerular Basement Membrane Disease*. Clin J Am Soc Nephrol, 2017. **12**(7): p. 1162-1172.
182. Kim, M., et al., *Antibody-mediated rejection in kidney transplantation: a review of pathophysiology, diagnosis, and treatment options*. Pharmacotherapy, 2014. **34**(7): p. 733-44.
183. Lawrence, E.A., D. Doherty, and R. Dhanda, *Function of the nephron and the formation of urine*. Anaesthesia & Intensive Care Medicine, 2018. **19**(5): p. 249-253.
184. C.J., L., *Principles of renal physiology*. Springer New York, 2012.
185. GJ, T. and D. B., *Principles of Anatomy and Physiology*. Hoboken NJ, 2010. **12**.
186. Curthoys, N.P. and O.W. Moe, *Proximal tubule function and response to acidosis*. Clin J Am Soc Nephrol, 2014. **9**(9): p. 1627-38.
187. Atherton, J.C., *Renal blood flow, glomerular filtration and plasma clearance*. Anaesthesia & Intensive Care Medicine, 2012. **13**(7): p. 315-319.
188. Reiser, J. and M.M. Altintas, *Podocytes*. F1000Res, 2016. **5**.
189. Pollak, M.R., et al., *The glomerulus: the sphere of influence*. Clin J Am Soc Nephrol, 2014. **9**(8): p. 1461-9.
190. Schell, C. and T.B. Huber, *The Evolving Complexity of the Podocyte Cytoskeleton*. J Am Soc Nephrol, 2017. **28**(11): p. 3166-3174.
191. Lennon, R., M.J. Randles, and M.J. Humphries, *The importance of podocyte adhesion for a healthy glomerulus*. Front Endocrinol (Lausanne), 2014. **5**: p. 160.
192. Sachs, N. and A. Sonnenberg, *Cell-matrix adhesion of podocytes in physiology and disease*. Nat Rev Nephrol, 2013. **9**(4): p. 200-10.

193. Pavenstadt, H., W. Kriz, and M. Kretzler, *Cell biology of the glomerular podocyte*. *Physiol Rev*, 2003. **83**(1): p. 253-307.
194. Martin, C.E. and N. Jones, *Nephrin Signaling in the Podocyte: An Updated View of Signal Regulation at the Slit Diaphragm and Beyond*. *Front Endocrinol (Lausanne)*, 2018. **9**: p. 302.
195. Kardasz, S., *The function of the nephron and the formation of urine*. *Anaesthesia & Intensive Care Medicine*, 2012. **13**(7): p. 309-314.
196. Kawachi, H. and Y. Fukusumi, *New insight into podocyte slit diaphragm, a therapeutic target of proteinuria*. *Clin Exp Nephrol*, 2020. **24**(3): p. 193-204.
197. Ruotsalainen, V., et al., *Nephrin is specifically located at the slit diaphragm of glomerular podocytes*. *Proc Natl Acad Sci U S A*, 1999. **96**(14): p. 7962-7.
198. Dlugos, C.P., et al., *Nephrin Signaling Results in Integrin beta1 Activation*. *J Am Soc Nephrol*, 2019. **30**(6): p. 1006-1019.
199. Solanki, A.K., et al., *Phosphorylation of slit diaphragm proteins NEPHRIN and NEPH1 upon binding of HGF promotes podocyte repair*. *J Biol Chem*, 2021. **297**(3): p. 101079.
200. Beltcheva, O., et al., *Mutation spectrum in the nephrin gene (NPHS1) in congenital nephrotic syndrome*. *Hum Mutat*, 2001. **17**(5): p. 368-73.
201. Savage, J.M., et al., *Improved prognosis for congenital nephrotic syndrome of the Finnish type in Irish families*. *Arch Dis Child*, 1999. **80**(5): p. 466-9.
202. Teitelbaum, I. and L. Kooienga, *Chapter 23. Nephrotic Syndrome versus Nephritic Syndrome, in CURRENT Diagnosis & Treatment: Nephrology & Hypertension*, E.V. Lerma, J.S. Berns, and A.R. Nissenson, Editors. 2009, The McGraw-Hill Companies: New York, NY.
203. Hashmi, M.S. and J. Pandey, *Nephritic syndrome*. StatPearls Publishing LLC., 2022.
204. Qunibi, W.Y., et al., *Nephrotic syndrome in anti-GBM antibody mediated glomerulonephritis*. *South Med J*, 1979. **72**(11): p. 1396-8.
205. Health, N.I.o., *Nephrotic Syndrome in Children*. National Institute of Diabetes and Digestive and Kidney Disease (NIDDK), 2021. **Health Information**.
206. Kodner, C., *Diagnosis and Management of Nephrotic Syndrome in Adults*. *Am Fam Physician*, 2016. **93**(6): p. 479-85.
207. Badoe, E. and R. Kumoji, *Congenital nephrotic syndrome of the finnish type*. *Ghana Med J*, 2008. **42**(1): p. 42-4.
208. Dumas De La Roque, C., et al., *Idiopathic Nephrotic Syndrome: Characteristics and Identification of Prognostic Factors*. *J Clin Med*, 2018. **7**(9).
209. Boyer, O., et al., *[Idiopathic nephrotic syndrome]*. *Arch Pediatr*, 2017. **24**(12): p. 1338-1343.
210. Pasini, A., et al., *Childhood Idiopathic Nephrotic Syndrome: Does the Initial Steroid Treatment Modify the Outcome? A Multicentre, Prospective Cohort Study*. *Front Pediatr*, 2021. **9**: p. 627636.
211. Hahn, D., et al., *Corticosteroid therapy for nephrotic syndrome in children*. *Cochrane Database Syst Rev*, 2015. **2015**(3): p. CD001533.
212. Zion, E., et al., *A Clinical Response-Adjusted Steroid Treatment Protocol for Children With Newly Diagnosed Idiopathic Nephrotic Syndrome*. *Am J Kidney Dis*, 2022. **80**(4): p. 473-482 e1.
213. Matalon, A., A. Valeri, and G.B. Appel, *Treatment of focal segmental glomerulosclerosis*. *Semin Nephrol*, 2000. **20**(3): p. 309-17.
214. Bagga, A., *Revised guidelines for management of steroid-sensitive nephrotic syndrome*. *Indian J Nephrol*, 2008. **18**(1): p. 31-9.
215. Ehren, R., et al., *Initial treatment of steroid-sensitive idiopathic nephrotic syndrome in children with mycophenolate mofetil versus prednisone: protocol for a randomised, controlled, multicentre trial (INTENT study)*. *BMJ Open*, 2018. **8**(10): p. e024882.
216. Campbell, R.E. and J.M. Thurman, *The Immune System and Idiopathic Nephrotic Syndrome*. *Clin J Am Soc Nephrol*, 2022. **17**(12): p. 1823-1834.

217. Menon, S. and R.P. Valentini, *Membranous nephropathy in children: clinical presentation and therapeutic approach*. *Pediatr Nephrol*, 2010. **25**(8): p. 1419-28.
218. Ronco, P., et al., *Membranous nephropathy*. *Nat Rev Dis Primers*, 2021. **7**(1): p. 69.
219. Ponticelli, C. and R.J. Glasscock, *Glomerular diseases: membranous nephropathy--a modern view*. *Clin J Am Soc Nephrol*, 2014. **9**(3): p. 609-16.
220. Lai, W.L., et al., *Membranous nephropathy: a review on the pathogenesis, diagnosis, and treatment*. *J Formos Med Assoc*, 2015. **114**(2): p. 102-11.
221. Seifert, L., et al., *The classical pathway triggers pathogenic complement activation in membranous nephropathy*. *Nat Commun*, 2023. **14**(1): p. 473.
222. Gipson, D.S., et al., *Comparing Kidney Health Outcomes in Children, Adolescents, and Adults With Focal Segmental Glomerulosclerosis*. *JAMA Netw Open*, 2022. **5**(8): p. e2228701.
223. D'Agati, V.D., F.J. Kaskel, and R.J. Falk, *Focal segmental glomerulosclerosis*. *N Engl J Med*, 2011. **365**(25): p. 2398-411.
224. Troyanov, S., et al., *Focal and segmental glomerulosclerosis: definition and relevance of a partial remission*. *J Am Soc Nephrol*, 2005. **16**(4): p. 1061-8.
225. Podesta, M.A. and C. Ponticelli, *Autoimmunity in Focal Segmental Glomerulosclerosis: A Long-Standing Yet Elusive Association*. *Front Med (Lausanne)*, 2020. **7**: p. 604961.
226. Pacic, A., et al., *IgM as a novel predictor of disease progression in secondary focal segmental glomerulosclerosis*. *Croat Med J*, 2017. **58**(4): p. 281-291.
227. Saha, T.C. and H. Singh, *Minimal change disease: a review*. *South Med J*, 2006. **99**(11): p. 1264-70.
228. Sellier-Leclerc, A.L., et al., *A humanized mouse model of idiopathic nephrotic syndrome suggests a pathogenic role for immature cells*. *J Am Soc Nephrol*, 2007. **18**(10): p. 2732-9.
229. Abdel-Hafez, M., et al., *Idiopathic nephrotic syndrome and atopy: is there a common link?* *Am J Kidney Dis*, 2009. **54**(5): p. 945-53.
230. Avila-Casado Mdel, C., et al., *Proteinuria in rats induced by serum from patients with collapsing glomerulopathy*. *Kidney Int*, 2004. **66**(1): p. 133-43.
231. Chan, C.Y., et al., *Low regulatory T-cells: A distinct immunological subgroup in minimal change nephrotic syndrome with early relapse following rituximab therapy*. *Transl Res*, 2021. **235**: p. 48-61.
232. Suarez-Fueyo, A., et al., *T cells and autoimmune kidney disease*. *Nat Rev Nephrol*, 2017. **13**(6): p. 329-343.
233. Paquissi, F.C. and H. Abensur, *The Th17/IL-17 Axis and Kidney Diseases, With Focus on Lupus Nephritis*. *Front Med (Lausanne)*, 2021. **8**: p. 654912.
234. Liu, L.L., et al., *Th17/Treg imbalance in adult patients with minimal change nephrotic syndrome*. *Clin Immunol*, 2011. **139**(3): p. 314-20.
235. May, C.J., et al., *Human Th17 cells produce a soluble mediator that increases podocyte motility via signaling pathways that mimic PAR-1 activation*. *Am J Physiol Renal Physiol*, 2019. **317**(4): p. F913-F921.
236. Jaiswal, A., et al., *Regulatory and effector T cells changes in remission and resistant state of childhood nephrotic syndrome*. *Indian J Nephrol*, 2014. **24**(6): p. 349-55.
237. Saleem, M.A. and Y. Kobayashi, *Cell biology and genetics of minimal change disease*. *F1000Res*, 2016. **5**.
238. Tuncay, S.C., et al., *Regulatory T-cell Changes in Patients with Steroid-Resistant Nephrotic Syndrome after Rituximab Therapy*. *Saudi J Kidney Dis Transpl*, 2021. **32**(4): p. 1028-1033.
239. Madanchi, N., M. Bitzan, and T. Takano, *Rituximab in Minimal Change Disease: Mechanisms of Action and Hypotheses for Future Studies*. *Can J Kidney Health Dis*, 2017. **4**: p. 2054358117698667.

240. Colucci, M., et al., *Immunology of idiopathic nephrotic syndrome*. *Pediatr Nephrol*, 2018. **33**(4): p. 573-584.
241. Oleinika, K., C. Mauri, and A.D. Salama, *Effector and regulatory B cells in immune-mediated kidney disease*. *Nat Rev Nephrol*, 2019. **15**(1): p. 11-26.
242. Kolovou, K., et al., *B-cell oligoclonal expansions in renal tissue of patients with immune-mediated glomerular disease*. *Clin Immunol*, 2020. **217**: p. 108488.
243. Ellis, J.S. and H. Braley-Mullen, *Mechanisms by Which B Cells and Regulatory T Cells Influence Development of Murine Organ-Specific Autoimmune Diseases*. *J Clin Med*, 2017. **6**(2).
244. Hsiao, C.C., et al., *Immunoglobulin E and G Levels in Predicting Minimal Change Disease before Renal Biopsy*. *Biomed Res Int*, 2018. **2018**: p. 3480309.
245. Yang, C.W., et al., *IgM mesangial deposition as a risk factor for relapses of adult-onset minimal change disease*. *BMC Nephrol*, 2021. **22**(1): p. 25.
246. Herlitz, L.C., et al., *IgA Nephropathy with Minimal Change Disease*. *Clinical Journal of the American Society of Nephrology*, 2014. **9**(6): p. 1033.
247. Ye, Q., et al., *The important roles and molecular mechanisms of annexin A(2) autoantibody in children with nephrotic syndrome*. *Ann Transl Med*, 2021. **9**(18): p. 1452.
248. Ye, Q., et al., *Seven novel podocyte autoantibodies were identified to diagnosis a new disease subgroup-autoimmune Podocytopathies*. *Clin Immunol*, 2021. **232**: p. 108869.
249. Hada, I., et al., *A Novel Mouse Model of Idiopathic Nephrotic Syndrome Induced by Immunization with the Podocyte Protein Crb2*. *J Am Soc Nephrol*, 2022.
250. Schlom, J., et al., *The role of soluble CD40L in immunosuppression*. *Oncoimmunology*, 2013. **2**(1): p. e22546.
251. Liu, J. and F. Guan, *B cell phenotype, activity, and function in idiopathic nephrotic syndrome*. *Pediatr Res*, 2022.
252. Chugh, S.S., L.C. Clement, and C. Mace, *New insights into human minimal change disease: lessons from animal models*. *Am J Kidney Dis*, 2012. **59**(2): p. 284-92.
253. Purohit, S., et al., *Molecular Mechanisms of Proteinuria in Minimal Change Disease*. *Front Med (Lausanne)*, 2021. **8**: p. 761600.
254. Shen, X., et al., *Lipopolysaccharide-induced podocyte injury is regulated by calcineurin/NFAT and TLR4/MyD88/NF-kappaB signaling pathways through angiopoietin-like protein 4*. *Genes Dis*, 2022. **9**(2): p. 443-455.
255. Bryant, C., et al., *Adriamycin-Induced Nephropathy is Robust in N and Modest in J Substrain of C57BL/6*. *Front Cell Dev Biol*, 2022. **10**: p. 924751.
256. Yang, J.W., et al., *Recent advances of animal model of focal segmental glomerulosclerosis*. *Clin Exp Nephrol*, 2018. **22**(4): p. 752-763.
257. Lee, V.W. and D.C. Harris, *Adriamycin nephropathy: a model of focal segmental glomerulosclerosis*. *Nephrology (Carlton)*, 2011. **16**(1): p. 30-8.
258. Wang, Y.M., et al., *Adriamycin nephropathy in BALB/c mice*. *Curr Protoc Immunol*, 2015. **108**: p. 15 28 1-15 28 6.
259. Pippin, J.W., et al., *Inducible rodent models of acquired podocyte diseases*. *Am J Physiol Renal Physiol*, 2009. **296**(2): p. F213-29.
260. Bertelli, R., et al., *Molecular and Cellular Mechanisms for Proteinuria in Minimal Change Disease*. *Front Med (Lausanne)*, 2018. **5**: p. 170.
261. Takeuchi, K., et al., *New Anti-Nephrin Antibody Mediated Podocyte Injury Model Using a C57BL/6 Mouse Strain*. *Nephron*, 2018. **138**(1): p. 71-87.
262. Moller-Kerutt, A., et al., *Crumbs2 Is an Essential Slit Diaphragm Protein of the Renal Filtration Barrier*. *J Am Soc Nephrol*, 2021. **32**(5): p. 1053-1070.

263. Udagawa, T., et al., *Altered expression of Crb2 in podocytes expands a variation of CRB2 mutations in steroid-resistant nephrotic syndrome*. *Pediatr Nephrol*, 2017. **32**(5): p. 801-809.
264. Tanoue, A., et al., *Podocyte-specific Crb2 knockout mice develop focal segmental glomerulosclerosis*. *Sci Rep*, 2021. **11**(1): p. 20556.
265. Ostalska-Nowicka, D., et al., *Ezrin--a useful factor in the prognosis of nephrotic syndrome in children: an immunohistochemical approach*. *J Clin Pathol*, 2006. **59**(9): p. 916-20.
266. Caplazi, P., et al., *Mouse Models of Rheumatoid Arthritis*. *Vet Pathol*, 2015. **52**(5): p. 819-26.
267. Constantinescu, C.S., et al., *Experimental autoimmune encephalomyelitis (EAE) as a model for multiple sclerosis (MS)*. *Br J Pharmacol*, 2011. **164**(4): p. 1079-106.
268. Awate, S., L.A. Babiuk, and G. Mutwiri, *Mechanisms of action of adjuvants*. *Front Immunol*, 2013. **4**: p. 114.
269. Bennett, B., et al., *A comparison of commercially available adjuvants for use in research*. *J Immunol Methods*, 1992. **153**(1-2): p. 31-40.
270. ThermoFisher, *Dialysis methods for protein research*. *Pierce Protein Methods*, 2009.
271. Assenmacher, M., J. Schmitz, and A. Radbruch, *Flow cytometric determination of cytokines in activated murine T helper lymphocytes: expression of interleukin-10 in interferon-gamma and in interleukin-4-expressing cells*. *Eur J Immunol*, 1994. **24**(5): p. 1097-101.
272. Ai, W., et al., *Optimal method to stimulate cytokine production and its use in immunotoxicity assessment*. *Int J Environ Res Public Health*, 2013. **10**(9): p. 3834-42.
273. ThermoFisher, *ELISA technical guide and protocols*. *Tech Tip*, 2010. **65**.
274. Herz, J., et al., *Peripheral T Cell Depletion by FTY720 Exacerbates Hypoxic-Ischemic Brain Injury in Neonatal Mice*. *Front Immunol*, 2018. **9**: p. 1696.
275. Tsai, H.C., et al., *Effects of sphingosine-1-phosphate receptor 1 phosphorylation in response to FTY720 during neuroinflammation*. *JCI Insight*, 2016. **1**(9): p. e86462.
276. Herlitz, L.C., et al., *IgA nephropathy with minimal change disease*. *Clin J Am Soc Nephrol*, 2014. **9**(6): p. 1033-9.
277. Ruiz, J.T., et al., *Adjuvants- and vaccines-induced autoimmunity: animal models*. *Immunol Res*, 2017. **65**(1): p. 55-65.
278. Rangachari, M. and V.K. Kuchroo, *Using EAE to better understand principles of immune function and autoimmune pathology*. *J Autoimmun*, 2013. **45**: p. 31-9.
279. Nakamura, A., et al., *Fcgamma receptor IIB-deficient mice develop Goodpasture's syndrome upon immunization with type IV collagen: a novel murine model for autoimmune glomerular basement membrane disease*. *J Exp Med*, 2000. **191**(5): p. 899-906.
280. Jones, B.E., et al., *Autoimmune receptor encephalitis in mice induced by active immunization with conformationally stabilized holoreceptors*. *Sci Transl Med*, 2019. **11**(500).
281. Allan, D., P. Jenkins, and F.I. Crampton, *The effect of Freund's complete adjuvant on the cellular immune response in mice to a porcine strain of Escherichia coli lipopolysaccharide*. *Res Vet Sci*, 1977. **23**(1): p. 97-101.
282. Fontes, J.A., et al., *Complete Freund's adjuvant induces experimental autoimmune myocarditis by enhancing IL-6 production during initiation of the immune response*. *Immun Inflamm Dis*, 2017. **5**(2): p. 163-176.
283. Vintar Spreitzer, M., et al., *Do C1q or IgM nephropathies predict disease severity in children with minimal change nephrotic syndrome?* *Pediatr Nephrol*, 2014. **29**(1): p. 67-74.
284. Fogo, A.B., et al., *AJKD Atlas of Renal Pathology: Minimal Change Disease*. *Am J Kidney Dis*, 2015. **66**(2): p. 376-7.
285. Liu, W., et al., *Immunological Pathogenesis of Membranous Nephropathy: Focus on PLA2R1 and Its Role*. *Front Immunol*, 2019. **10**: p. 1809.

286. Nakatsue, T., et al., *Nephrin and podocin dissociate at the onset of proteinuria in experimental membranous nephropathy*. *Kidney Int*, 2005. **67**(6): p. 2239-53.
287. Katafuchi, R., et al., *Comprehensive evaluation of the significance of immunofluorescent findings on clinicopathological features in IgA nephropathy*. *Clin Exp Nephrol*, 2019. **23**(2): p. 169-181.
288. Chen, X. and P.E. Jensen, *The role of B lymphocytes as antigen-presenting cells*. *Arch Immunol Ther Exp (Warsz)*, 2008. **56**(2): p. 77-83.
289. Zhang, J.M. and J. An, *Cytokines, inflammation, and pain*. *Int Anesthesiol Clin*, 2007. **45**(2): p. 27-37.
290. Houglum, J.E., *Interferon: mechanisms of action and clinical value*. *Clin Pharm*, 1983. **2**(1): p. 20-8.
291. Kojima, F., et al., *Reduced T cell-dependent humoral immune response in microsomal prostaglandin E synthase-1 null mice is mediated by nonhematopoietic cells*. *J Immunol*, 2013. **191**(10): p. 4979-88.
292. Ivetic, A., H.L. Hoskins Green, and S.J. Hart, *L-selectin: A Major Regulator of Leukocyte Adhesion, Migration and Signaling*. *Front Immunol*, 2019. **10**: p. 1068.
293. Baaten, B.J., et al., *Regulation of Antigen-Experienced T Cells: Lessons from the Quintessential Memory Marker CD44*. *Front Immunol*, 2012. **3**: p. 23.
294. Gerberick, G.F., et al., *Selective modulation of T cell memory markers CD62L and CD44 on murine draining lymph node cells following allergen and irritant treatment*. *Toxicol Appl Pharmacol*, 1997. **146**(1): p. 1-10.
295. Lohning, M., et al., *Expression of ICOS in vivo defines CD4+ effector T cells with high inflammatory potential and a strong bias for secretion of interleukin 10*. *J Exp Med*, 2003. **197**(2): p. 181-93.
296. Linsley, P.S. and J.A. Ledbetter, *The role of the CD28 receptor during T cell responses to antigen*. *Annu Rev Immunol*, 1993. **11**: p. 191-212.
297. Dong, C., et al., *ICOS co-stimulatory receptor is essential for T-cell activation and function*. *Nature*, 2001. **409**(6816): p. 97-101.
298. Thornton, A.M., et al., *Helios(+) and Helios(-) Treg subpopulations are phenotypically and functionally distinct and express dissimilar TCR repertoires*. *Eur J Immunol*, 2019. **49**(3): p. 398-412.
299. Nakagawa, H., et al., *Instability of Helios-deficient Tregs is associated with conversion to a T-effector phenotype and enhanced antitumor immunity*. *Proc Natl Acad Sci U S A*, 2016. **113**(22): p. 6248-53.
300. Getnet, D., et al., *A role for the transcription factor Helios in human CD4(+)CD25(+) regulatory T cells*. *Mol Immunol*, 2010. **47**(7-8): p. 1595-600.
301. Thornton, A.M. and E.M. Shevach, *Helios: still behind the clouds*. *Immunology*, 2019. **158**(3): p. 161-170.
302. Vazquez, M.I., J. Catalan-Dibene, and A. Zlotnik, *B cells responses and cytokine production are regulated by their immune microenvironment*. *Cytokine*, 2015. **74**(2): p. 318-26.
303. Justiz Vaillant, A.A. and A. Qurie, *Interleukin*, in *StatPearls*. 2022: Treasure Island (FL).
304. Zhu, J. and W.E. Paul, *Heterogeneity and plasticity of T helper cells*. *Cell Res*, 2010. **20**(1): p. 4-12.
305. Liu, Q., et al., *FTY720 demonstrates promising preclinical activity for chronic lymphocytic leukemia and lymphoblastic leukemia/lymphoma*. *Blood*, 2008. **111**(1): p. 275-84.
306. Bail, K., et al., *Differential effects of FTY720 on the B cell compartment in a mouse model of multiple sclerosis*. *J Neuroinflammation*, 2017. **14**(1): p. 148.
307. Sic, H., et al., *Sphingosine-1-phosphate receptors control B-cell migration through signaling components associated with primary immunodeficiencies, chronic lymphocytic leukemia, and multiple sclerosis*. *J Allergy Clin Immunol*, 2014. **134**(2): p. 420-8.

308. Fan, J., et al., *Advances in Infectious Disease Vaccine Adjuvants*. Vaccines (Basel), 2022. **10**(7).
309. Krummel, M.F., F. Bartumeus, and A. Gerard, *T cell migration, search strategies and mechanisms*. Nat Rev Immunol, 2016. **16**(3): p. 193-201.
310. Kitching, A.R. and S.R. Holdsworth, *The renal draining lymph nodes in acute inflammatory kidney disease*. Kidney Int, 2019. **95**(2): p. 254-256.
311. Gough, S.C. and M.J. Simmonds, *The HLA Region and Autoimmune Disease: Associations and Mechanisms of Action*. Curr Genomics, 2007. **8**(7): p. 453-65.
312. Ishina, I.A., et al., *MHC Class II Presentation in Autoimmunity*. Cells, 2023. **12**(2).
313. Jurewicz, M.M. and L.J. Stern, *Class II MHC antigen processing in immune tolerance and inflammation*. Immunogenetics, 2019. **71**(3): p. 171-187.
314. Van Regenmortel, M.H.V., *Antigenicity and Immunogenicity of Viral Proteins*. Encyclopedia of Virology, 2008. **3**: p. 137-142.
315. Zhang, J. and A. Tao, *Antigenicity, Immunogenicity, Allergenicity*. Allergy Bioinformatics, 2015: p. 175-86.
316. eBioscience, *Mosue haplotype table*. ThermoFisher Scientific, 2023.
317. Schulte, S., G.K. Sukhova, and P. Libby, *Genetically programmed biases in Th1 and Th2 immune responses modulate atherogenesis*. Am J Pathol, 2008. **172**(6): p. 1500-8.
318. Lund, F.E. and T.D. Randall, *Effector and regulatory B cells: modulators of CD4+ T cell immunity*. Nat Rev Immunol, 2010. **10**(4): p. 236-47.
319. Granato, A., et al., *IL-4 regulates Bim expression and promotes B cell maturation in synergy with BAFF conferring resistance to cell death at negative selection checkpoints*. J Immunol, 2014. **192**(12): p. 5761-75.
320. Ramachandran, R., et al., *Regulatory B Cells Are Reduced and Correlate With Disease Activity in Primary Membranous Nephropathy*. Kidney Int Rep, 2020. **5**(6): p. 872-878.
321. Zhao, Q., et al., *Helper T Cells in Idiopathic Membranous Nephropathy*. Front Immunol, 2021. **12**: p. 665629.
322. Kuroki, A., et al., *Th2 cytokines increase and stimulate B cells to produce IgG4 in idiopathic membranous nephropathy*. Kidney Int, 2005. **68**(1): p. 302-10.
323. Doria-Rose, N.A. and M.G. Joyce, *Strategies to guide the antibody affinity maturation process*. Curr Opin Virol, 2015. **11**: p. 137-47.
324. Elsner, R.A. and M.J. Shlomchik, *Germinal Center and Extrafollicular B Cell Responses in Vaccination, Immunity, and Autoimmunity*. Immunity, 2020. **53**(6): p. 1136-1150.
325. Auner, H.W., et al., *The life span of short-lived plasma cells is partly determined by a block on activation of apoptotic caspases acting in combination with endoplasmic reticulum stress*. Blood, 2010. **116**(18): p. 3445-55.
326. Roth, K., et al., *Tracking plasma cell differentiation and survival*. Cytometry A, 2014. **85**(1): p. 15-24.
327. Tellier, J. and S.L. Nutt, *Plasma cells: The programming of an antibody-secreting machine*. Eur J Immunol, 2019. **49**(1): p. 30-37.
328. Lanzavecchia, A. and F. Sallusto, *Human B cell memory*. Curr Opin Immunol, 2009. **21**(3): p. 298-304.
329. Elkon, K. and P. Casali, *Nature and functions of autoantibodies*. Nat Clin Pract Rheumatol, 2008. **4**(9): p. 491-8.
330. Zhai, S., et al., *Respiratory Syncytial Virus Aggravates Renal Injury through Cytokines and Direct Renal Injury*. Front Cell Infect Microbiol, 2016. **6**: p. 112.
331. Pedersen, G.K., et al., *Vaccine Adjuvants Differentially Affect Kinetics of Antibody and Germinal Center Responses*. Front Immunol, 2020. **11**: p. 579761.

332. Ebsensen, T., et al., *The Combination Vaccine Adjuvant System Alum/c-di-AMP Results in Quantitative and Qualitative Enhanced Immune Responses Post Immunization*. Front Cell Infect Microbiol, 2019. **9**: p. 31.
333. Henker, L.C., et al., *Immune protection conferred by recombinant MRLC (myosin regulatory light chain) antigen in TiterMax Gold(R) adjuvant against experimental fasciolosis in rats*. Vaccine, 2017. **35**(4): p. 663-671.
334. Becerra, E., et al., *Effect of rituximab on B cell phenotype and serum B cell-activating factor levels in patients with thrombotic thrombocytopenic purpura*. Clin Exp Immunol, 2015. **179**(3): p. 414-25.
335. Ye, Q., et al., *Autoimmune Podocytopathies: A Novel Sub-Group of Diseases from Childhood Idiopathic Nephrotic Syndrome*. J Am Soc Nephrol, 2022. **33**(3): p. 653-654.
336. Leclerc, S., et al., *Minimal Change Disease With Severe Acute Kidney Injury Following the Oxford-AstraZeneca COVID-19 Vaccine: A Case Report*. Am J Kidney Dis, 2021. **78**(4): p. 607-610.
337. Hummel, A., et al., *Idiopathic nephrotic syndrome relapse following COVID-19 vaccination: a series of 25 cases*. Clin Kidney J, 2022. **15**(8): p. 1574-1582.
338. Ebarasi, L., et al., *Defects of CRB2 cause steroid-resistant nephrotic syndrome*. Am J Hum Genet, 2015. **96**(1): p. 153-61.
339. Hamano, S., et al., *Association of crumbs homolog-2 with mTORC1 in developing podocyte*. PLoS One, 2018. **13**(8): p. e0202400.
340. Tonsawan, P., et al., *Knockout of the neonatal Fc receptor in cultured podocytes alters IL-6 signaling and the actin cytoskeleton*. Am J Physiol Cell Physiol, 2019. **317**(5): p. C1048-C1060.
341. Goldwisch, A., et al., *Podocytes are nonhematopoietic professional antigen-presenting cells*. J Am Soc Nephrol, 2013. **24**(6): p. 906-16.
342. Thurman, J.M., et al., *Complement alternative pathway activation in the autologous phase of nephrotoxic serum nephritis*. Am J Physiol Renal Physiol, 2012. **302**(12): p. F1529-36.
343. Dylewski, J.F., et al., *Podocyte-specific knockout of the neonatal Fc receptor (FcRn) results in differential protection depending on the model of glomerulonephritis*. PLoS One, 2020. **15**(12): p. e0230401.
344. Ahmadian, E., et al., *The Role of Cytokines in Nephrotic Syndrome*. Mediators Inflamm, 2022. **2022**: p. 6499668.
345. Yang, Y.Q., et al., *Case Report: The Application of Dupilumab in Atopic Dermatitis Children Complicated With Nephrotic Syndrome*. Front Med (Lausanne), 2022. **9**: p. 813313.
346. Dimitrov, J.D., S. Lacroix-Desmazes, and S.V. Kaveri, *Important parameters for evaluation of antibody avidity by immunosorbent assay*. Anal Biochem, 2011. **418**(1): p. 149-51.
347. Lasagni, L., et al., *Podocyte Mitosis - A Catastrophe*. Current Molecular Medicine, 2013. **13**(1): p. 13-23.
348. Sakairi, T., et al., *Conditionally immortalized human podocyte cell lines established from urine*. Am J Physiol Renal Physiol, 2010. **298**(3): p. F557-67.
349. Endlich, N., et al., *Palladin is a dynamic actin-associated protein in podocytes*. Kidney Int, 2009. **75**(2): p. 214-26.
350. Ding, W.Y. and M.A. Saleem, *Current concepts of the podocyte in nephrotic syndrome*. Kidney Res Clin Pract, 2012. **31**(2): p. 87-93.
351. Agrawal, S., et al., *Albumin-induced podocyte injury and protection are associated with regulation of COX-2*. Kidney Int, 2014. **86**(6): p. 1150-60.
352. Wu, J., et al., *A p38alpha-BLIMP1 signalling pathway is essential for plasma cell differentiation*. Nat Commun, 2022. **13**(1): p. 7321.
353. Chan, O.T., et al., *A novel mouse with B cells but lacking serum antibody reveals an antibody-independent role for B cells in murine lupus*. J Exp Med, 1999. **189**(10): p. 1639-48.

354. Chegade, H., et al., *Two new families with hereditary minimal change disease*. BMC Nephrol, 2013. **14**: p. 65.
355. Jia, X., et al., *Strong Association of the HLA-DR/DQ Locus with Childhood Steroid-Sensitive Nephrotic Syndrome in the Japanese Population*. J Am Soc Nephrol, 2018. **29**(8): p. 2189-2199.